



# Contribution to the Study of 3D Interaction Techniques and Sensory Feedbacks for Improving Navigation and Walking in Virtual Reality

Léo Terziman

## ► To cite this version:

Léo Terziman. Contribution to the Study of 3D Interaction Techniques and Sensory Feedbacks for Improving Navigation and Walking in Virtual Reality. Graphics [cs.GR]. INSA de Rennes, 2012. English. NNT: . tel-00767488

**HAL Id: tel-00767488**

**<https://theses.hal.science/tel-00767488>**

Submitted on 20 Dec 2012

**HAL** is a multi-disciplinary open access archive for the deposit and dissemination of scientific research documents, whether they are published or not. The documents may come from teaching and research institutions in France or abroad, or from public or private research centers.

L'archive ouverte pluridisciplinaire **HAL**, est destinée au dépôt et à la diffusion de documents scientifiques de niveau recherche, publiés ou non, émanant des établissements d'enseignement et de recherche français ou étrangers, des laboratoires publics ou privés.

Thèse



**THÈSE INSA Rennes**

*sous le sceau de l'Université Européenne de Bretagne*

*pour obtenir le grade de*

**DOCTEUR DE L'INSA DE RENNES**

*Spécialité : Informatique*

présentée par

**Léo TERZIMAN**

**ÉCOLE DOCTORALE : MATISSE**

**LABORATOIRE : INRIA Rennes - IRISA**

# Contribution to the Study of 3D Interaction Techniques and Sensory Feedbacks for Improving Navigation and Walking in Virtual Reality

**Thèse soutenue le 13.12.2012**

devant le jury composé de :

**Guillaume Moreau**

Professeur, École Centrale de Nantes / *Président*

**Frank Steinicke**

Professeur, University of Würzburg, Germany / *Rapporteur*

**Jean-Louis Vercher**

Directeur de Recherche CNRS, ISM / *Rapporteur*

**Sabine Coquillart**

Directrice de Recherche, INRIA Rhône-Alpes / *Examinatrice*

**Anatole Lécuyer**

Directeur de Recherche, INRIA Rennes / *Directeur de thèse*

**Maud Marchal**

Maître de Conférences, INSA de Rennes / *Encadrante*

**Bruno Arnaldi**

Professeur, INSA de Rennes / *Encadrant*



# Remerciements

TROIS ans, cinq papiers, des centaines d'heures de travail, pas mal de prises de tête, encore plus de bon temps. Bref, j'ai fait une thèse.

J'en profite donc pour remercier avant tout la team de choc qui m'a encadré, dirigé, conseillé, parfois contre mon gré, tout au long de ces trois ans. Tout d'abord Dr. Anatole Lécuyer, pour m'avoir ouvert les portes de la recherche et permit de me lancer dans cette aventure. Ensuite, Dr Maud Marchal pour sa présence au quotidien, et enfin Pr. Franck Multon et Pr. Bruno Arnaldi. Tous ensemble, de très nombreuses idées furent échangées et ont permis de nourrir ma créativité tout au long de cette thèse, afin de produire toutes ces techniques aux noms plus surprenant les uns que les autres. Ce fut un réel plaisir de travailler avec vous, et j'espère sincèrement que nous auront l'opportunité de collaborer ensemble à nouveaux.

Je souhaite également remercier chaleureusement les membres de mon jury pour m'avoir fait l'honneur de prendre le temps de s'intéresser à mes travaux. Tout d'abord Pr. Frank Steinicke et Dr. Jean-Louis Vercher pour avoir accepté de relire mon manuscrit et pour les remarques pertinentes qu'ils ont fait dessus. Ensuite, Dr. Sabine Coquillart et Pr. Guillaume Moreau pour avoir participé à ma soutenance et pour leurs nombreuses questions qui ont suivies. Finalement, je souhaite remercier encore une fois Pr. Guillaume Moreau pour avoir présidé ma soutenance.

Mes remerciements vont également aux membres de l'équipe Bunraku pour les bon moments passés ensemble le midi, aux pauses et surtout durant les pots. Je tiens également à remercier tout particulièrement les différents joueurs des Bugs, l'équipe mythique de hockey sur glace de l'IRISA. Les victoires contre l'INSA resteront gravées dans les annales. Finalement, je souhaite remercier Dr. Gabriel Cirio et Dr. Loeïz Glondu pour avoir partagé ce bureau pendant ces dernières années. Les questions improbables de Loeïz me manqueront sûrement.

Enfin, je souhaite remercier ma famille, et tout particulièrement Élodie (ma petite marmotte), pour m'avoir soutenu et encouragé durant ces trois années, et surtout durant la rédaction de ce manuscrit.





# Contents

<b>Contents</b>	<b>1</b>
<b>List of figures</b>	<b>6</b>
<b>List of tables</b>	<b>8</b>
<b>Introduction</b>	<b>9</b>
<b>1 Related Work: 3D Navigation Techniques and Sensory Feedbacks for Walking in Virtual Reality</b>	<b>15</b>
1.1 A brief Overview of the Properties of Human Walk . . . . .	16
1.1.1 Physical Description . . . . .	16
1.1.1.1 Senses Used During the Walk . . . . .	16
1.1.1.2 Description of the Lower Limbs . . . . .	18
1.1.1.3 Walking Cycle . . . . .	18
1.1.2 Biomechanical Description . . . . .	20
1.1.2.1 Biomechanics of Walking . . . . .	20
1.1.2.2 Differences Between the Locomotion States . . . . .	20
1.1.2.3 Biomechanical Models . . . . .	22
1.1.3 Neuroscience Description . . . . .	23
1.1.3.1 Orientation Strategies Involved During the Walk . . . . .	23
1.1.3.2 Visual Attention Strategies . . . . .	24
1.1.4 Conclusion . . . . .	26
1.2 Locomotion Interfaces for Navigating in VE . . . . .	26
1.2.1 Pedaling Devices . . . . .	27
1.2.2 Foot-based Devices . . . . .	27
1.2.2.1 Shoe-based Devices . . . . .	27
1.2.2.2 Foot Platforms . . . . .	28
1.2.3 Recentering Devices . . . . .	28
1.2.3.1 Treadmills . . . . .	28
1.2.3.2 Tiles . . . . .	30
1.2.3.3 Spheres . . . . .	30
1.2.4 Conclusion . . . . .	31
1.3 3D Interaction Techniques for Navigating in VE . . . . .	31
1.3.1 3D Interaction Techniques for In-Place Use . . . . .	32
1.3.1.1 Static Navigation . . . . .	32
1.3.1.2 Step World in Miniature . . . . .	32
1.3.1.3 Walking in Place . . . . .	33
1.3.2 3D Interaction Techniques Involving Real Physical Walking . . . . .	34
1.3.2.1 Resetting Techniques . . . . .	35

1.3.2.2	Redirected Walking	36
1.3.2.3	Motion Compression	37
1.3.2.4	Impossible Spaces	38
1.3.3	Conclusion	38
1.4	Sensory Feedback Techniques for Navigating in VE	39
1.4.1	Haptic Feedback	39
1.4.1.1	Foot Devices	39
1.4.1.2	Floor Devices	40
1.4.2	Visual Feedback	41
1.4.3	Vestibular Feedback	43
1.4.4	Auditory Feedback	44
1.4.4.1	Step-contact Sounds	44
1.4.4.2	Surfaces Sound Properties	44
1.4.5	Multimodal Feedback	45
1.4.6	Conclusion	47
1.5	Conclusion	47
<b>2</b>	<b>Shake-Your-Head: a Navigation Technique Revisiting Walking-In-Place for Desktop Virtual Reality</b>	<b>49</b>
2.1	The Shake-Your-Head Technique	50
2.1.1	Input/Output Interfaces	51
2.1.1.1	Input: Tracking Based on Head Motions	51
2.1.1.2	Output: Immersive and Desktop Visual Displays	53
2.1.2	Walking Simulation	53
2.1.2.1	Walking States	53
2.1.2.2	Forward State	53
2.1.2.3	Jump and Crawl States	54
2.1.2.4	Turn State	55
2.1.3	Visual Feedback Based on Camera Motions	55
2.1.3.1	Advance Oscillations	55
2.1.3.2	Lateral Oscillations	56
2.1.3.3	Vertical Oscillations	56
2.1.4	Conclusion	56
2.2	Evaluation of the Shake-Your-Head	57
2.2.1	Method	57
2.2.1.1	Virtual Environment	57
2.2.1.2	Population	57
2.2.1.3	Experimental Conditions	58
2.2.1.4	Experimental Apparatus	58
2.2.1.5	Experimental Plan	59
2.2.1.6	Collected Data	59
2.2.2	Results	60
2.2.2.1	Task Completion Time	60
2.2.2.2	Accuracy	61
2.2.2.3	Subjective Questionnaire	61
2.2.3	Discussion	62
2.3	Analysis of the Virtual Trajectories Generated with the Shake-Your-Head	63
2.3.1	Trajectories Analysis	63
2.3.1.1	Spatial Analysis	64

2.3.1.2	Temporal Analysis . . . . .	67
2.3.2	Discussion . . . . .	67
2.3.3	Conclusion . . . . .	68
2.4	Conclusion . . . . .	68
<b>3</b>	<b>King-Kong Effects: Improving Sensation of Walking with Visual and Tactile Vibrations at each Step</b>	<b>69</b>
3.1	Concept of King Kong Effects . . . . .	70
3.1.1	Step Simulator . . . . .	71
3.1.2	Visual King Kong Effects . . . . .	73
3.1.3	Tactile King Kong Effects . . . . .	74
3.1.4	Conclusion . . . . .	76
3.2	Evaluations of the King Kong Effects . . . . .	76
3.2.1	Method . . . . .	76
3.2.1.1	Experimental Apparatus . . . . .	76
3.2.1.2	Virtual Environment . . . . .	76
3.2.1.3	Collected Data . . . . .	77
3.2.2	Experiment 1: Selecting the Best Visual Vibration Pattern for KKE . . . . .	77
3.2.2.1	Population . . . . .	77
3.2.2.2	Experimental Conditions . . . . .	77
3.2.2.3	Results . . . . .	78
3.2.2.4	Conclusion . . . . .	78
3.2.3	Experiment 2: Testing the Combination of Visual KKE and Oscillating Camera Motions . . . . .	79
3.2.3.1	Population . . . . .	79
3.2.3.2	Experimental Conditions . . . . .	79
3.2.3.3	Results . . . . .	79
3.2.3.4	Conclusion . . . . .	80
3.2.4	Experiment 3: Selecting the Best Tactile Vibration Pattern for KKE . . . . .	81
3.2.4.1	Population . . . . .	81
3.2.4.2	Experimental Conditions . . . . .	81
3.2.4.3	Results . . . . .	81
3.2.4.4	Conclusion . . . . .	82
3.2.5	Experiment 4: Testing Participant Preference for Multimodal KKE . . . . .	82
3.2.5.1	Population . . . . .	83
3.2.5.2	Experimental Conditions . . . . .	83
3.2.5.3	Collected Data . . . . .	83
3.2.5.4	Results . . . . .	83
3.2.5.5	Conclusion . . . . .	84
3.3	Discussion . . . . .	84
3.4	Conclusion . . . . .	85
<b>4</b>	<b>Personified and Multi-States Camera Motions for First-Person Navigation in Virtual Reality</b>	<b>87</b>
4.1	Multi-States and Personified Camera Motions . . . . .	88
4.1.1	Approach . . . . .	89
4.1.2	Existing Models of Camera Motions . . . . .	89
4.1.3	Our Novel Model of Camera Motions . . . . .	90
4.1.4	Personified Camera Motions . . . . .	90

4.1.4.1	Influence of the Physical Condition of the Virtual Human . . .	91
4.1.4.2	Influence of the Physical Properties of the Virtual Human . . .	91
4.1.4.3	Energy Expenditure Estimation . . . . .	92
4.1.5	Multi-states Camera Motions . . . . .	93
4.1.5.1	Oscillations Amplitude . . . . .	93
4.1.5.2	Vibrations . . . . .	94
4.1.5.3	Locomotion Modes . . . . .	94
4.1.6	Advance Speed of Camera Motions . . . . .	95
4.1.6.1	Advance Speed . . . . .	95
4.1.6.2	Oscillations Phase and Frequency . . . . .	95
4.1.6.3	Slope-Dependant Camera Motions . . . . .	96
4.1.6.4	Speed Computation . . . . .	96
4.1.7	Results and Performance . . . . .	97
4.1.7.1	Benchmark . . . . .	97
4.1.7.2	Influence of Slope . . . . .	97
4.1.7.3	Influence of Virtual Human Morphology . . . . .	98
4.1.7.4	Influence of Virtual Human Fatigue . . . . .	99
4.1.8	Conclusion . . . . .	99
4.2	Perceptual Evaluation of Personified and Multi-States Camera Motions . . . .	101
4.2.1	Method . . . . .	101
4.2.1.1	Population . . . . .	101
4.2.1.2	Virtual Environment . . . . .	102
4.2.1.3	Experimental Apparatus . . . . .	102
4.2.1.4	Collected Data . . . . .	102
4.2.2	Experiment 1: Detection of the Locomotion Modes . . . . .	102
4.2.2.1	Experimental Conditions . . . . .	103
4.2.2.2	Results . . . . .	103
4.2.3	Experiment 2: Detection of the Transitions Between Locomotion Modes . . . .	103
4.2.3.1	Experimental Conditions . . . . .	103
4.2.3.2	Results . . . . .	104
4.2.4	Experiment 3: Perception of the Virtual Human Properties . . . . .	104
4.2.4.1	Experimental Conditions . . . . .	104
4.2.4.2	Results . . . . .	105
4.2.5	Experiment 4: Influence of VR on the Detection of the Locomotion Modes . . . .	105
4.2.5.1	Experimental Conditions . . . . .	105
4.2.5.2	Results . . . . .	106
4.2.6	Discussion . . . . .	106
4.2.7	Conclusion . . . . .	108
4.3	Influence of Camera Motions on Perception of Traveled Distances in Virtual Environments . . . . .	108
4.3.1	Method . . . . .	109
4.3.1.1	Participants . . . . .	109
4.3.1.2	Set-up . . . . .	109
4.3.1.3	Distracting task . . . . .	110
4.3.1.4	Interaction . . . . .	110
4.3.1.5	Experimental plan . . . . .	110
4.3.2	Collected Data . . . . .	111
4.3.3	Results . . . . .	111
4.3.3.1	Signed Distance Errors . . . . .	111

4.3.3.2	Absolute Distance Errors . . . . .	112
4.3.3.3	Questionnaire . . . . .	113
4.3.4	Discussion . . . . .	113
4.3.5	Conclusion . . . . .	115
4.4	Conclusion . . . . .	115
<b>Conclusion</b>		<b>117</b>
<b>A Appendix: Résumé Long en Français</b>		<b>123</b>
A.1	Approche . . . . .	125
A.2	Contributions . . . . .	126
A.2.1	Le Shake-Your-Head . . . . .	126
A.2.2	Les King Kong Effects . . . . .	127
A.2.3	Mouvements de Caméra Personnifiés et Multi-États . . . . .	128
A.3	Perspectives et Prochain Travaux . . . . .	129
A.3.1	Prochain Travaux . . . . .	129
A.3.1.1	Le Shake-Your-Head . . . . .	129
A.3.1.2	Les King Kong Effects . . . . .	129
A.3.1.3	Mouvements de Caméra Personnifiés et Multi-États . . . . .	130
A.3.2	Perspectives . . . . .	130
A.3.2.1	Vers des Navigations Multimodales à Bas Coût en EV . . . . .	130
A.3.2.2	Vers des Navigations Biomécaniquement Réalistes en EV . . . . .	131
<b>Author's Publications</b>		<b>133</b>
<b>Bibliography</b>		<b>135</b>

# List of Figures

1	Interaction loop for navigation in Virtual Reality. . . . .	9
2	Objectives . . . . .	11
1.1	Time spent on each limb during a gait cycle. . . . .	18
1.2	Main events of the human gait cycle. . . . .	19
1.3	Phases of the VGRF during one running step. . . . .	21
1.4	Different VGRF profiles depending on the locomotion state. . . . .	21
1.5	Demonstration of the Bottom-up (a) and Top-down (b) strategies. . . . .	24
1.6	Visual attention model by Itti et al. . . . .	25
1.7	Examples of shoes-based devices. . . . .	27
1.8	Examples of foot platforms devices. . . . .	28
1.9	Examples of unidirectional treadmills. . . . .	29
1.10	The Torus Treadmill. . . . .	29
1.11	The Cyberwalk treadmill. . . . .	30
1.12	The CirculaFloor prototype. . . . .	30
1.13	Two examples of sphere devices: the CyberSphere and the Virtusphere. . . . .	31
1.14	The Step WIM technique. . . . .	32
1.15	The Gaiter interface. . . . .	33
1.16	The Gait-Understanding-Driven Walking-In-Place. . . . .	34
1.17	The Magic Barrier Tape. . . . .	36
1.18	Example of path obtained with Redirected Walking. . . . .	36
1.19	Example of path obtained with Motion Compression. . . . .	37
1.20	Motion compression. . . . .	38
1.21	Impossible Spaces. . . . .	38
1.22	Shoe-based device for vibrotactile feedback. . . . .	39
1.23	The ALive Floor. . . . .	40
1.24	The EcoTile. . . . .	40
1.25	Oscillation of the eyes during the walk. . . . .	41
1.26	Compensation of the gaze orientation during the walk. . . . .	42
1.27	Example of depth-of-field blur effect. . . . .	42
1.28	The Height, orientation and speed can be used to simulate slopes in the VE. . . . .	43
1.29	The GVS System. . . . .	43
1.30	The footstep sounds are used to estimate the GRF. . . . .	45
1.31	The sound produced is substituted with a sound generated. . . . .	45
1.32	Multimodal simulation of walking on snow and ice. . . . .	46
1.33	Multimodal simulation of walking in water. . . . .	47
2.1	Slalom navigation in a Virtual Environment with the Shake-Your-Head technique. . . . .	50
2.2	Overview of the Shake-Your-Head. . . . .	51
2.3	Extracted head motions. . . . .	52
2.4	Walking state automaton. . . . .	54

2.5	Virtual environment.	58
2.6	Description of the experimental setup.	58
2.7	Task completion time.	61
2.8	Results of the subjective questionnaires.	62
2.9	Accumulated trajectories for the first path.	64
2.10	Samples of the mean trajectories of SYH and joystick.	65
2.11	Curvatures of trajectories.	66
3.1	Concept of the King Kong Effects.	70
3.2	Architecture of the KKE.	71
3.3	Walking cycle.	72
3.4	Vibration patterns for the Visual KKE.	74
3.5	Vibrotactile tiles.	74
3.6	Vibration patterns for the tactile KKE.	75
3.7	Experimental apparatus.	77
3.8	Results of the questionnaires for the first experiment.	79
3.9	Results of the questionnaires for the second experiment.	80
3.10	Results of the questionnaires for the third experiment.	82
3.11	Museum scene of the 5th experiment.	83
3.12	Results of the questionnaires for the fourth experiment.	84
4.1	Vibrations of the camera at each step.	90
4.2	State Automaton.	95
4.3	Benchmark of the locomotion simulator.	98
4.4	Influence of the slope and virtual human fitness and fatigue.	100
4.5	Example of vertical oscillations.	101
4.6	Virtual Environment.	102
4.7	Detection rates for the three locomotion modes.	103
4.8	Detection rates for the virtual human properties.	107
4.9	Experimental setup.	109
4.10	Visual display with random lifetime dots.	110
4.11	Distances reproduced by the participants.	112
4.12	Absolute distance errors.	113
4.13	Subjective evaluation of camera motions.	114
4.14	Novel architecture of interaction loop.	121
A.1	Boucle d'interaction pour la navigation en Réalité Virtuelle.	123
A.2	Objectifs	125
A.3	Implémentation du SYH.	127
A.4	Concept des KKE	128
A.5	Nouvelle architecture de boucle d'interaction.	131



# List of Tables

1.1	Comparison of different biomechanical models for the human locomotion. . . .	23
1.2	Overview of existing Walking-In-Place techniques. . . . .	35
2.1	Results of the ANOVA on the curvature criteria. . . . .	66
4.1	Parameters of the vibration model. . . . .	90
4.2	Amplitude factors depending on virtual human fitness. . . . .	91
4.3	Amplitude factors of oscillating CM depending on the locomotion mode. . . . .	94
4.4	Maximal advance speeds for the different locomotion modes. . . . .	95
4.5	Mean and standard deviation of the percentages of correct answers. . . . .	104
4.6	Mean and standard deviation depending on the speed factor. . . . .	106

# Introduction

MANY Virtual Reality (VR) applications rely on navigation tasks and must allow users to walk and navigate freely in the Virtual Environment (VE). Navigation is often essential for training applications. For example, the SNCF (French railway company) developed a training simulation for railroad engineers who have to walk along the railways to perform several maintenance operations [David 01]. Moreover, architectural reviews of buildings [Fuchs 01] or virtual visits of museums [Miller 92] also require the possibility for the user to navigate easily and efficiently in the VE.

Navigating in a large VE can be a very exciting experience. As an example, first-person video games often feature large and rich environments to explore. For example, in the video game “The Elder Scrolls V: Skyrim” an island of more than 35 km<sup>2</sup> can be freely explored by the player. As a result users can spend countless hours exploring and discovering various landscapes while achieving the different missions of the game.

Navigation within VE can be described as an interaction loop [Bowman 05] (Figure 1). The user manipulates interaction devices (1) which generate inputs for the VR system. Then, the interactions techniques (2) convert the user inputs into instructions and commands that can modify the content of the VE (3). In return, sensory feedback techniques (4) compute the various sensory rendering of the VE and its modifications. Finally, the sensory feedbacks are displayed to the user using different kinds of devices (visual interfaces such as CAVE or HMD, haptic interfaces, etc) (5), allowing the user to finally perceive changes occurring in the VE and, notably his/her navigation.

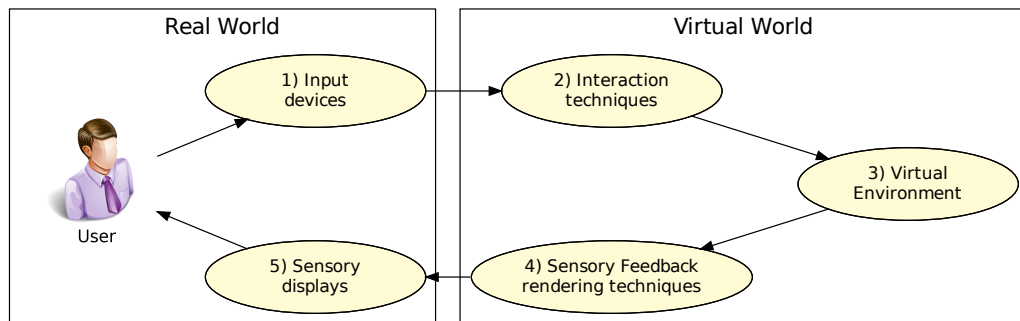


**Figure 1** – Interaction loop for navigation in Virtual Reality.

Numerous interaction devices (1) have been proposed for navigation in VR [Bowman 05]. Up to now, the possible locomotion devices range from simple keyboard/joystick [Stanney 02] to complex mechanical devices. One classical solution consisting in tracking the 3D motions of the user and use them as inputs for the simulation. For example, the Walking-In-Place (WIP) [Slater 95] is based on this approach. This technique tracks the motions of the user when “walking in place” to control the navigation in the VE. Other complex mechanical

devices, such as treadmills [Iwata 99a] or foot platforms [Iwata 01] can also be used. These devices are designed to track and control the motions of the user. As such, they also often provide some sensory feedback (5).

The interaction techniques (2) translate the inputs of the user into commands to interact with the VE. In particular, interaction techniques can be used to compensate some of the limitations of the interaction device. For instance, the user can be confronted to situations where the VE is larger than the physical workspace. Therefore, the navigation techniques must find a way to maintain the user position into the range of the available workspace. For example, the Redirected Walking [Steinicke 08a] can use visual feedback to fool the user and make him/her walk in curved lines in the real world when walking in straight line in the VE. If the workspace is large enough, the user will walk in circles and therefore never notice the limits of the workspace.

However, the existing interaction devices/techniques still suffer some limitations. Interaction techniques must achieve many concurrent goals. Indeed, interaction techniques and devices must often be efficient, ecological<sup>1</sup>, solve the problem of the limited workspace and not have a prohibitive cost. For example, the Redirected Walking technique [Steinicke 08a] seems efficient and ecological but requires a large workspace. Therefore, an interaction technique that would achieve all these goals at the same time still remains an open research question.

Concerning the sensory feedbacks (4 and 5), the users should perceive the VE through different modalities and multiple sensory feedbacks. Indeed, during the walk, humans can perceive their motions through visual, auditory, vestibular and proprioceptive senses [Harris 99]. For example, the material composing the virtual ground can be displayed using different modalities. Snow, gravel, sand or concrete can be rendered using the auditory modality [Nordahl 10] with sound synthesis methods. These materials can also be rendered with the vibrotactile modality [Visell 08] using small actuators placed on the user's shoes or under the floor. The Camera Motions (CM) [Lécuyer 06] can also be used for the visual modality. The CM were introduced to simulate the visual flow corresponding to the motions of the head during the walk. The virtual camera oscillates along the three axes and reproduces the head movements. Interestingly enough, this technique was found to increase the sensation of walking, as well as the immersion in the VE [Lécuyer 06].

The existing sensory feedback devices/techniques also suffer from limitations. Many techniques are often based on only one modality. The range of sensory feedbacks provided decreases, and the sense of immersion in the VE is often limited or impaired. On the other hand, each technique simulates only one precise type of feedback. Therefore, many techniques are required to provide a global sensory simulation. Thus, new sensory feedback are required to improve the immersion and the sensations of the users during navigation in VE.

Therefore, new navigation techniques seem necessary to achieve efficient and ecological navigations in VR applications while remaining affordable. Moreover, new sensory feedback techniques are necessary to improve immersion, using new modalities or multimodal approaches.

---

<sup>1</sup>Ecological interactions are defined by Gibson's ecological theory of visual perception [Gibson 86]: the affordances, i.e. the correlation between perception and action, eliminates the need to distinguish between real and virtual worlds because valid perception is one that makes successful action in the environment possible [Gibson 86].

## Approach

The remainder of this dissertation will study and design new interaction techniques and new sensory feedback to improve navigation in VR. In particular, we propose to study the natural human walking as a mode of interaction to design navigation techniques as ecological as possible. Indeed, one of our objectives is to make the frontier between the real world and the virtual world fade as much as possible during the navigation. Ideally, the user should interact and navigate with the VE in the same way he can interact in the real world (Figure 2). Moreover, navigations based on the natural human walk would also free the user hands for other tasks.



**Figure 2** – Our objectives are to improve navigation in VR by increasing either navigation performance, ecological interaction, immersion and sensation of walking in VE. For example, the navigation should be as similar as possible as navigations in real world.

We first study the design of new interaction techniques with four main objectives in mind:

- **Compliance and extension of the real workspace:** The navigation technique should address the problem of the limits of the real workspace to allow navigations in large and potentially infinite VE.
- **Efficient navigation:** The navigation technique should for instance enable fast and precise navigations in the VE.
- **Ecological navigation:** The navigation technique should be as ecological as possible to allow seamless interaction with the VE.
- **Moderate cost:** The cost of the technique should avoid prohibitive costs to allow a large panel of possible applications.

Second, we study how to increase the range of sensory feedback to improve immersion and sensation of walking during the navigation in VE [Lécuyer 06]. Three different objectives are considered:

- Propose **novel effects** which reproduce existing sensory cues available in real worlds.

- Propose **novel metaphors** of sensory feedbacks to extend the range of information rendered to the users, sometimes with non-realistic but very evocative effects.
- Create **multimodal rendering** of the walk to improve the immersion in VE with multiple sensory modalities.

For each of our novel techniques, we have adopted a user-centered approach. In particular, in each case, we have conducted quantitative and qualitative experiments to evaluate their performances as well as users' preferences.

## Contributions

### 1 Novel Interaction Technique for Walking in VR

In [chapter 2](#) we propose a new navigation technique for controlling navigation in VR, called Shake-Your-Head (SYH). Our technique, based on the Walking-In-Place technique, requires actual motions of the user body and measures specifically the motions produced by the head when Walking-In-Place to control the navigation. The user can either be standing or sitting (such as in traditional video games or desktop VR configurations). The head movements are captured using a low-cost optical tracking composed of a standard webcam. The locomotion simulation proposes the computation of a virtual walking motion, as well as turning, jumping, and crawling possibilities. We conducted an experiment to evaluate the efficiency of our technique compared to keyboard and joystick. We measured the time required to complete a slalom trajectory, as well as the learning time of the technique. We also evaluated the subjective appreciation of the users on various criteria, such as immersion or sensation of walking. Finally, we propose an in-depth evaluation of the trajectories produced with SYH, compared to trajectories produced using a joystick.

### 2 Novel Sensory Feedback for Improving the Sensation of Walking in VR

In [chapter 3](#) we introduce a new sensory feedback technique called the “King Kong Effects” (KKE) for navigation in VR. The KKE simulates the contacts of the feet with the ground at each virtual step. Visual and tactile vibration patterns are used to enhance the sensation of walking in VE. The KKE are inspired from famous Hollywood movies such as “King Kong” or “Godzilla” where the walk of gigantic creatures is emphasized to make the spectators “feel” the steps of the incoming creature. Our effects are, in a way, reproducing the special effects demonstrated in these movies for desktop VR technologies in an interacting way. We conducted a set of experiments to identify the best parameters of our KKE and reach a better sensation of walking using the KKE. Finally, we evaluated the different components of the KKE in a multimodal context, i.e. with auditory, visual and tactile feedback.

Moreover, in [chapter 4](#) we propose a new approach for designing Camera Motions (CM) for first-person navigation in VR. Previous models of CM were limited to the simulation of the walk. Our CM are multi-states: they are adapted to the different locomotion modes of the human locomotion and can thus render: walk, run and sprint. Moreover, existing CM do not take into account the morphology and physiology of the virtual human. We propose new personified CM adapted to the virtual human. The visual feedback of CM is

different if the virtual human is heavier or is in a better physical condition for example. Moreover, contrary to existing CM, our CM are adapted to the slope of the VE. Finally, we demonstrated that the CM improve the immersion in VE, as well as the perception of distances for small distances. We conduct a set of experiments to evaluate if the different locomotion modes and the transitions are well perceived by the users and if the participants were able to correctly perceive the age, weight and fitness of the virtual human.

Finally, the last chapter provides conclusions and perspectives concerning the work presented in this manuscript.



# Related Work: 3D Navigation Techniques and Sensory Feedbacks for Walking in Virtual Reality

# 1

## Contents

<b>1.1 A brief Overview of the Properties of Human Walk</b>	<b>16</b>
1.1.1 Physical Description	16
1.1.2 Biomechanical Description	20
1.1.3 Neuroscience Description	23
1.1.4 Conclusion	26
<b>1.2 Locomotion Interfaces for Navigating in VE</b>	<b>26</b>
1.2.1 Pedaling Devices	27
1.2.2 Foot-based Devices	27
1.2.3 Recentering Devices	28
1.2.4 Conclusion	31
<b>1.3 3D Interaction Techniques for Navigating in VE</b>	<b>31</b>
1.3.1 3D Interaction Techniques for In-Place Use	32
1.3.2 3D Interaction Techniques Involving Real Physical Walking	34
1.3.3 Conclusion	38
<b>1.4 Sensory Feedback Techniques for Navigating in VE</b>	<b>39</b>
1.4.1 Haptic Feedback	39
1.4.2 Visual Feedback	41
1.4.3 Vestibular Feedback	43
1.4.4 Auditory Feedback	44
1.4.5 Multimodal Feedback	45
1.4.6 Conclusion	47
<b>1.5 Conclusion</b>	<b>47</b>

In this chapter, we propose a bibliographical study of the *3D Navigation Techniques and Sensory Feedbacks for Walking in Virtual Reality (VR)*. In order to improve the users' navigation in VE, numerous types of 3D user interfaces have been proposed. In particular, these techniques and devices are designed to address some important challenges. Indeed, interaction techniques and devices aim at **efficient** and **ecological** navigations, while maintaining the user in the **limits of the workspace** in the real world. Moreover, the **cost** of the technique can also be an issue in some contexts. Similarly, the sensory feedbacks try to improve the **immersion** and **sensations** during the navigation.



The natural human walk is one possible solution to the challenge of ecological navigation. Indeed, the walk is used in most navigations in the real world and therefore offers a natural and elegant solution to navigate in VE. Many navigation techniques and sensory feedbacks are therefore based on this approach.

However, the walk is a complex mode of locomotion that can be considered at different levels. First, at physical and anatomical level, the walk is a cyclic motion of the lower limbs involving different senses. Second, The biomechanical level focuses on the kinematics and dynamics of the motion to allow a better understanding of the subtleties of the human locomotion. Last, insight on the objectives and strategies used during the locomotion can be found at the neurological level. A good understanding of all those levels is necessary in order to understand and design techniques and devices for Virtual Reality based on the walking metaphor.

In this chapter, we propose a survey of these techniques. In particular, we propose to study the locomotion devices developed for walking in VR, as well as the navigation techniques based on the walk paradigm. Finally, we present the existing sensory feedback designed to improve the immersion and sensation of walking in the VE. However, we propose first to briefly consider different properties of the walk that could have an impact on the studied techniques.

## 1.1 A brief Overview of the Properties of Human Walk

The walk is a natural navigation paradigm for human beings. It is learned early during a child development and becomes completely natural. This specificity makes it a good paradigm to navigate in the VE. However, the human walk is a very complex phenomenon. We propose to separate it in three distinct aspects: physical, neurological and biomechanical.

### 1.1.1 Physical Description

One way to describe the process of walking is to look at it as a physical and mechanical phenomenon, which can be measured and quantified.

#### 1.1.1.1 Senses Used During the Walk

The senses used during the walk are important physiological aspects. Indeed, during the walk, our body receives plenty of information from various receptors. Therefore, we present a very succinct description of the senses used during the walk.

**Proprioceptive Sense.** First of all, the proprioceptive information an important feedback to control any motion. Indeed, the proprioception is the awareness of movement derived from muscular, tendon and articular sources, as defined by Charles Scott Sherrington in 1906. To plan a motion and coordinate the different parts of the body, it is necessary to be aware, even unconsciously, of the position and kinematic of the different limbs involved [Berthoz 97]. For example, during the walk, the legs should not bump into each

other, or into any obstacle to avoid any unexpected fall. The proprioceptive information is transmitted by various receptors located in various places in the different limbs [Berthoz 97, Olivier 08]. The stretch receptors in the muscles provide information about the deformation of the various muscles. The Golgi tendon organ placed in the tendons measure the forces applied to the joints. Finally, the Ruffini corpuscles placed in the deep layers of the skin near the joints register the deformation within joints.

**Tactile Sense.** In the same idea, the perception of contacts between the foot and the ground plays also an important role, especially since the sole of the foot is one of most innervated part of the body [Berthoz 97]. The tactile sense is provided by multiple sensory receptors, like the Pacinian corpuscles and Meissner's corpuscles [Berthoz 97] which measure rapid changes of pressure applied to the skin. The Pacinian corpuscles have an optimal sensitivity at 250 Hz, when the Meissner's corpuscles have a lower threshold (50 Hz) and thus allow a better sensitivity to slight contacts. The skin also has a lot of other receptors, like the thermoreceptors for the perception of the temperature, the nociceptors for pain or other receptors associated to the hairs which allow us to perceive rubbing and caresses.

**Vestibular Sense.** The vestibular system is the sense that provides information about the global movement and orientation of the head. This sense is primarily used to maintain our balance and our sense of spatial orientation. The vestibular system is situated in the vestibulum in the inner ear and is a part of the auditory system. This system is separated in two different organs with specific functions: the semicircular canal system allows us to perceive rotational movements, and the otoliths allow the linear accelerations [Berthoz 97, Olivier 08]. Combined together, those organs detect both rotations and translations. The vestibular system is composed of three semicircular canals in each ear disposed orthogonally on the three main euclidean planes [Berthoz 97]. The semicircular canals are composed of a fluid, which movements push the hair cells of the cupula, resulting in an electrical signal. On the same idea, the otoliths are composed of the otoconia crystals immersed in a viscous gel layer. The vestibular system is composed of two otoliths in each ear called utricle and saccule. One interesting consequence of the way otoliths are designed is that they not only allow to perceive linear acceleration, but because of the constant acceleration of the gravity they also provide information regarding the inclination of the head in Earth referential.

**Visual Sense.** Finally, the last used during the walk is the visual sense. Not only this sense is necessary to perceive the environment and plan the trajectory of the body, but it also plays an important role in equilibrium and perception of the motion [Berthoz 97]. The visual system is composed of the eyes, the optic nerve and the visual cortex of the brain. The eyes are the entry points of the visual system. They are composed of a lens that projects the light on the retina on their back [Breedlove 07]. The retina is composed of two different kinds of photo-receptor: the rod and cone cells [Breedlove 07]. The cone cells are used for the day vision, while the rod cells have a lower threshold, but cannot perceive the colors. The cone cells are concentrated on the fovea, the pit in the retina which allows for maximum acuity of vision, but only for an angle of 2 degrees. The rod cells are placed around the fovea, and their density progressively decreases as the distance to the fovea increases. As a consequence, the human eye allows a very sharp perception

on a very small part of the field of view, but they allow a good perception of the motions on the rest of the field of view, even in the dark.

An interesting point is the existing link between the visual system and the vestibular system at a neural level. A good example of this link is the vestibulo-ocular reflex [Berthoz 97], which stabilizes images on the retina during head movement by producing an eye movement in the direction opposite to head movement, thus preserving the image on the center of the visual field. However, this reflex is also affected by visual tracking mechanisms [Gauthier 90]. Another example of this link is the illusion ofvection: in some circumstances, humans can have the illusion of moving even without actually moving for real. A classic illustration of this phenomenon can be experienced on a train: before the departure, when another train on the other side of the gate leaves it can give the strong impression of actually moving. This phenomenon is a good illustration of the importance of the visual system in the perception of self-motions [Berthoz 97].

### 1.1.1.2 Description of the Lower Limbs

Another approach to study the walk is to consider the kinematics and dynamics of the body, and more specifically the lower limbs, during one or more steps. According to Terminologia Anatomica [FCAT 98], the lower limb of the human body is composed of, from top to bottom: the pelvic girdle, the buttocks, the hip, the thigh, the knee, the leg, the ankle and finally the foot. The major (long) bones of the human leg are the femur, tibia, and fibula. The patella is the bone in front of the knee. In the normal case, the large joints of the lower limb are aligned on a straight line which represents the mechanical longitudinal axis of the leg, the Mikulicz line. This line stretches from the hip joint, through the knee joint, and down to the center of the ankle.

### 1.1.1.3 Walking Cycle

The walk can be viewed as a good approximation of a periodic event [Boulic 90]. Indeed each step follows a given pattern, which is reproduced over the time. Moreover, the left and right foots follow the same pattern, with a phase shift of half of the step period. Thus, the stride is also a periodic event. As a consequence, the studies are usually based on the description of one step or stride. The step cycle can be divided in two main phases: the stance phase where the foot is on the ground, and the swing phase where the leg is swinging in the air in preparation of the next foot strike [Vaughan 92, Multon 98]. At the beginning of the stance phase, both foot are in contact with the ground. The other leg will then start swinging and only one foot stay in contact with the ground. Finally the other foot will reach the ground again and a double support is achieved again. The stance phase represents about 62% of the total cycle, and the swing phase 38%. Integrating the symmetry between both legs, we can summarize the average gait cycle over the time with the Figure 1.1.

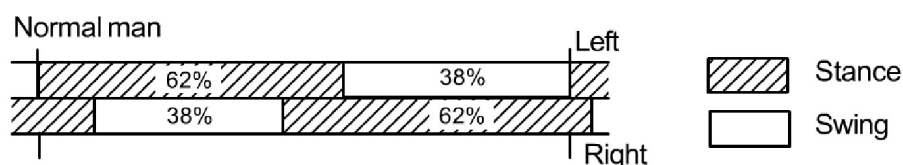


Figure 1.1 – Time spent on each limb during a gait cycle. [Vaughan 92]

However, the gait cycle can be described even more precisely. The stance and swing phases can be subdivided in five and three distinct events respectively (Figure 1.2). Those events, based on the movement of the foot, are as follows [Cochran 82, Vaughan 92]:

■ Stance phase events:

1. Heel strike initiates the gait cycle and represents the point at which the body's center of gravity is at its lowest position.
2. Foot-flat is the time when the plantar surface of the foot touches the ground.
3. Midstance occurs when the swinging (contralateral) foot passes the stance foot and the body's center of gravity is at its highest position.
4. Heel-off occurs as the heel loses contact with the ground and pushoff is initiated via the triceps surae muscles, which plantar flex the ankle.
5. Toe-off terminates the stance phase as the foot leaves the ground.

■ Swing phase events:

1. Acceleration begins as soon as the foot leaves the ground and the subject activates the hip flexor muscles to accelerate the leg forward.
2. Midswing occurs when the foot passes directly beneath the body, coincidental with midstance for the other foot.
3. Deceleration describes the action of the muscles as they slow the leg and stabilize the foot in preparation for the next heel strike.

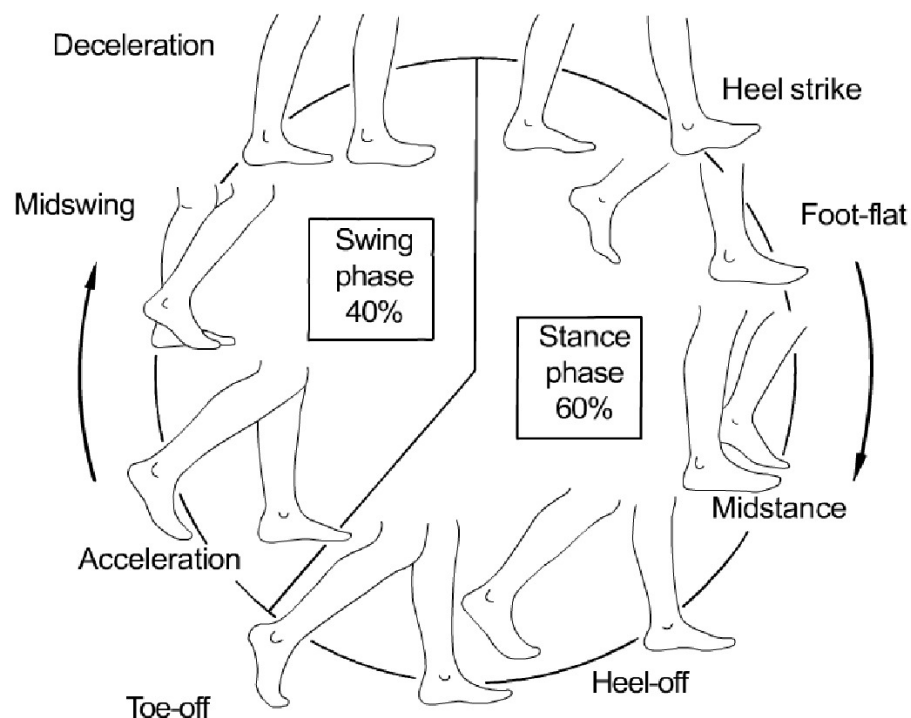


Figure 1.2 – Main events of the human gait cycle. [Vaughan 92]

### 1.1.2 Biomechanical Description

Another approach of the problem consists in analyzing the internal processes of kinematic, dynamic, transfer of energy, work and metabolic costs involved during the motion of the limbs.

#### 1.1.2.1 Biomechanics of Walking

The walk can also be described from a biomechanical point of view. Indeed, human walk follows some common mechanical laws and thus can be represented by simple approximate models.

**Step Length.** The most basic example is the relation between step length and frequency. Indeed, the speed is defined by  $v = L * f$ , with  $L$  the stride length and  $f$  the stride frequency [Alexander 03]. Moreover, the step length, i.e. the distance traveled while a particular foot remains on the ground, is defined by  $l = \alpha * L$ , where  $\alpha$  is the fraction of the time for which a foot remains on the ground. If  $\alpha$  is greater than 0.5, at some point both feet are simultaneously on the ground and the motion is defined as walking. Otherwise, running motions are defined when  $\alpha < 0.5$ .

**Speed of Comfort.** Other relations have also been found, for example, to determine the step length from the speed. Grieve [Grieve 68] showed empirically that the approximate relation  $l \sim v^\beta$  is verified when people walk at comfort speed, thus minimizing the involved energies. The value of  $\beta$  is around 0.42 for adults.

#### 1.1.2.2 Differences Between the Locomotion States

The human locomotion is not limited to the walk. Indeed, the human locomotions can also be composed of running and sprinting periods. Each state has different properties, that can be studied through their biomechanical description. The differences between the states of locomotion include the types of events produced during the locomotion, as well as the type of forces applied to the ground at each step or the energy consumed during the locomotion.

**Events.** The walk can also be described by the succession of events produced during the cycle. The moments of contact and separation of the different parts of the feet with the ground are specific to the type of locomotion [Novacheck 98]. For example, the events of the heel and toes can be used to describe the type of locomotion. Indeed, the difference between walking and running is defined by the fact that during walking motions both feet can be simultaneously on contact with the ground, while running motions are characterized by moments where both feet are off the ground [Novacheck 98]. Therefore, during the walk, the time between the heel strike and toe-off events is superior to the half gait cycle duration. On the contrary, the time between those two events is inferior to the half gait cycle duration for the run. Moreover, the sprinting motions can also be characterized by

the generated events of the locomotion. Indeed, the sprint can be defined by a type of running where the heel stops touching the ground at each step [Novacheck 98]. Therefore, the sprinting locomotion produces only events for the toes.

**Ground Reaction Forces.** The locomotion can also be defined by the vertical ground reaction forces (VGRF) at each step. Indeed, the profile of the force applied on the ground is very specific and depends on the gait and type of locomotion [Novacheck 98, Tongen 10]. Indeed, the contact of the feet with the ground can be decomposed into two phases: (1) a phase of absorption of the energy produced by the previous step and (2) a phase a generation for the next step [Novacheck 98] (Figure 1.3).

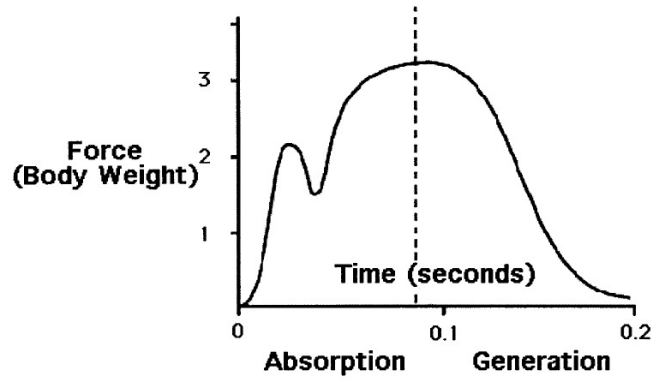


**Figure 1.3** – Phases of the VGRF during one running step [Novacheck 98].

Moreover, the profile of the VGRF depends on the type of locomotion [Tongen 10]. Indeed, the VGRF corresponding to the walk is relatively constant, except for two small peaks corresponding to the absorption and generation phases. However, as the speed increase, the VGRF becomes less and less symmetric. Indeed, the absorption phase gradually fades and the generation peak become preminent: all the energy is used for the motion and the energy losses decrease (Figure 1.4).

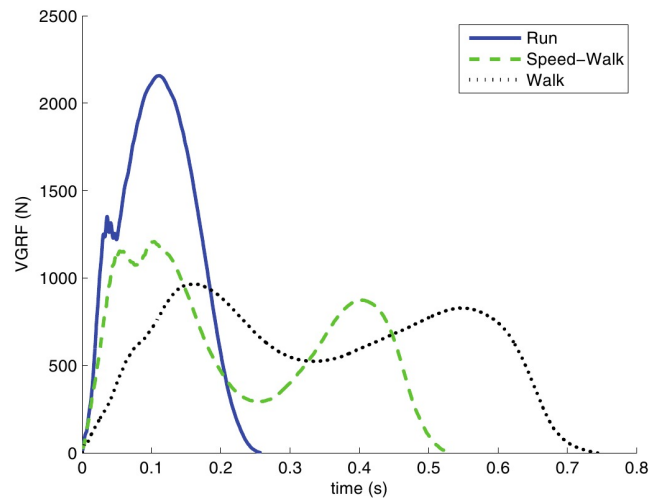


**Figure 1.4** – Different VGRF profiles depending on the locomotion state [Tongen 10].

**Energy Consumption.** The energy consumed during the locomotion is also an important factor. Some types of locomotion like running and especially sprinting require more energy than the walk [Wilmore 94], and different methods exist to measure the energy used by a given motion. One method consists in measuring the volume of oxygen  $VO_2$  consumed during the effort [Wilmore 94]. Indeed, the oxygen is consumed to produce the energy for the motion, therefore the metabolic energy is correlated to  $VO_2$ . The oxygen consumption is measured by analyzing the gas exchanges during each breath. The analysis can be done using portable devices and provide an estimation of the energy spent. Moreover, the estimation of the maximal oxygen consumption  $VO_{2max}$  is an important factor to determine the maximal effort that can be produced by a given athlete. Finally, an approximative linear relationship exists between the advance speed and the  $VO_2$  for the walking, running and sprinting locomotions. Another method to estimate the metabolic cost of a motion is to measure the athlete pulse [Wilmore 94]. Indeed, the heart beat frequency is correlated to the metabolic cost of the motion. However, this method is not as accurate as the measure of the oxygen consumption. Finally, a direct measure of the lactate concentration in the blood stream is another very precise measure [Wilmore 94]. However, this method can not be used to monitor the evolution of the effort during the motions. Indeed, this method is limited to instantaneous measures.

Depending on the intensity of the effort, the time to exhaustion and the recuperation time are also impacted. Indeed, depending on the speed of a run, the time to exhaustion of the athletes will change [Blondel 01]. Moreover, the recuperation time after the motions is also an important factor that depends on the kind of motions performed. Indeed, the length and intensity of the motions influence the recuperation time. One possibility to measure the recuperation time is to monitor the Excess Post-Exercise Oxygen Consumption (EPOC) [Gore 90]. The difference between oxygen consumption at rest and after the effort can be used to determine the metabolic state of the athlete and therefore the time needed for the recuperation [Firstbeat 05].

### 1.1.2.3 Biomechanical Models

Different models have been proposed to simulate the human locomotion based on biomechanical knowledge. They are usually based on a set of mechanical and physics equations that describe the motions of the limbs during the walk. For example, biomechanical models can predict the gait of young and old adults [Dean 07] and provide interesting insights of the origin of the differences in the observed gait. On the same idea, experiments have shown that, for a given speed, humans will instinctively adjust their step length and frequency to minimize the metabolic cost induced by the limb motions [Donelan 01]. Using models to compute and minimize this cost, it is then possible to determine dynamically which step length and frequency are the best suited [Kuo 01]. This problem of minimization of the metabolic cost is a recurrent pattern, as it is generally the solution of the system of equations defined by a given model [Doke 05, Doke 07]. However, given the complexity of the phenomena involved, the models need to be opposed to experimental data to be validated [Park 04, Gordon 09]. Kinematics and dynamics of the different parts of the limb can be measured, but work and metabolic costs are more complex to evaluate. Moreover, the performances are specific to each model, depending the considered criterion [Gard 04, Fraysse 09]. The following non-exhaustive list describes briefly some of the existing models (Table 1.1).



References	Model	Description
[Alexander 76]	Heel Strike	One of the first to include some energetic features
[McGeer 90]	McGeer's	Passive dynamics alone, no force input
[Kuo 01]	Antropomorphic	Add hip torque & toe-off impulse to the McGeer's Model
[Kuo 05]	Postural Balance	Uses state feedback control to maintain human postural balance
[Kuo 07]	Dynamic Walking	Focuses on the use of works

**Table 1.1** – Comparison of different biomechanical models for the human locomotion.

### 1.1.3 Neuroscience Description

The walk can be observed from a neuroscience point of view. Indeed, past the physical description, the walk highly depends to various cerebral processes [Berthoz 97]. However, in this section we will focus on cognitive aspects only. Indeed, if low level cerebral processes are very important to understand the inner mechanisms of walk, they are less significant to model the navigation, contrary to high level cognitive aspects.

#### 1.1.3.1 Orientation Strategies Involved During the Walk

One example of the involved processes concerns the strategies used for controlling and planning the global motions.

**Path Integration.** Path integration is the method used for dead reckoning. Dead reckoning is the process of estimating one's current position based upon a previously determined position, or fix, and advancing that position based upon known or estimated speeds over elapsed time, and course. Understanding the inner processes involved during path integration is essential to simulate efficiently some navigation task in a given VE. For example, some experiments show that the visual flow alone can be enough for path integration [Riecke 02]. However, in that case some people will mistake the left and right directions [Riecke 07]. Those informations can be precious to explain the behavior of the users during navigation tasks.

**Wayfinding.** Wayfinding is also a phenomenon that should be taken into account. Wayfinding encompasses all the ways in which people and animals orient themselves in physical space and navigate from place to place. For example, naturally blind, blinded and blindfolded people will have the same poor results during some wayfinding task [Riecke 09], which suggest that wayfinding strongly depends and visual clues, and is independent from any form of learning through vestibular information. Another surprising result is that



people are faster and slightly more accurate for more complex paths when only optic flow is provided [Wiener 06]. Moreover, Peruch et al. [Péruch 95] found that active exploration of an environment helps to improve the performance of future wayfinding tasks compared to passive exploration. Finally, wayfinding interfere more with verbal and spatial tasks than with visual tasks [Meilinger 08]. With this information in mind, it is possible to avoid or limit any possible disruption in the navigation task.

### 1.1.3.2 Visual Attention Strategies

Orientation strategies are not the only high level cognitive aspects involved during the walk. Indeed, as specified by Berthoz [Berthoz 97], “I go where I’m looking”, and not “I look where I’m going”. Thus, the visual attention strategies must be understood. The visual strategies can be split in two categories based on parameters either:

- Independent of the virtual human, like the properties of the viewed images;
- Dependent on the virtual human, like the tasks that must be accomplished.

**Bottom-up.** The focus zone is influenced by the perceived image at a low cerebral level. Thus, for a given stimuli, the human eyes will be attracted by some primitives in the perceived image depending on their spatial properties. For example, in the Figure 1.5a, the human eye is automatically attracted by red “T” because of it’s color.

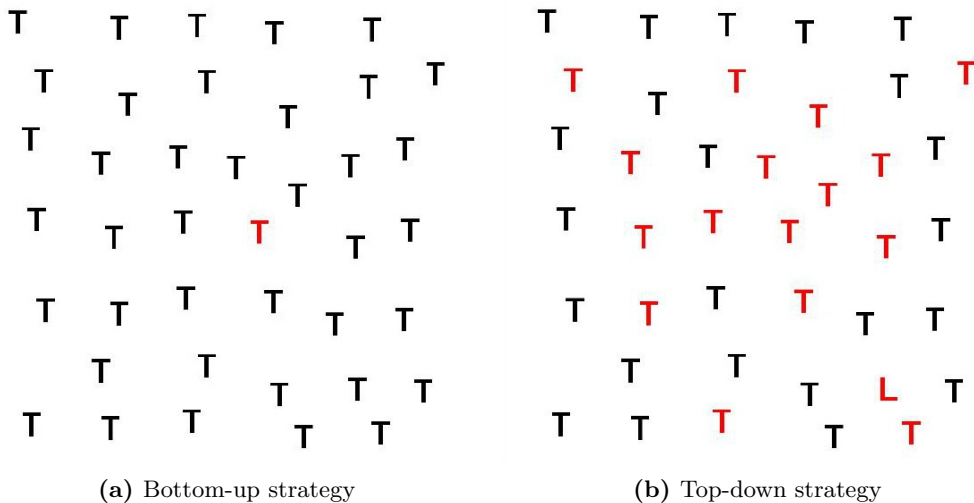


**Figure 1.5** – Demonstration of the Bottom-up (a) and Top-down (b) strategies.

The feature-integration model proposed by Treisman et al. [Treisman 80] is one of the theories designed to explain the bottom-up strategies. In this theory, part of the visual information is processed in a parallel and preattentive fashion. Thus, the human eyes are sensitive to a large panel of stimuli, such as color, shapes, intensity and motions. As a consequence, the properties of the different primitives of an image will make some parts more salient than others, thus more appealing for the eyes. This process can be modeled with the saliency map algorithm proposed by Itti et al. [Itti 98]. Basically, this algorithm (Figure 1.6) compute the saliency of each pixel of an image. It can be decomposed in the following main steps:

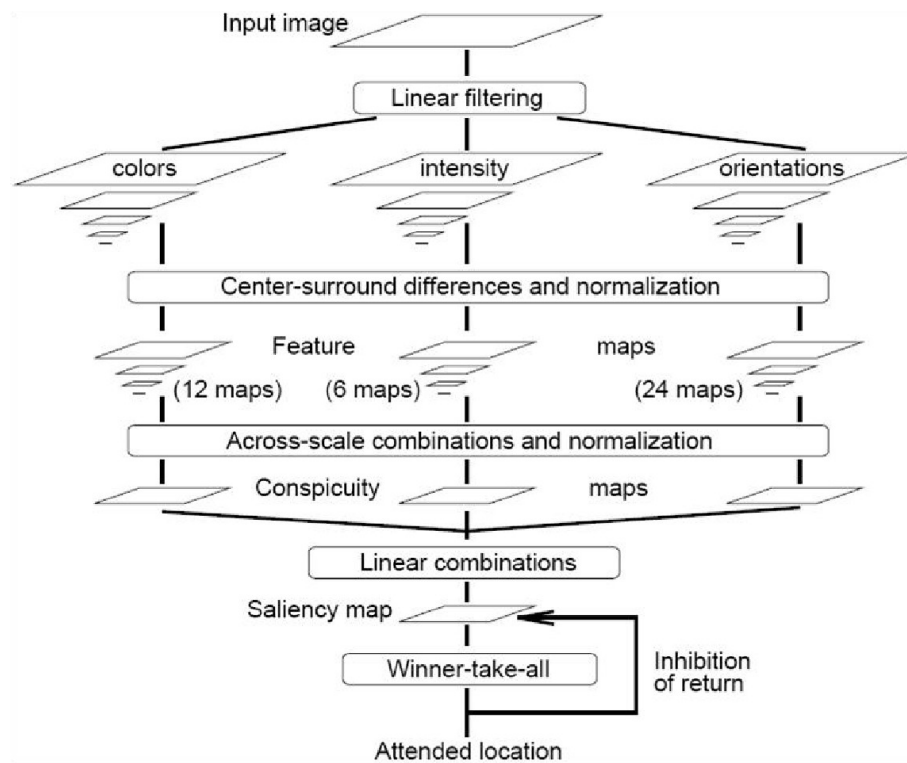


**Figure 1.6** – Visual attention model by Itti et al. [Itti 98]

- Compute the primitive information, such as color, intensity and orientation for each pixel. The resulting maps are then rescaled in a pyramid form to allow multi-resolution comparisons.
- Center-surround differences and normalization are applied to the maps to produce the feature maps.
- Cross-scale combination and normalization of the feature maps to produce the conspicuity maps.
- Linear combination of the conspicuity maps obtained for each primitives to produce the saliency map.
- The most salient point on the image is chosen as the focus point [Courty 02].
- The area of the focus point is inhibited for the next round of the algorithm, thus simulating the phenomenon of inhibition of return.

**Top-down.** The visual attention is not only controlled by reflex strategies. Indeed, the visual attention is also dependent on the task to accomplish. For example, on the [Figure 1.5b](#), the search strategy for the red “L” will be different from one person to another. Moreover, depending of the required task, the strategy used will change. This phenomenon demonstrates the existence of high level visual strategies combined to the low level ones. To model this behavior, the theory used is not based on space anymore, but is based on visual objects instead [Sun 03]. The strategies rely on the perceived objects, recognized by the brain, to work. However, because it is a high level cognitive process, behavioral parameters should be considered, such as absent mindedness, anticipation, self-confidence, etc [Courty 02]. Different methods have been proposed to simulate the top-down strate-

gies depending on the required tasks. For example, Bordeux et al. [Bordeux 99] proposed a complete pipeline to search some objects on the scene perceived by a virtual human through the use of a combination of filters applied to a database of the existing objects. This model also provides a simulation of the short term memory for the encountered objects. Another example is the model proposed by Kuffner et al. [Kuffner 99] which is designed for the navigation of virtual humans who have to avoid collisions with moving and static objects. The perceived objects are memorized with their properties, like their velocity or the observation date. The objects are then kept in memory for an amount time that depends on the importance of the object for the current task.

**Application to Walk.** Some visual attention strategies are specific to the walk. Indeed, visual attention tends to anticipate the curves during navigation [Olivier 08], and Hillaire et al. [Hillaire 09a] showed that this phenomenon is still respected when working in a Virtual Environment (VE). In particular, this property of the human gaze can be integrated as a parameter in the computation of the saliency maps for bottom-up strategies. Indeed, it can be implemented as a post-processing filter for the saliency map: the saliency of the pixels can be increased depending on the curve angle, thus making the primitives in the trajectory more likely to be focused on.

#### 1.1.4 Conclusion

The walk is a complex phenomenon that can be studied at different levels. First, at the physical and anatomical level, the walk is a cyclic motion involving the lower limbs, but also different senses. At the biomechanical level, the study of the kinematics and dynamics of the motion allows a better understanding of the subtleties of the human locomotion. Finally, the neurological level provides also important insight on the objectives and strategies used during the locomotion. Therefore, a good understanding of all those levels is necessary in order to design techniques and devices for Virtual Reality based on the walk metaphor.

## 1.2 Locomotion Interfaces for Navigating in VE

Many devices have been used as 3D user interfaces for navigation, going from the mouse/keyboard to Brain Computer Interfaces [Bowman 08]. Locomotion interfaces are a natural solution for navigation and walking in VE. Indeed, locomotion interfaces allow the user to interact directly with his/her body, providing not only sensory haptic feedback, but also transforming the body motions into commands for the VE. Usually, sensorimotor devices are used to move some part of the user's body, but they can also allow the user to move freely in the VE while physically maintaining him within a limited space in the real world for example. Locomotion interfaces for walking in VE can be decomposed into two main categories: devices which control the position of the user's feet, and devices which maintain the user in place by shifting the ground under his/her feet. Additionally, we will briefly present some pedaling devices which could be used to simulate the walk to some extent.

### 1.2.1 Pedaling Devices

The pedaling devices, like bicycles [Fuchs 01, Stanney 02], allow an easy and intuitive interaction with the VE. With these devices, the user provides linear motion data to the system by pedaling. Moreover, the system can provide some additional haptic feedback through pedaling resistance. The steer is used to provide the direction data. The Sarcos Uniport [Fuchs 01, Stanney 02] is characterized by the absence of steer. Instead, the seat rotates thanks to body pressure which provides the direction of the motion. In addition, it keeps the hands of the user free. Moreover, the user actually have to turn its/her body thus having a better vestibular perception of the virtual rotational motion. On the one hand, pedaling devices are intuitive and easy to use, but on the other hand they are not specifically designed to simulate the walk.

### 1.2.2 Foot-based Devices

A first approach to keep the user in a limited space is to control the trajectory of his feet. Although, this action, ideally, must not be perceived by the user.

#### 1.2.2.1 Shoe-based Devices

Shoes-based devices are basically systems built upon special shoes worn by the user. Those shoes are designed to slide on the ground when the rest of the system keeps the user stationary. Iwata et al. designed numerous of such interfaces, like the Virtual Perambulator [Iwata 99b] (Figure 1.7a) and the String Walker [Iwata 07] (Figure 1.7b). The Virtual Perambulator is composed of a pair of roller skates and a hoop around the user's waist. Thus, the user can slide in place with a motion close to walking. In contrast, the String Walker uses another approach: the user's foots are re-centered during the stance phase by strings attached to the shoes and pulled by actuators.

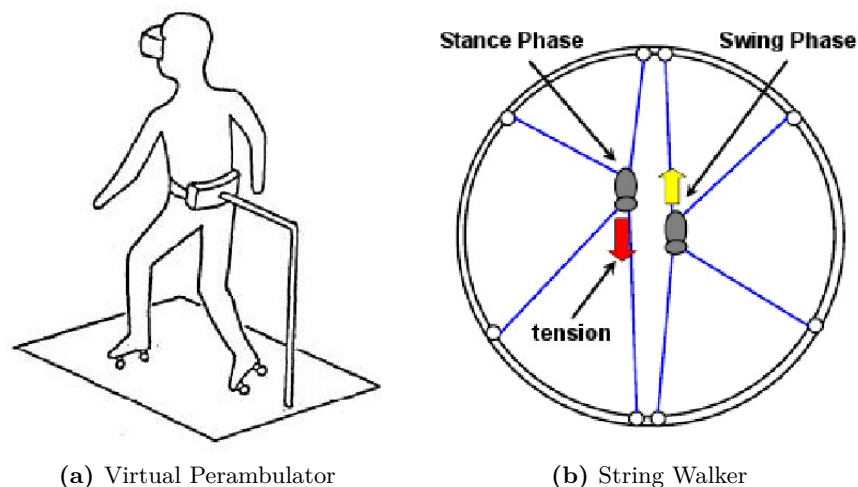


**Figure 1.7** – Examples of shoes-based devices.

### 1.2.2.2 Foot Platforms

Another type of sensorimotor interface, designed for locomotion, is based on platforms attached to the user's feet. The platforms can be moved in three dimensions. If the user moves his feet, the platforms follow their movements without any resistance. When the user's feet touch the virtual ground, the platforms are servoed to simulate a rigid surface. The platforms can be moved jointly in order to keep the user at the same position, even if he has the sensation to walk normally in the VE. The Gait Master (Figure 1.8a) [Yano 00, Iwata 01, Stanney 02] and the Sarcos Biport (Figure 1.8b) [Stanney 02] are good examples of foot platforms. These devices have respectively three and four Degrees of Freedom (DOF), even if the original specifications of the Gait Master present a 6 DOF device. Both devices can simulate either flat or uneven grounds, but due to mechanical constraints only moderate walking is possible.



**Figure 1.8** – Examples of foot platforms devices.

### 1.2.3 Recentering Devices

A different approach to keep the user in a limited space while walking relies on moving the ground under his/her feet during the walk.

#### 1.2.3.1 Treadmills

The treadmills are the most common sensorimotor interfaces used for navigation in VE. The most common treadmills are exercise machines that allow the user to run or walk while staying in place. Such kind of interfaces are composed of a moving belt which compensate the displacements of the user [Fuchs 01]. Usually, the treadmills are composed of a single



conveyor belt actuated linearly from the rear. Basically, such treadmills are similar to those used by athletes. However, treadmills used to walk in VE need to detect the user's speed in order to adapt dynamically the speed of the motors. For example, in the Sarcos Treadport (Figure 1.9a), a mechanical tether is attached to the user's back and provides the required information to the system [Fuchs 01, Stanney 02]. However, classical treadmills only allow the user to move on a flat ground. In order to walk on uneven grounds, more sophisticated have been proposed. For example, the ATLAS system (Figure 1.9b) is a classical treadmill installed on a platform that can pitch, yaw and roll [Yano 00, Stanney 02].

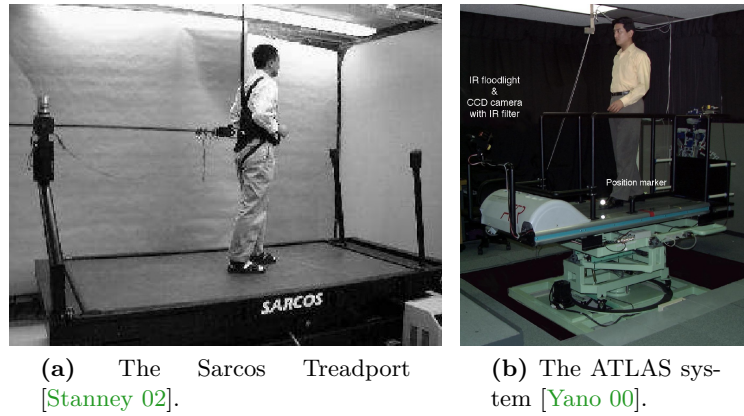


**Figure 1.9** – Examples of unidirectional treadmills.

Nevertheless, treadmills generally allow the user to move in only one direction. In order to solve this problem, Iwata proposed the Torus Treadmill [Iwata 99a, Iwata 99b, Iwata 99c, Fuchs 01, Stanney 02]. This system consists of 12 small treadmills, ten of them connected side-by-side and forming a bigger conveyor belt, while the others provides in the perpendicular direction (Figure 1.10). With this system, the user can walk in every directions on a plane surface. The Torus Treadmill is not the only 2D treadmill. For example, the Omni-Directional Treadmill (ODT) designed by Virtual Space Devices offers also a two-dimensional surface to walk in [Stanney 02]. Another approach for omni-directional treadmills consists in using small balls instead of conveyor belts. For example, the Cyberwalk (Figure 1.11) [Schwaiger 07] is based on this concept. However, contrary to other omni-directional treadmills, this device offer one linear and one rotational DOF, instead of two linear DOF.

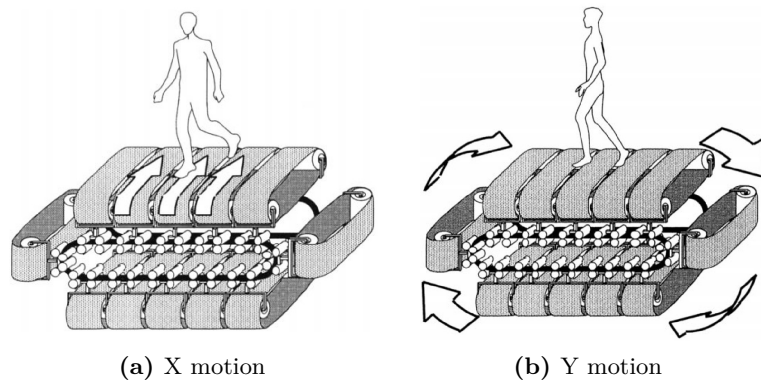


**Figure 1.10** – The Torus Treadmill: a torus composed of a group of belts [Iwata 99a].

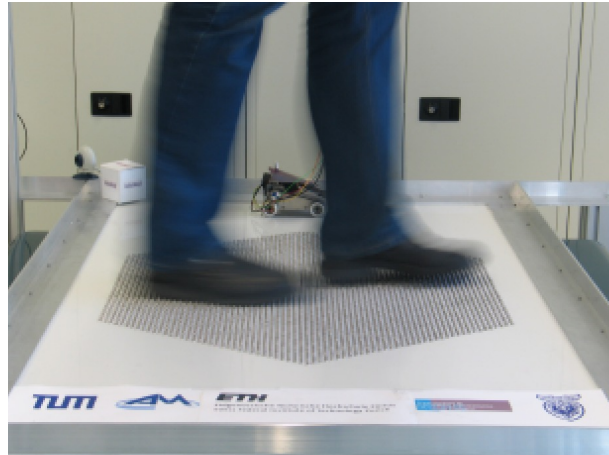


Figure 1.11 – The Cyberwalk treadmill [Schwaiger 07].

### 1.2.3.2 Tiles

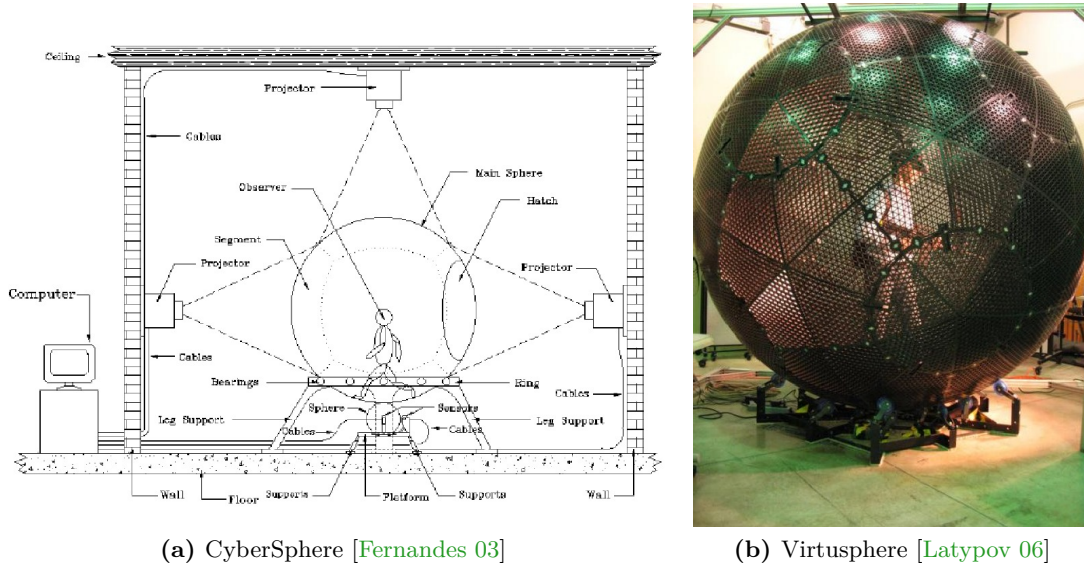
Another approach maintains the user in place with tiles moving freely on the ground. The CirculaFloor prototype [Iwata 05] is composed of tiles that coordinate themselves anticipating the trajectory of the user, placing themselves according to the user's feet (Figure 1.12). When the user has one of his/her foot placed on one tile, the tile will move in the opposite way of the user motion in order to keep the user's body at a constant position in the workspace. However, for now the prototype is only able to handle slow motions and does not allow a normal locomotion speed.



Figure 1.12 – The CirculaFloor prototype [Iwata 05].

### 1.2.3.3 Spheres

The last approach uses a sphere in which the user can freely walk. The sphere rolls on its base without actually moving. Thus the user is constantly recentered, allowing free infinite displacements in every direction. The CyberSphere [Fernandes 03] and Virtusphere [Latypov 06] are two examples of that kind of devices (Figure 1.13).



**Figure 1.13** – Two examples of sphere devices: the CyberSphere and the Virtusphere.

#### 1.2.4 Conclusion

We presented a panel of locomotion interfaces designed for walking in VE. These locomotion interfaces use different mechanical methods to maintain the user in a constant position in the workspace. For example, some interfaces control the trajectories of the user's feet, while other interfaces move the ground under the user's feet. However, most of these techniques allow the user to walk naturally in the real world in order to navigate in the VE. Therefore, these interfaces are generally efficient and ecological by design. Moreover, they provide kinesthetic and proprioceptive feedback to the user. Therefore, they offer a great all-in-one solution for navigation in VE. However, these interfaces are generally costly and therefore can not be used in some contexts. Thus, other approaches and techniques are required to solve this limitation.

### 1.3 3D Interaction Techniques for Navigating in VE

3D Interaction Techniques allow the user to perform different types of task in 3D space [Bowman 05]. They can be decomposed into four main categories: selection of virtual objects, manipulation of virtual objects, navigation in VE and system control [Bowman 05]. This section will focus on navigation techniques, i.e. techniques designed to move from the current location in the VE to a desired point. In addition to the locomotion interfaces, navigation techniques have been developed to control the navigation in the VE. Moreover, these techniques also address the problem posed by the limited size of the workspace: some techniques maintain the user in place, while other are designed to manage the available working space. We propose to decompose those techniques into two main categories: (1) techniques where the user remains in place and (2) techniques where the user can walk freely inside a predefined space. Therefore, these techniques can be classified depending on the size of the necessary working space.



### 1.3.1 3D Interaction Techniques for In-Place Use

For some of the navigation techniques, the size of the working space is too small to allow the users to move freely. Therefore, the users have to remain in place in the real world during the interaction.

#### 1.3.1.1 Static Navigation

Mouse, keyboard and joystick are devices commonly associated to navigation techniques which do not require body interactions. For example, navigation can be achieved with a mouse by pointing on a virtual map the place to go [Fuchs 01, Stanney 02]. A joystick can also be used to control the position and orientation of the camera in the VE. The Image-Based Walk-Through System [Endo 98] is one example of that kind of interaction techniques, video games are many others. The World in Miniature (WIM) technique [Pausch 95, Fuchs 01, Stanney 02] is a little more complex. Indeed, the user holds a miniature graphical representation of the VE in his hand and interacts with the VE through this miniature. Thus, navigation is achieved by changing the position of an avatar representing the user inside the WIM. However, the camera will fly automatically to the new position of the avatar. This aspect limits considerably the possibility of the navigation tasks, as the user do not have the possibility to wander in the VE.

#### 1.3.1.2 Step World in Miniature

An improvement of the World in Miniature technique (Figure 1.14) is to use a miniature projected on the ground instead of being hand-held. The user can directly walk in the miniature to be transported to the location he wants to visit in the VE. This technique is called Step WIM [LaViola 01].



Figure 1.14 – The Step WIM technique [LaViola 01].

### 1.3.1.3 Walking in Place

Walking-In-Place (WIP) is an interaction paradigm designed for both an improved sensation of walking and an efficient navigation in virtual environments [Slater 95]. The WIP technique consists in consciously walking in place in the real world (Figure 1.15). The user motions are tracked and used to control the navigation in the VE. Different implementations of the WIP have been proposed and are summarized in Table 1.2.

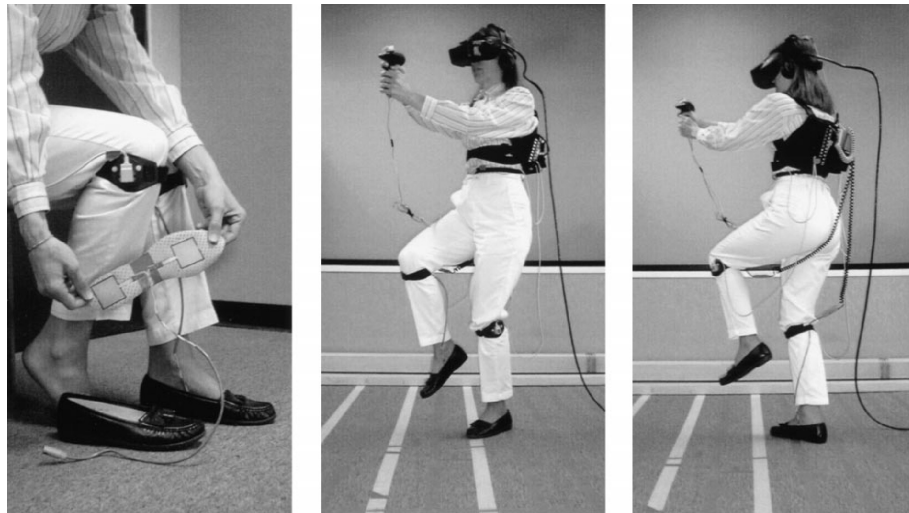
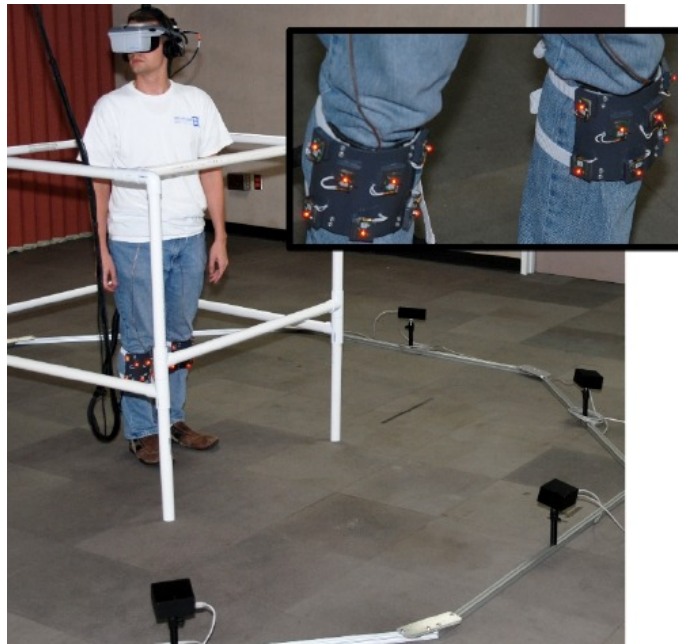


Figure 1.15 – The Gaiter interface [Templeman 99].

The first implementation proposed for WIP used an HMD. Head tracking was used to predict and detect the steps of the user using a neural network [Slater 95]. When user's steps were detected, the viewpoint automatically moves forward in the VE. The advance direction was only related to the head's direction. In the next implementations of WIP, the processing of head movements with a neural network was abandoned. The next systems tracked the motions of the user's knees or heels (Figure 1.16). Then, the user's steps could be detected and translated into a variable navigation speed depending on the steps' frequency. In order to detect the steps, Templeman et al. [Templeman 99] proposed to use pattern recognition. Feasel et al. [Feasel 08] proposed to use frequency analysis for the detection, and Wendt et al. [Wendt 10] proposed to use biomechanically inspired state automaton.

Using only the legs offers an additional benefit: the user has his/her hands free, allowing him/her to perform other tasks. Therefore, the user's hands are free and can be used for other tasks. For example, with the WIP, the user can navigate and manipulate objects in the VE simultaneously. Turning in the virtual world is often achieved using the orientation of one of the tracked points (e.g., head, waist, chest) [Templeman 99]. In other cases, the user relies on a gamepad or joystick for turning [Feasel 08]. In addition, the WIP can also be combined with natural walking. The user can move freely in the available workspace and simply start to walk-in-place when the limits of the workspace are reached. Therefore, WIP is used only when absolutely needed and the user can walk normally otherwise. When considering Table 1.2, all the WIP techniques described in the literature so far are meant for highly immersive virtual environments and use either HMDs or CAVEs as visual displays [Razzaque 02]. However, recent implementation of WIP using smartphones as wireless input captors [Kim 12] might allow a more widespread use for WIP.

Unfortunately, very few evaluations of WIP comparing it with other existing navigation



**Figure 1.16** – The Gait-Understanding-Driven Walking-In-Place [Wendt 10].

techniques have been carried out up to now. Moreover, these rare studies have mostly used subjective questionnaires, except for Whitton et al. [Whitton 05]. Considering the data available in the literature, it seems that WIP can increase presence compared to classical joystick-based interaction [Razzaque 02, Usoh 99]. WIP is also perceived as a more natural technique [Yan 04]. However, WIP might also result in an increased cyber-sickness [Usoh 99]. WIP has been found to be less efficient in terms of usability compared to real walking [Feasel 08]. Whitton et al. [Whitton 05] have performed a quantitative study comparing the WIP, natural walking and joystick-based First-Person Shooter (FPS) techniques, in terms of task performance and kinematics of the task criteria, but only for linear navigations. In particular, they found that the variability between techniques can be explained by the peak velocity and deceleration parameters. Moreover, the correlation of those variables suggests a coarse ordering of the techniques by “naturalness”. Other studies compared the trajectories produced by different interaction techniques, but only on qualitative criteria [Zanbaka 05]. However, navigation techniques are usually used in complex navigations, including turns and changes of speed. To the authors’ best knowledge, the WIP has never been evaluated in such kind of scenario so far.

### 1.3.2 3D Interaction Techniques Involving Real Physical Walking

The purpose of interaction techniques involving real physical walking is to manage the available working space during the navigation. The user can benefit of the available space to navigate, while the interaction techniques keep the consistency between the real and virtual world.

References	Input/Output Interfaces		Interaction Technique	
	Display	Tracking	Control Law	Available Motions
[Slater 95]	HMD	Head	Neural network	Turn, Forward
[Usoh 99]	HMD	Head	Neural network	Turn, Forward
[Templeman 99]	HMD	Knees, waist, hands, head	Knee pattern	Turn, Forward, Backward, Diagonal, Sidestep
[Razzaque 02]	CAVE	Head	Neural network	Turn, Forward
[Yan 04]	CAVE	Legs, waist, head	Leg speed relation	Turn, Forward
[Feasel 08]	HMD	Shins	Filtered heels speed	Turn, Forward (various speeds)
[Wendt 10]	HMD	Shins	Biomechanical state machine	Turn, Forward (various speeds)
[Kim 12]	HMD	Ankles	Acceleration / Sensor-fusion	Turn, Forward

**Table 1.2** – Overview of existing Walking-In-Place techniques.

### 1.3.2.1 Resetting Techniques

Resetting Techniques are a set of navigation techniques based on natural walking which address the issue of the limitation of the workspace. The objective of these techniques is to reset the user's position in the real world when reaching the limits of the workspace without breaking the user immersion. Williams et al. [Williams 07] proposed three different navigation techniques based on this approach. With the Freeze-Backup technique, the VE is frozen whenever the user is reaching the limits of the workspace. The user must then make a few steps backward to recenter himself in the workspace before continuing his navigation. Similarly, the Freeze-Turn techniques wait for the user to make a 180° rotation before continuing the navigation in the VE. Finally, the 2:1-Turn do not freeze the VE when the user reach the limits of the workspace. Instead, the rotations in the VE are twice the rotations in the real world. Therefore, when the user rotates of 360° in the VE, the corresponding rotation in the real world is only 180°. Thus, the user can continue to navigate without risking to reach the limits of the workspace.

The Magic Barrier Tape [Cirio 09] technique is another resetting technique based on a metaphor which allows the user to navigate in an infinite virtual scene while confined in a restricted walking workspace. The physical boundaries of the workspace are materialized in the virtual environment as a barrier tape that should not be crossed by the user (Figure 1.17). Thus, the user can manage its position with a hybrid method based both on the natural walk in the workspace and the use of a classic static method like a joystick. Experiments showed that this metaphor is more efficient and more appreciated by the users than the Freeze-Backup and the 2:1-Turn Resetting techniques [Cirio 09]. A similar approach for navigations in CAVEs, the Walking in a Cube metaphor [Cirio 12b], has also been proposed. In addition to the limits of the working space, the technique also manages the orientation avoiding the user to see the walls of the CAVE without projected content. Indeed, many CAVEs are composed of only 3 faces and the floor. Therefore, to maintain the immersion, the user must stay oriented in the direction of the screens. This technique

also relies on the metaphor of virtual wall to indicate the limits of the field of view.



**Figure 1.17** – The Magic Barrier Tape [Cirio 09]

### 1.3.2.2 Redirected Walking

The method called “Redirected Walking” [Razzaque 01] is designed to control the user and makes him/her stay in a reasonably small workspace even when walking in straight lines in the VE. When walking in straight line in the VE, the user is tricked into walking into curved lines in the real world (Figure 1.18). If the workspace is large enough, the user will walk in circles and therefore never notice the limits of the workspace.

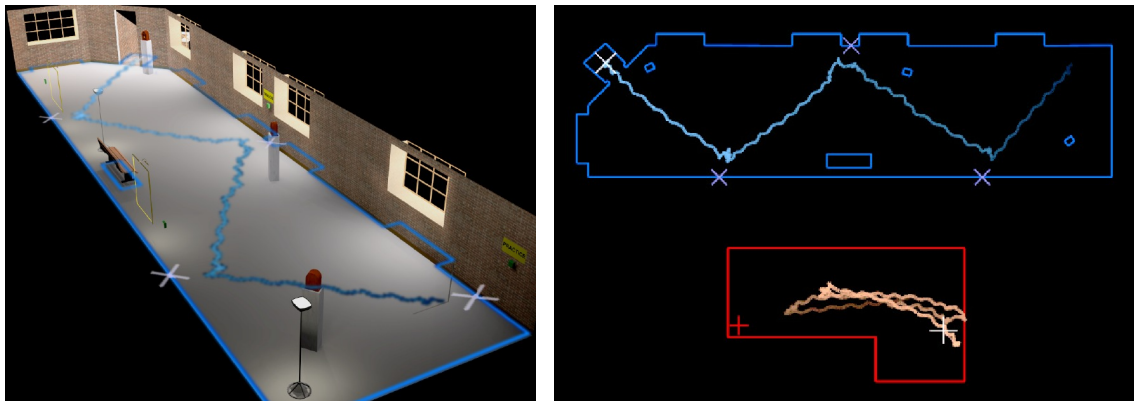


**Figure 1.18** – Example of path obtained with Redirected Walking: (a) the virtual path followed by the user in the VE and (b) the real (red) and virtual (blue) paths traveled by the user [Razzaque 01].

This technique relies on imperceptible rotations of the VE around the user when the user is walking with a head mounted display. The difference between the visual feedback and the actual trajectory makes the user turn without noticing it to correct the deviation of the images. This technique always tries to orientate the user in direction of the farthest wall of the workspace. However, if the workspace is too small, it is not possible to inject enough rotations to keep the user away from the limits of the workspace. Indeed, if the injected rotations are too important, the user would perceive them. A possible solution to overcome this limitation is to artificially introduce secondary tasks, increasing the cognitive load of the user which allow to inject greater rotations. A first study showed that a VE of 8 m



by 20 m can be safely simulated in a physical workspace of half that size [Razzaque 01]. Moreover, Steinicke et al. [Steinicke 08b, Steinicke 08a] proposed to statistically quantify the maximum distortion that could be introduced without being noticed by the users. A first preliminary evaluation showed that this effect will be unnoticed in 80% of cases by the user as long as the rotation distortion stay below 30%. They also showed that it is possible to expand or shrink the distances traveled by the user in the real world by 45% and 15% respectively [Steinicke 08b]. Moreover, more detailed evaluation showed that a virtual trajectory in straight line can be redirected in a 24 m radius circle without the users noticing [Steinicke 08a]. However, the perception of the distortions is subjective and variates from one user to another. Moreover, the navigation speed also influence the effectiveness of the curvature gain. Therefore, a more recent approach proposed a controller to dynamically adapt the gains based on the user's velocity [Neth 11]. Redirected Walking can also be adapted to be used in CAVes, in association with Walking-In-Place [Razzaque 02]. Indeed, this technique can be used to avoid the user looking at the CAVE missing screens. Finally, Redirected Walking is also well suited for driving simulation [Bruder 12] for example. Therefore, the same technique can be used for either small or long navigation in the VE.

### 1.3.2.3 Motion Compression

The underlying idea of Motion Compression [Nitzsche 04] is very close to the Redirected Walking technique. However, contrary to the previous technique where gains were applied to the curvature, rotations are injected only during the rotations of the user, but may be greater than with Redirected Walking. Therefore, the user might slightly perceive the rotations, especially when staying close to the border of the allocated space (Figure 1.19). As a consequence, the working space can potentially be smaller compared to Redirected Walking.

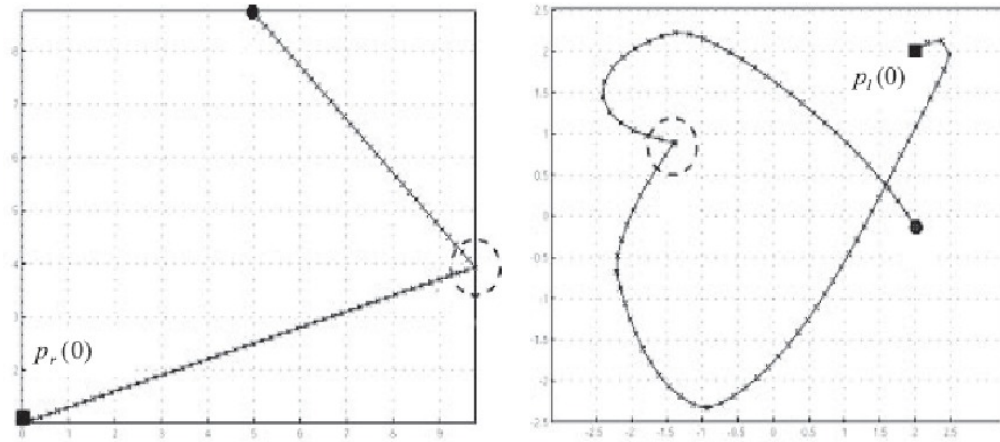


**Figure 1.19** – Example of path obtained with Motion Compression: (a) the virtual path followed by the user and (b) the real path traveled by the user after correction. [Su 07]

Moreover, Engel et al. [Engel 08] proposed a real-time controller to further reduce the necessary space. The algorithm first computes a prediction of the user's path. Based on the constraints of the working space, a new path is computed to match the constraints, and then the user is redirected as smoothly as possible. This results in a reduction of the necessary space while being almost not noticeable for the user (Figure 1.20).

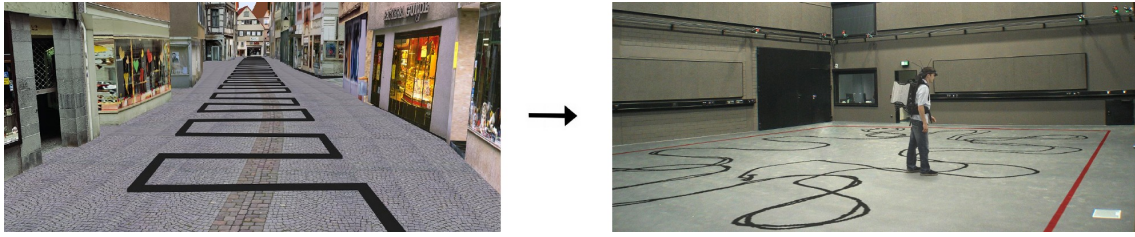


**Figure 1.20** – Motion compression: the user stays in a reasonably small workspace [Engel 08].

#### 1.3.2.4 Impossible Spaces

More recently, Suma et al. [Suma 12] proposed to violate the rules of Euclidean geometry to optimize the working space. The Impossible Spaces technique overlaps different virtual rooms to fit the VE into a smaller workspace (Figure 1.21). Therefore, one position in the real world can potentially correspond to two or more different positions in the VE. Moreover, the technique also propose to expand the virtual rooms to fill the available tracking space. However, in order to maintain the visual coherency during the navigation, the technique uses corridors between the virtual rooms to do the transitions. Suma et al. found that, for a workspace of 9.14 m by 9.14 m, the virtual rooms can overlap up to 56% for fixed size rooms and 31% for expanded rooms [Suma 12].



**Figure 1.21** – Impossible Spaces: the virtual rooms overlaps on the real workspace [Suma 12].

### 1.3.3 Conclusion

We presented different interaction techniques to navigate in VE. Some of these techniques keep the user on a constant position in the real world. However, it does not mean that the user's motions can not be used to control the navigation. On the other hand, some techniques use the position of the user during real walk in the workspace as input for the position in the VE. However, these techniques are designed to prevent the user to reach the limits of the workspace, or to allow him to continue his/her navigation in another direction in the real workspace. The presented techniques allows efficient navigations, but some are more ecological than others. In particular, techniques based on the user real motions of walking are more ecological compared to the static techniques. Finally, these techniques are generally more affordable than the locomotion interfaces presented in section 1.2, but requires larger workspaces or provides less sensory feedback.

## 1.4 Sensory Feedback Techniques for Navigating in VE

Sensory feedback are designed to provide simulated feedback to the senses through various modalities. Sensory feedback can be used to induce the feeling of immersion for the user. For navigation, sensory feedback can also be used to improve the sensation of walking for example.

The presented techniques in this section are classified depending on the modality simulated: haptic, visual, vestibular, auditory and finally some multimodal techniques.

### 1.4.1 Haptic Feedback

The haptic sense includes the perception of forces, stiffness, roughness, textures, vibrations, as well as the kinesthetic and proprioceptive senses. Some techniques are based on haptic feedback to provide information to the user. Simulation of the kinesthetic and proprioceptive senses can be used to increase the perception of the motions during navigation, while other haptic senses can be used to simulate properties of the VE.

#### 1.4.1.1 Foot Devices

Some devices can provide haptic feedback directly to the foot of the user to allow perception of the ground properties inside the VE. The Fantastic Phantom Slipper [Kume 98] is a pair of shoes with vibrators placed on the sole which provide haptic rendering. Thus, with a tracking of the user's shoes, the user can feel objects on the floor of the VE. However, the Fantastic Phantom Slippers are not designed to be used for real walk. The FootIO [Rovers 05] is another device designed to provide haptic feedback to the foot of the user. However, this prototype uses actuator to stimulate the user's foot with 15 different levels of intensity on a wide frequency range. Like the Fantastic Phantom Slippers, this prototype can not be used for real walking yet. Vibrotactile information can also be provided through shoe-based devices [Papetti 10]. Using contact sensors and vibrators, the shoes can simulate different ground types by producing adapted vibrotactile feedback at each step (Figure 1.22). The vibrotactile information can be used to simulate solid materials, as well as aggregate floors such as snow, sand or gravels.

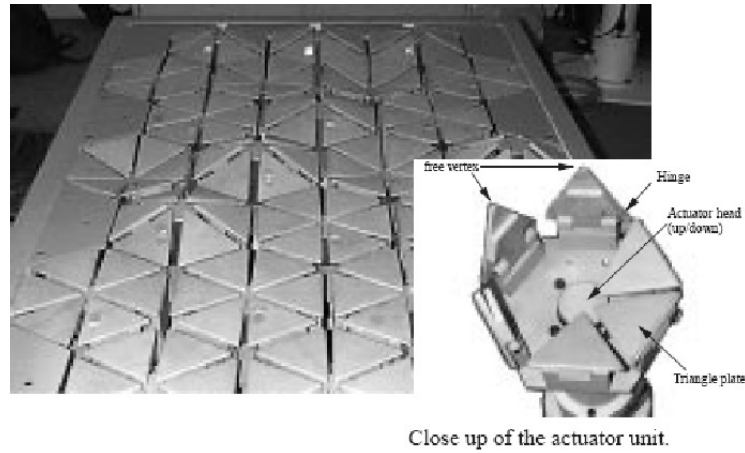


Figure 1.22 – Shoe-based device for vibrotactile feedback [Papetti 10].



### 1.4.1.2 Floor Devices

Another possibility is to use deformable floors to provide the haptic information. For example, the ALive Floor [Sugihara 98] device is a floor made of tiles whose tilt is controlled by actuators. Thus, the device can simulate uneven floors in real time (Figure 1.23).



**Figure 1.23** – The ALive Floor.

Other devices can also provide vibrotactile information. For example, the EcoTile [Visell 08, Visell 10a] is a vibrotactile tile that can be used to create enhanced floors (Figure 1.24). This device generates vibrational stimuli according to the user's footsteps. The vibrations are created by a single actuator placed below the floor tile. Moreover, contact/pressure captors are used to detect the user's feet pressure. Therefore, a ground composed of multiple tiles can track the displacements of the users and generate localized feedback accordingly. The vibrotactile simulation allows different kind of rendering . For example, this device can render different ground textures, like snow or ice [Visell 08]. Moreover, the vibrations can also be used to render the contact of the user's feet with fluids [Cirio 12a], like water for example.

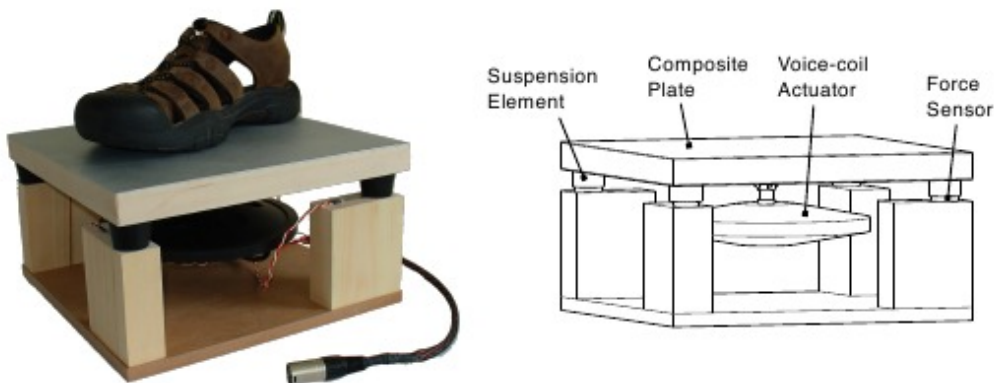


**Figure 1.24** – The EcoTile [Visell 10a].

### 1.4.2 Visual Feedback

Visual-based techniques can be used for applications of Virtual Reality that cannot afford expensive locomotion interfaces that would provide users with vestibular and proprioceptive cues. Even if passive physical motion appears to be a more effective cue, Harris et al. [Harris 02] showed that visual flow also influences the perception of self-motion. Moreover, it can provide enough information alone to carry out even the most complex tasks. However, the display device used may have an impact on a given task. For example, ego-motion perception depends more of the device than the provided field-of-view [Riecke 05]. In this case, large curved projection screen gives better results than head mounted displays (HMDs).

Visual information can also be used to enhance the sensation of walking in VE. For example, effects on the virtual camera can be created [Lécuyer 06]. Camera Motions (CM) simulate the motions of the user's head and its associated visual flow during the walk [Lécuyer 06]. The point of view of the user oscillates to follow the head motions that would be produced by a real walk. (Figure 1.25). Using subjective questionnaires they found that oscillating motions were preferred by the participants over the “classical” linear motions. Moreover, they found that CM improve the immersion and sensation of walking in the VE.

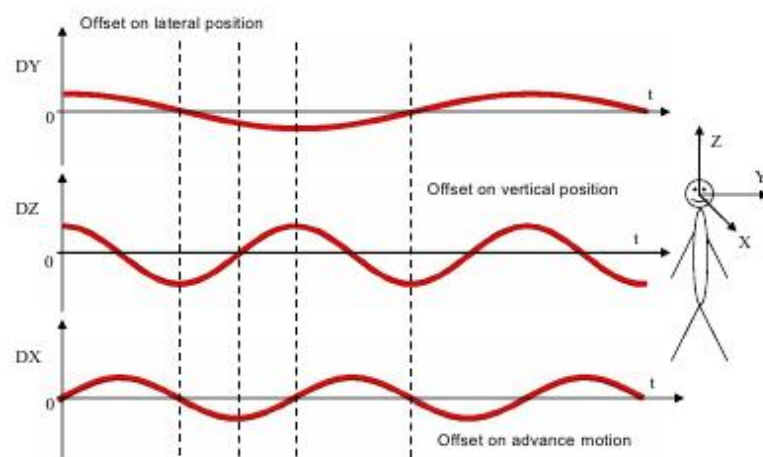


**Figure 1.25** – Oscillation of the eyes during the walk [Lécuyer 06].

Compensation of the head orientation to focus the gaze on the objects is known as the oculomotor reflex. This reflex can also be integrated into the Camera Motions [Hillaire 08] (Figure 1.26). Using questionnaires, they found that compensated oscillating camera motions were also preferred by the participants over the regular oscillating camera motions. Moreover, Hillaire et al. [Hillaire 09b] proposed to use an eye-tracking system in order to improve the use of compensated oscillating camera motions. They dynamically adapted the focus point of the camera to match the participants' gaze. By this means they were able to simulate more realistic camera motions. Still using questionnaires they found that participants have globally preferred the compensated camera motions adapted with the eye-tracking system.

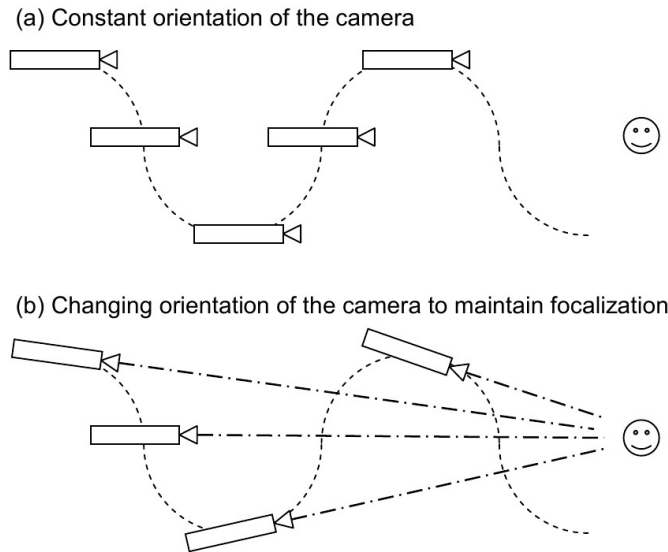


**Figure 1.26** – Compensation of the gaze orientation during the walk [Lécuyer 06].

Hillaire et al. also proposed to simulate the depth-of-field blur effect [Hillaire 07] (Figure 1.27), as well as more complex ocular reflexes, such as the orientation of the gaze depending on the trajectories [Hillaire 09a]. Indeed, the gaze anticipates the turns of the trajectories. Therefore, the orientation of the gaze can be approximated depending on the rotation speed.

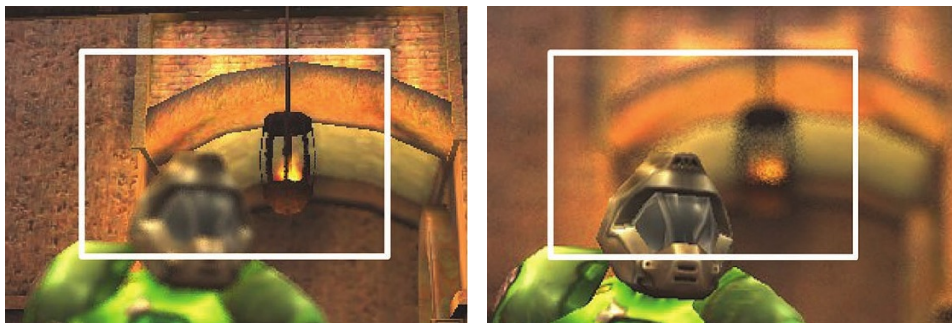


**Figure 1.27** – Example of depth-of-field blur effect: (a) focus on the background (b) focus on the foreground [Hillaire 07].

Camera Motions can also be used to suggest slopes for example [Marchal 10]. The height, advance speed and orientation of the camera can be used separately or together to inform about the slope. When the three parameters are combined the perception of slopes increase [Marchal 10]. Interestingly, orientating the camera up and down produce the impression of walking on uneven grounds, even when the camera height is always kept at a given height (Figure 1.28).

However, the current models do not account for the exact motions of the head. Precise measures of the position of the head during the walk have been made [Hirasaki 99], but surprisingly users seems to prefer less realistic models over the more physically accurate ones [de Barros 09a, de Barros 09b]. Indeed, the models the users preferred only used translations over the right and upward axes, without any rotation. On the other hand, the model using translations and rotations over the three axes was the less liked of all the models, including a pseudo-random model.

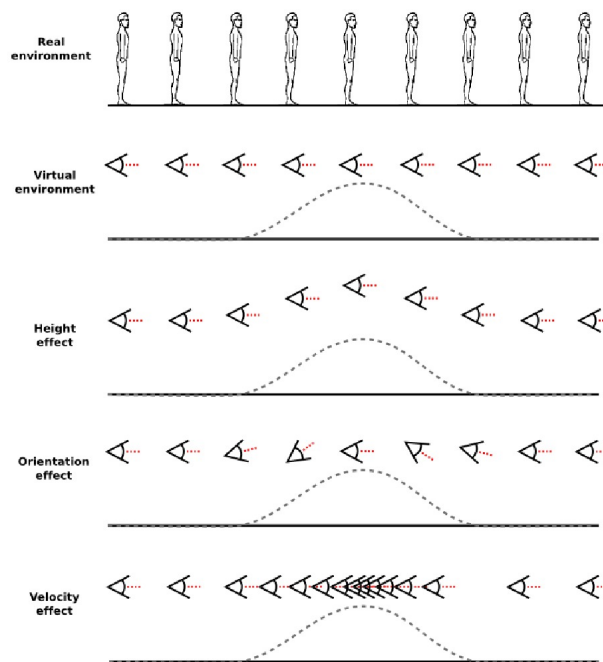


**Figure 1.28** – The Height, orientation and speed can be used to simulate slopes in the VE [Marchal 10].

### 1.4.3 Vestibular Feedback

The Galvanic Vestibular Stimulation (GVS) is a technique which can alter the balance of the user and induce vection (virtual sense of acceleration) [Maeda 05]. The GVS is composed of two electrodes placed on the mastoids behind the ears and which emit small electrical impulses (Figure 1.29). Those impulses temporarily alter the vestibular system of the inner ears, depending on the frequency and intensity of the current [Nagaya 05]. The user will then perceive a modification of the position of his/her center of gravity towards the anode.



**Figure 1.29** – The GVS System [Nagaya 05].

This method can be used to provide the user with vestibular information while remaining in place. For example, Reed-Jones et al. used the GVS in a car simulation in order to provide vection matching the acceleration produced by the inertial force when driving a real car [Reed-Jones 07]. Main advantages of GVS are its low-cost (just two electrodes and a few transistors) and its small size and weight. However, this device can only act on the vestibular sense of the users, contrary to the sensorimotor devices.

#### 1.4.4 Auditory Feedback

Another modality which is not strictly speaking part of the senses involved during the natural human walk can still prove to be immersive when navigating. For example, Riecke et al. [Riecke 09] showed that auditory stimuli can increase the phenomenon of circular vection for the user, as well as the presence in the VE. Thus, auditory stimuli must be taken into account when walking in VE. For example, auditory feedback can provide information with specific footstep sounds. Audio feedback can be adapted to simulate the different ground materials in the VE. Serafin et al. [Serafin 09] proposed a technique to extract the components of a real footstep sound in real time. This technique allows them to dynamically generate a new footstep sound, in real time, matching the properties of the virtual ground to be simulated. For example, a user walking on concrete in the real world could hear sounds of footsteps on snow. The physical simulation used allows a large variety of simulation of footstep sounds matching many types of virtual grounds such as snow, water, leaves, wood, concrete, gravel and so on [Nordahl 10].

##### 1.4.4.1 Step-contact Sounds

One kind of sounds that can be simulated is the one made by the footsteps. For example, Fontana et al. [Fontana 03] proposed a model based on a physical impact model and control rules. With this model, they successfully simulated sounds resulting from walking, running and crushing objects like cans. Still based on physical models, Nordahl et al. [Nordahl 06] implemented a multimodal audio and visual architecture, which can generate the sound produced by the footsteps of the virtual human for different surfaces. One interesting specificity of this architecture is the ability to render a fully spatialized sound, with 8 channels, and tracking the user's position for an optimal effect. Using microphones, Nordahl et al. [Nordahl 10] estimated the ground reaction forces (GRF) at each step. The GRF is then used to control precisely the synthesis of the virtual footsteps (Figure 1.30).

##### 1.4.4.2 Surfaces Sound Properties

The sound produced by the footsteps changes depending on the surface the user is walking on. Some devices have been designed to simulate the sound made by some specific textures, like snow for example. The EcoTile [Visell 08] presented in section 1.4.1.2 is one of them. However, some other approaches with less limitations have also been developed. For example, with a physical resonator model, Serafin et al. [Serafin 09] successfully separated the sound produced by footsteps in two different components: (1) the sound produced by the exciter, i.e. the shoes themselves and (2) the sound produced by the resonator, i.e. the ground. Thus, they manage to substitute in real time the sound produced by the ground with a sound generated by a ground with different properties (Figure 1.31). As



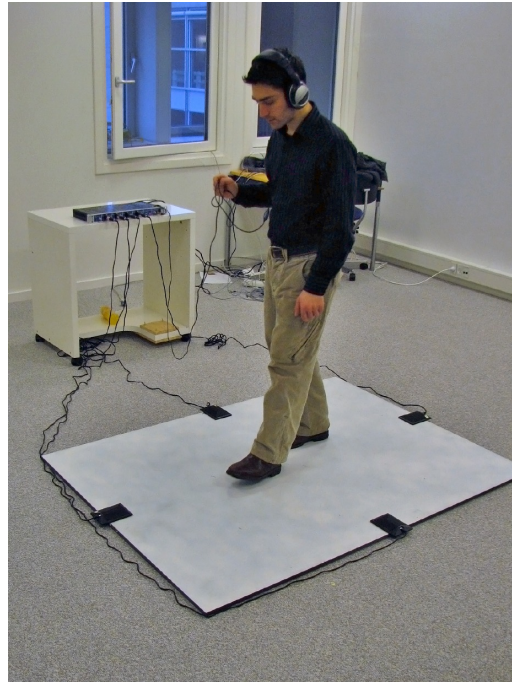


**Figure 1.30** – The footstep sounds are used to estimate the ground reaction forces [Nordahl 10].

a consequence, the user can walk on a concrete floor but hear his footsteps as if he was walking on snow for example.



**Figure 1.31** – The sound produced is substituted in real time with a sound generated by a ground with different properties [Serafin 09].

### 1.4.5 Multimodal Feedback

Most of the time, more than one modality is used to render walking in the VE. In that case, the coherency between the modalities must be preserved to allow the feeling of presence for the user and to avoid possible side-effects such as Cybersickness [LaViola 00]. In some

cases, some modalities can improve other modalities, providing the same information that will be assimilated by the user in a similar way. For example, Serafin et al. [Serafin 07] showed that auditory cues can significantly influence the haptic perception of virtual textures. Thus, the perception of textures seems not to rely exclusively on haptic perception, but can also be simulated in some part as an auditory stimuli. On the same idea, Harris et al. [Harris 99] quantified the ratio relation between visual and vestibular information. Indeed, to estimate the magnitude of the perceived motion more accurately, the VE should provide vestibular information in a ratio of one to four with the visual information. However, this study stands out as very few other ever tried to precisely measure the parameters that should be used to obtain the better combination of two or more modalities.

Different modalities can also be combined to improve immersion when walking in VE. For example, shoe-based devices can be associated with real time audio simulation [Papetti 10]. Contact sensors embedded in shoes are used to detect footsteps and both vibrotactile and auditory feedbacks are provided to match a specific virtual ground surface. Tactile tiles can also be used with visual and auditory feedbacks in a CAVE to provide a complete simulation using the haptic, auditory and visual modalities. Different scenarios have been experimented so far:

- The frozen pond [Visell 10b] simulates walking on a frozen surface: each step is detected and generates cracks on the ice. The cracks produce tactile and auditory feedbacks located under the user feet, in addition to the visual display of the cracks propagating in the ice (Figure 1.32b).
- Similarly, the snow field scenario renders the sound and vibrations produced at each step in the snow. Moreover, the position of the steps are detected precisely to generate accurate foot tracks (Figure 1.32a).
- This system have also been used for multimodal rendering of fluids [Cirio 12a]: the footsteps of the user are detected and used to generate in real-time realistic sounds of fluids using visual, audio and vibrotactile modalities (Figure 1.33a). Each step generates bubbles in the water which produce in turn realistic perception of sound and vibration of water under the user's feet.
- Finally, the same model can also be used to simulate rushing waves on a beach: the user perceives the contact with each wave through the three modalities (Figure 1.33b).

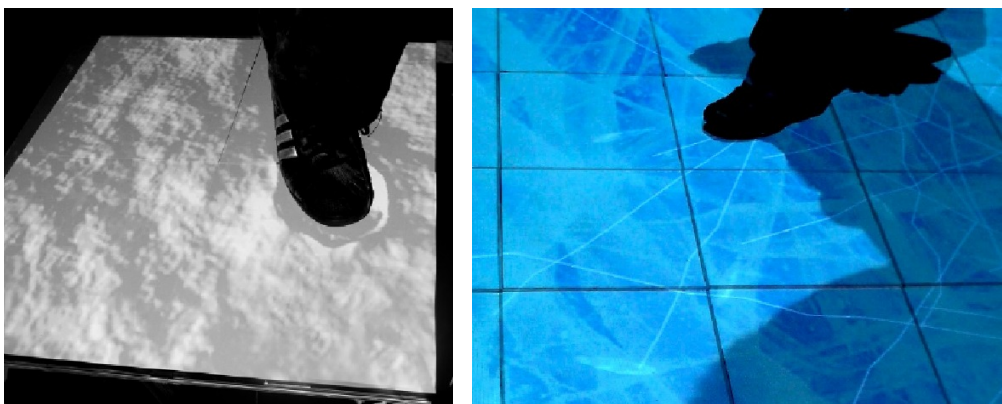


**Figure 1.32** – Multimodal simulation of walking on snow and ice: (a) ground made of snow (b) ground made of ice [Visell 10b].



**Figure 1.33** – Multimodal simulation of walking in water: visual, audio and vibrotactile feedbacks. Scenarios: a shallow water pool (a) and a wave rushing on a beach (b) [Cirio 12a].

#### 1.4.6 Conclusion

We presented different sensory feedbacks for walking in VE. These techniques can be used to simulate different modalities during the virtual walk. In particular, such techniques can be used together with the navigation techniques to improve the immersion and sensations of walking of the users. The majority of the sensory feedback techniques only simulate one modality. Moreover, the multimodal techniques usually focus on one scenario of navigation. Therefore, new sensory feedbacks are necessary to extend the range of modalities and scenarios available during the walk in VE.

### 1.5 Conclusion

In this chapter, we presented the *3D Navigation Techniques and Sensory Feedbacks for Walking in Virtual Reality*. In a first part, we presented some of the properties of the human walk through different aspects. We focused on descriptions of the physical, biomechanical and neurological aspects of the human walk. In a second part, we presented some of the locomotion interfaces designed for walking in VE. In the third part, we focused on different interaction techniques for walking in VR. Finally, the fourth part presented sensory feedbacks to increase the immersion and sensation of walking during the navigation.

The walk is a complex phenomenon that can be studied at different levels. First, at the physical and anatomical level, the walk is a cyclic motion involving the lower limbs, but also different senses. At the biomechanical level, the study of the kinematics and dynamics of the motion allows a better understanding of the subtleties of the human locomotion. Finally, the neurological level also provides important insight on the objectives and strategies used during the locomotion. Therefore, a good understanding of all those levels is necessary in order to design techniques and devices for Virtual Reality based on the walking metaphor.

Locomotion interfaces can be used to simulate the walk in VE. Indeed, locomotion interfaces are devices which interact directly with the body of the user. Therefore, the motions



of the user are used to control the navigation. Moreover, these devices also provide sensory information to the user, like haptic feedback of objects within the VE. Therefore, locomotion interfaces generally provide efficient and ecological navigation in the VE while solving the problem of the size of the workspace. However, these interfaces are also generally expensive and therefore not affordable for many applications.

In addition to the locomotion interfaces which act directly on the user's body, navigation techniques have been developed to navigate in the VE without acting directly on the user. Those techniques are also designed to address the problem raised by the limited size of the workspace. Some techniques maintain the user in place, while others are designed to manage the available working space. However, the efficiency varies depending on the technique. Moreover, some techniques are not as ecological as the others, or are less affordable. Therefore, no navigation technique is adapted to all kind of applications.

Finally, the sensory feedbacks can be used to simulate one or more modality of the user. Therefore, these techniques can be used to complete the chosen navigation techniques/devices in order to increase the immersion and sensation of walking in the VE. Different techniques have been proposed for each of the possible modalities. However, most techniques only use one modality. Moreover, each technique focus on one type of feedback. Therefore, new sensory feedbacks are necessary to extend the range of modalities or types of feedback. Moreover, new models to coordinate the different sensory feedbacks together would also improve complex simulation of navigation.

Through this overview of 3D navigation techniques and sensory feedbacks for walking in VR, and considering the objectives of this Ph.D. thesis, several issues stand out. First to this point, there is no navigation technique that would achieve all our fixed goals, i.e. an **efficient**, **ecological** and **low-cost** navigation techniques requiring only a **small workspace**. Second, the number of sensory feedbacks for walking in VR is still limited, and the proposed feedbacks are either unimodal or limited to specific simulations, such as ground properties for example. New sensory feedbacks could be developed to simulate **new scenarios** or increase the **range of modalities**.

# Shake-Your-Head: a Navigation Technique Revisiting Walking-In-Place for Desktop Virtual Reality

# 2

## Contents

<b>2.1 The Shake-Your-Head Technique</b>	<b>50</b>
2.1.1 Input/Output Interfaces	51
2.1.2 Walking Simulation	53
2.1.3 Visual Feedback Based on Camera Motions	55
2.1.4 Conclusion	56
<b>2.2 Evaluation of the Shake-Your-Head</b>	<b>57</b>
2.2.1 Method	57
2.2.2 Results	60
2.2.3 Discussion	62
<b>2.3 Analysis of the Virtual Trajectories Generated with the Shake-Your-Head</b>	<b>63</b>
2.3.1 Trajectories Analysis	63
2.3.2 Discussion	67
2.3.3 Conclusion	68
<b>2.4 Conclusion</b>	<b>68</b>

Natural human walking in VR is often limited by the size of the workspace. Indeed, the simulated VE are generally larger than the workspace. The navigation and immersion of the users can be perturbed when the users reach the limits of the workspace. Therefore, specific navigation techniques are necessary to solve the problem of the limited workspace.

The Walking-In-Place (WIP) technique has been introduced by Slater et al. [Slater 95] to enable a real physical walking movement and an efficient navigation technique in 3D virtual environments. The user has to consciously walk in place while motions of his body are tracked and analyzed (Figure 2.1). The tracked Walking-In-Place motion is used as input for the locomotion simulation inside the VE. First implementations of WIP were all based on the processing of head positions using a neural network [Slater 95]. More recent models track the positions of the heels or knees of the user to compute the resulting virtual locomotion [Feasel 08, Wendt 10]. However, all existing WIP techniques require the user to stand up, and they focus on immersive VR applications based on sophisticated tracking devices and head-mounted-displays or CAVE setups.



**Figure 2.1** – Slalom navigation in a Virtual Environment with the Shake-Your-Head technique.

In this chapter, we propose a novel approach to the WIP technique. Our intention is to extend it to match a larger set of configurations, by notably applying it to desktop setups. As a result, we propose to improve the WIP technique on three main aspects, corresponding to the three main innovations claimed in this chapter:

- **Novel user interface capacities.** We introduce (1) the possibility for the user to stand or sit (using classical interaction paradigms of desktop VR with mouse), and (2) the possibility to use screens (with limited field of view) and low-cost tracking (webcam) by using the use of head movements as main input of WIP control laws.
- **Novel locomotion simulation.** We extend the range of possible motions with WIP to: walking, turning, jumping and crawling, using heuristics and control laws based exclusively on users' head movements.
- **Novel visual feedback of walking.** We introduce the possibility to combine our approach with more realistic visual feedback of walking, i.e. camera motions, that are known to improve the sensation of walking [Lécuyer 06].

The remainder of this chapter is organized as follows: In [section 2.1](#) we introduce the Shake-Your-Head (SYH) technique, a new interaction technique based on the Walking-In-Place (WIP) paradigm. In [section 2.2](#) we describe the results of a set of experiments conducted to evaluate the ease and efficiency to navigate with our technique. Finally, in [section 2.3](#) we conduct an in-depth analysis of the trajectories produced by the SYH.

## 2.1 The Shake-Your-Head Technique

We propose a novel approach to the Walking-In-Place technique to match a larger set of configurations and apply it to the context of desktop Virtual Reality. Our approach is summarized in [Figure 2.2](#). The figure highlights the main differences between our approach and the classical and existing WIP techniques.

With the Shake-Your-Head (SYH) technique, the user can stand or sit (such as in tradi-

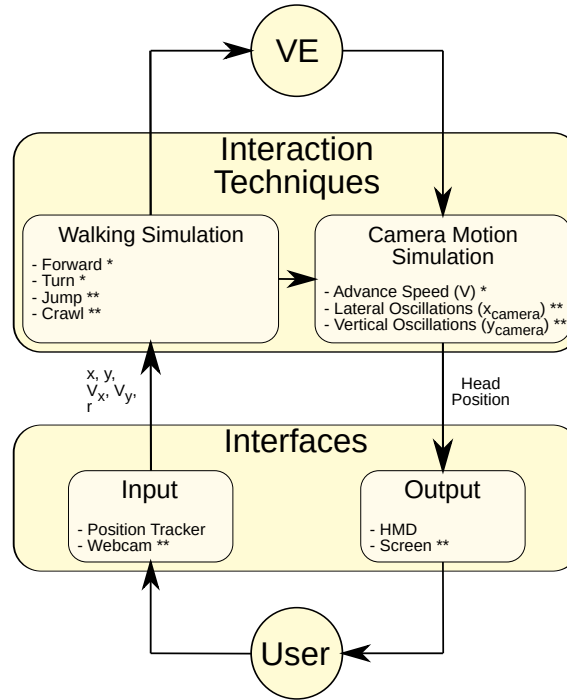


**Figure 2.2** – Overview of our novel approach for Walking-In-Place (one star stresses improvement of existing component, two stars stress additional components).  $x$  and  $y$  correspond to the tracking coordinates of the user’s head,  $V_x$  and  $V_y$  are the user’s head velocity and  $r$  is the user’s head orientation.

tional video games or desktop VR configurations). The user interacts with the system by means of head movements. These head movements can be captured using different tracking interfaces, but we insist on the use of low-cost optical tracking with standard webcams. The locomotion simulation proposes not only the computation of a virtual walking motion but also turning, jumping, and crawling possibilities. As a result, the user can perceive the locomotion in the virtual world by means of integrated virtual camera motions on the three axes of motion, to further enhance the sensation of walking.

In the following section, we will successively describe the different parts of our approach, namely: (1) the 3D user interface input/output, (2) the interaction techniques developed for the computation of the virtual locomotion, and (3) the visual feedback relying on camera motions.

### 2.1.1 Input/Output Interfaces

Our method proposes new features in terms of interfaces in order to extend the set of configurations where WIP can be applied, especially for Desktop VR. Thus, we propose to incorporate new devices for both input and output user interfaces in the VE.

#### 2.1.1.1 Input: Tracking Based on Head Motions

The input interface of our method is only based on head motions. In our implementation, the input interface is reduced to a webcam, allowing the use of our method for Desk-

top configuration without any additional peripheral. However, our method can also be implemented with other classical VR tracking systems.

**Use of Head Movements.** The main concept of our method is to exploit the head oscillations as a transposition of the one observed during natural walking. While walking, the head of the user oscillates along the lateral, vertical and forward axes [Lécuyer 06]. The oscillations are strongly correlated to gait events and foot steps. Moreover, these oscillations also occur while walking in place. Our approach is based on the measurement of those oscillations to control the navigation.

The head motions are classically retrieved in the existing WIP techniques thanks to the use of regular position trackers [Slater 95]. More generally, any tracking device can be used, as long as its accuracy is within the range of 1 cm. Moreover, the acquisition process of the required position does not have any influence, as long as the real time constraint is maintained. In our method, we propose the use of a video camera system to handle the tracking of the user head. Thus, our interaction technique can be deployed on a large scale at low cost for training purpose or video games for example.

**Extracted Data.** In our method, we propose to use 3 Degrees of Freedom (DOF) that can be easily accessed in the image frame provided by the webcam:

- The lateral position  $x$  (and the computed speed  $V_x$ );
- The vertical position  $y$  (and the computed speed  $V_y$ );
- The rotation of the head in the frontal plan  $r$ .

These three head motions are illustrated in Figure 2.3.

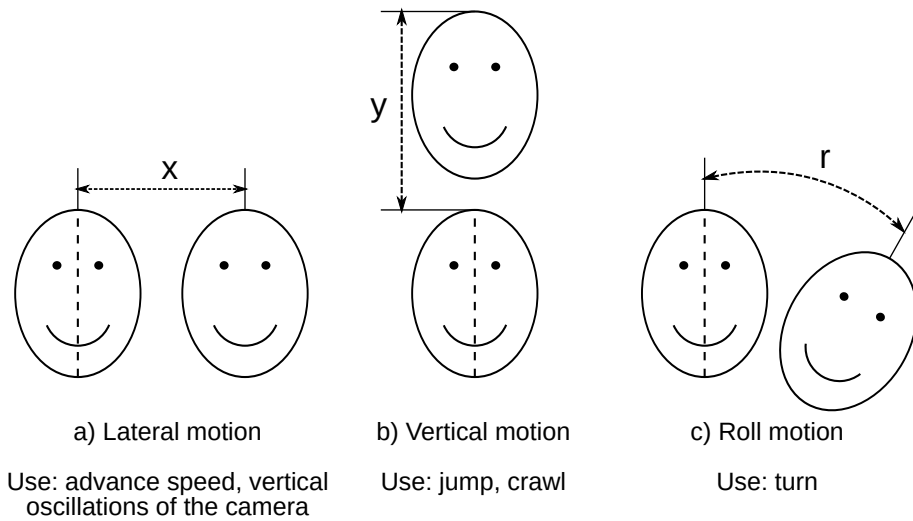


**Figure 2.3** – Extracted head motions: (a) lateral motion, (b) vertical motion, (c) roll motion.

**Implementation.** The use of the webcam to track the 3D position of the user head without using markers requires the implementation of real time constraints for the algorithms, i.e. more than 25 frames per seconds. Our implementation is based on the Camshift (Continuously Adaptive Mean Shift) algorithm [Bradski 98] implemented in the OpenCV

[OpenCV 10] library. This algorithm is based on color tracking and is well-suited for real-time tracking of features of a given color, such as the face of the user.

While the user is standing in front of the webcam, our algorithm recognizes him as an ellipsoid. The position of the head  $(x, y)$  can be deduced from the center of the ellipse and the orientation angle of the head  $r$  is given by the angle with the vertical of the ellipse. However,  $x$  and  $y$  depend on the resolution of the used webcam. Thus, we compute a normalized position  $(x_n, y_n)$  on  $[-1; 1]$  on both axes. From the normalized positions of the head  $(x_n, y_n)$ , we compute the instantaneous speeds  $V_x$  and  $V_y$ , and we use Kalman filters on all values to reduce the noise produced by the algorithm.

### 2.1.1.2 Output: Immersive and Desktop Visual Displays

Our method can be used with both immersive and regular screens as output interface with the VE. A requirement of desktop VR applications was to propose a technique that is usable with a limited Field of View (FoV). In regular WIP techniques, the provided FoV is always  $360^\circ$ , except in [Razzaque 02] where they used the redirected walking technique to simulate a  $360^\circ$  FoV in a 4-walls CAVE. In this chapter, our technique is evaluated with both LCD laptop screens to fulfill the Desktop VR pre-requisite or video projected output. Our method can also be used with the classical output used with WIP, i.e. with HMDs or CAVEs.

## 2.1.2 Walking Simulation

The main goal of our interaction technique is to translate the inputs of the user, i.e. head motions, into virtual motions in the VE. The user should be able to perform various motions while navigating in the VE. The lateral oscillations of the user's head are used to force the step duration, the locomotion state, as well as the advance speed. However, the WIP paradigm provide a larger range of inputs. Therefore, we propose another simple locomotion model for the SYH which integrates jumping and crawling locomotions.

### 2.1.2.1 Walking States

We implemented different locomotion states: walking, turning, jumping and crawling. To manage these different states, we added a state automaton to our algorithm (Figure 2.4). The state transitions are governed by the user head motions and the main inputs are the lateral velocity  $V_x$  and the vertical velocity  $V_y$ .

### 2.1.2.2 Forward State

The forward movements in the VE are governed by the lateral oscillations as main input. Our technique is designed to emphasis the idea of walking with a varying advance speed depending on the user head motions. The advance velocity  $V_a$  oscillates regularly, accordingly to the lateral head motions. One head oscillation period corresponds to one step. The footstep events are simulated by a null advance speed and correspond to a modification of the lateral velocity sign of the user's head. Thus, when the user's head reaches the

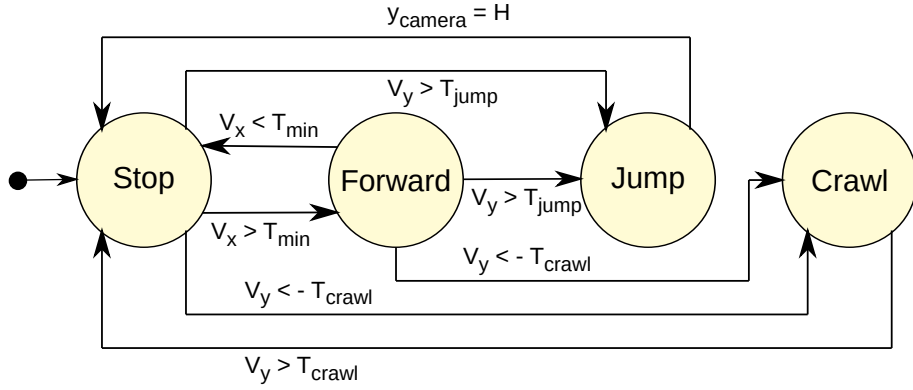


**Figure 2.4** – Walking state automaton: the main inputs are the velocities  $V_x$  and  $V_y$ .  $V_x$  allows the transition from the Stop state to the Forward motion;  $V_y$  allows the transition to the Jump or Crawl states.  $T_{min}$ ,  $T_{jump}$  and  $T_{crawl}$  are threshold parameters used to control the transitions.  $H$  is the reference height of the camera during the walk. The Turn motion is not represented as it can be activated in any state, depending on the head orientation.

maximal amplitude of the oscillations, the oscillating speed is null, as well as the advance speed, simulating a foot step.

For more realistic movements, we introduced two thresholds  $T_{min}$  and  $T_{max}$ .  $T_{min}$  allows to stop the forward movements when the lateral head motions are too small.  $T_{max}$  allows to avoid unrealistic high speed walks. The advance velocity  $V_a$  is computed in two steps in order to test these thresholds. The equations of  $V_a$  are:

$$\begin{aligned}
 V_{n1} &= \frac{\min(\text{abs}(V_x), T_{max})}{T_{max}} \\
 V_{n2} &= \begin{cases} 0 & \text{if } V_{n1} < T_{min} \\ V_{n1} & \text{otherwise} \end{cases} \\
 V_a &= V_{n2} * V_{max}
 \end{aligned} \tag{2.1}$$

Finally, the advance speed  $V$  of the camera inside the VE is adapted in function of the current locomotion state and is given by:

$$V = \begin{cases} V_a & \text{if } state = walk \\ 0.4 * V_a & \text{if } state = crawl \\ V_{max} & \text{if } state = jump \end{cases} \tag{2.2}$$

We chose normalized thresholds with the following values:  $T_{min} = 0.05$  and  $T_{max} = 0.5$ . We also set  $V_{max}$  to  $3.5 \text{ m} \cdot \text{s}^{-1}$ , corresponding to the maximal speed that can be achieved.

### 2.1.2.3 Jump and Crawl States

Comparing to existing WIP techniques, we chose to add 2 new states to the navigation possibilities in the VE: Jump and Crawl motions. The jump and crawl states are governed by the vertical oscillations of the user's head. If the vertical velocity exceeds normalized thresholds  $T_{jump}$  in upward direction and  $T_{crawl}$  in downward direction, the user can jump and crawl respectively in the VE. In practice, it means that the user will need to slightly jump or bend forward if he is seated, or jump or crouch down if he is standing. The user has to stand-up to stop crawling.

When a jump is detected, the vertical position of the camera is set to follow a classical parabolic trajectory defined by:

$$y_{camera} = \frac{1}{2} * g * t^2 + V * t \quad (2.3)$$

with  $g$  the gravity acceleration and  $t$  the time. The jumping state is left automatically while landing, i.e. when the camera reaches again its normal height  $H$  (known as the reference state when the algorithm starts). After preliminary testings, we set  $T_{jump} = 0.3$  and  $T_{crawl} = 0.4$ . While the crawling state is activated, the vertical position of the virtual camera  $y_{camera}$  is lowered by 1 m.

### 2.1.2.4 Turn State

In parallel to Forward, Jump and Crawl states, the user has the possibility to turn inside the VE in order to modify his navigation direction. During a turn in a normal walk, the human body leans slightly in direction of the center of the turn to compensate the centrifugal force [Courtime 03]. This phenomenon is often reproduced by video games players which can tend to lean in the direction of the turn even if it does not have any influence on their in-game trajectory. Thus, we choose to use this property to implement turns in our system as a control law based on the head orientation on the roll axis. To turn in the VE, the user has to lean his head in the left or right side respectively to turn left or right in the VE. The rotation speed  $V_r$  of the virtual camera is given by:

$$V_r = \begin{cases} V_{r_{max}} & \text{if } r > r_{max} \\ -V_{r_{max}} & \text{if } r < -r_{max} \\ 0 & \text{otherwise} \end{cases} \quad (2.4)$$

where  $r_{max}$  is the minimum angle of head inclination to start the rotation and  $V_{r_{max}}$  is the maximal angular speed of the rotations. In our experiment, we set  $r_{max} = 15^\circ$  and  $V_{r_{max}} = 45^\circ \cdot s^{-1}$ .

### 2.1.3 Visual Feedback Based on Camera Motions

To further emphasize the perception of walking in the VE, we extended the visual rendering of the WIP using camera motions driven by the user's head oscillations. There are existing models in the literature that make the virtual camera oscillating along the three axes ([Lécuyer 06] for example). However, the oscillations are totally independent from the user interactions.

We introduce a new model of camera motions adapted to the user's head motions. The camera oscillations along the different axes must follow the user in real time to maintain the coherency of the system. Thus we have implemented a novel visual feedback with camera motions along the vertical, lateral and advance axes.

#### 2.1.3.1 Advance Oscillations

The advance speed  $V$  of the view point already oscillates. The camera motions are indeed intrinsically linked to the advance velocity of the control law presented in [section 2.1.2.2](#).



As a result, extra camera motion is not necessary along this axis and the advance camera velocity corresponds exactly to  $V$ .

### 2.1.3.2 Lateral Oscillations

In order to move in the VE, the user has to make his head oscillating from left to right. Thus, as the user moves in front of the screen, his view point of the scene is modified to follow the head oscillations.

The lateral oscillations of the camera are computed as a function of the user's position. If  $d$  is the distance of the user to the screen and  $\alpha$  and  $\beta$  the opening angles of the webcam, the real world position of the user in front of the screen depends on the normalized coordinates  $x_n$  and  $y_n$ . The real world position of the user's head is given by the following coordinates:

$$\begin{cases} x_{real} &= x_n * d * \tan(\alpha/2) \\ y_{real} &= y_n * d * \tan(\beta/2) \end{cases} \quad (2.5)$$

Finally, the virtual camera is moved along the lateral axis by a distance  $x_{camera}$  equals to:  $x_{camera} = A_x * x_{real}$ . We set the scale factor  $A_x = 1$  to match the user's head displacement and thus generate the illusion that the screen is a window through which the user can observe directly the VE. However, other values can be used to amplify the camera motions for example. The webcam used during the experiment was such as  $\alpha = 30^\circ$  and  $\beta = 45^\circ$ .

### 2.1.3.3 Vertical Oscillations

The vertical oscillations of the camera can not be computed with the same algorithm as for lateral oscillations. In a desktop VR context the user can be seated and not be able to produce high vertical oscillations.

In our method, we propose to generate pseudo-sinusoidal vertical camera oscillations based on the current phase of the virtual gait cycle. Similarly to advance speed control law, the vertical amplitude  $y_{camera}$  of the camera oscillations is given by:

$$y_{camera} = V_{n2} * y_{camera}^{max} \quad (2.6)$$

where  $y_{camera}^{max}$  is the amplitude of the vertical oscillations for velocities greater or equal to the  $T_{max}$  threshold. For smaller speeds, the amplitude of the oscillations is proportional to this maximum, thus increasing the perception of the variations in advance speeds. Using the same factor between the camera motions and the advance velocity forces the synchronization, resulting in a smooth final visual rendering. In our implementation, we set  $y_{camera}^{max} = 15$  cm.

### 2.1.4 Conclusion

To summarize, our approach is composed of (1) an input interface based on the sole user's head movements, (2) a locomotion simulation in the VE composed of various possibilities such as jumping, crawling, turning, and (3) a visual feedback of walking relying on oscillating camera motions. The head motions are tracked along 3 DOF: lateral, vertical and

roll axis (Figure 2.3). These different physical motions are transposed in virtual movements thanks to a locomotion automaton (Figure 2.4). We then added oscillating camera motions (Equation 2.2, Equation 2.5 and Equation 2.6) to the visual feedback to enhance the walking sensation. The different control laws were parametrized after preliminary testings. But of course some parameters can be modified in order to amplify/decrease some effects during the locomotion simulation. Besides, other movement possibilities could also be envisaged and added to our automaton such as running state or backward movement.

## 2.2 Evaluation of the Shake-Your-Head

The evaluation of the proposed technique was performed using a comparison with classical techniques in Desktop VR. We chose keyboard and joystick peripherals for seated and standing positions respectively as they are often used in Desktop VR context. The experiments were conducted using 3D VE displayed on a screen and we investigated the effectiveness of our technique to travel complex paths composed of different gates placed in the VE.

In this chapter, we choose to not compare our technique to existing WIP techniques, and instead used more common interfaces that followed our low cost requirement. We conducted the evaluation of the proposed technique in both immersive Standing Up (SU) position and Desktop Sitting Down (SD) position. The keyboard and joystick were chosen respectively as the control conditions in the SD position and the SU position. Both keyboard and joystick peripherals are referred as Control techniques (Ctrl) in the following paragraphs. Our technique is referred with the “WIP” suffix.

### 2.2.1 Method

#### 2.2.1.1 Virtual Environment

The evaluation was performed within a 3D virtual environment without any contextual cues. The only landmarks were the gates that the user had to navigate through. A fog effect was added to mask the distant gates, allowing to perceive only the 2 or 3 closest gates. A texture on the ground provided useful visual flow information during the navigation. The scene was normally illuminated, and no shadows were drawn as illustrated in Figure 2.5.

#### 2.2.1.2 Population

Twelve participants (10 males and 2 females) aged from 22 to 35 (Mean  $M = 25.4$ , Standard Deviation  $SD = 3.35$ ) performed the experiment. Two participants were left-handed and none of them had known perception disorders. All participants were used to VEs but were naïve with respect to the proposed technique, as well as to the experimental setup and purpose of the experiment.

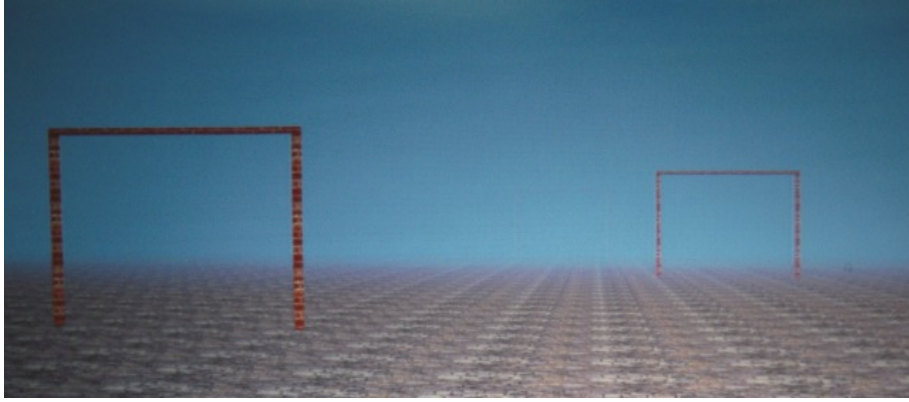
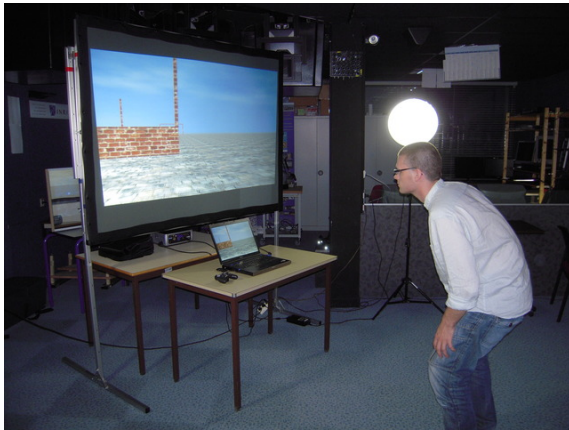


**Figure 2.5** – Virtual environment with different gates to represent the path that the user has to navigate through.

### 2.2.1.3 Experimental Conditions

The experiment was carried out in a room with controlled luminosity (using two projectors). There were two visual conditions corresponding to the two different configurations (SD and SU). The two configurations are illustrated in [Figure 2.6](#). For the SU configuration, participants were at a distance of 1.5 m in front of a 1.72 m large and 1.24 m height back-projected screen (physical field of view of  $60^\circ$  horizontally and  $45^\circ$  vertically). During the SD configuration, they sat in front of a 17 inches widescreen laptop screen (physical field of view of  $30^\circ$  horizontally and  $18.5^\circ$  vertically). In both cases, the resulting image had a resolution of  $1600 \times 1200$  pixels. We used monoscopic rendering, with a frame rate of 60 Hz. The projector used was a DepthQ Stereoscopic.



(a)



(b)

**Figure 2.6** – Description of the experimental setup for (a) the Stand-Up (SU) configuration, and (b) the Sit-Down (SD) configuration.

### 2.2.1.4 Experimental Apparatus

In our experiment, the goal was to compare our technique to classical interface devices (keyboard and joystick). During the experiment, the participants had to navigate in the VE through 3 different paths composed of 8 gates each. The 2 first paths, called Normal, were composed of 3 meters by 3 meters wide gates regularly disposed in order to form

a slalom. The third path, called Steeple, was composed of 1.5 meters high tunnels and 80 cm high fences (4 of each). For this path, the users had to jump and crawl to pass the gates, while the 2 other paths only required a simple navigation.

The classical interface devices were implemented as follows:

- **Keyboard:** Forward and turn motions were triggered using the forward, left and right arrow keys. The jumping was triggered by the left Shift key and the crawling by the left Control key.
- **Joystick:** Forward and turn motions were triggered using the left joystick of a gamepad. Jumping and crawling were triggered with two of the right buttons.

To provide a fair comparison between WIP and Ctrl conditions, the oscillating camera motions were also implemented in the two Ctrl conditions. To do so, we used the best implementation described in [Lécuyer 06]. Moreover, the Ctrl condition advance speed was set to match the WIP condition average advance speed, which had been measured in a preliminary phase.

The participants had to press the “Enter” key at the beginning of each block of conditions to launch the experiment. At any time during the experiment they had the possibility to make a break by pressing the “Space” key. After each trial, the participants were automatically teleported to the beginning of the next trial. A black screen displayed 2 s notified the beginning of the new trial.

#### **2.2.1.5 Experimental Plan**

The participants were exposed to 4 blocks of 18 trials each: one block for each of the possible combinations of the experimental conditions. The combinations were the following: (1) Sitting Down, using the keyboard (SD-Ctrl); (2) Sitting Down, using the our technique (SD-WIP); (3) Standing Up, using the joystick (SU-Ctrl); (4) Standing Up, using the proposed technique (SU-WIP).

The participants were split in 4 groups equally composed of 3 people each. Two groups started with the SD configuration and the 2 other with the SU configuration. We counter-balanced the conditions between them, meaning that the group starting with Ctrl condition in the SD configuration starts with WIP condition in the SU configuration. For each of the 18 trials of a block, the participants had to navigate through the 3 paths. The 12 first trials were composed only of the normal paths (6 for each, in a random order), and the last 6 trials corresponded to the steeple path.

#### **2.2.1.6 Collected Data**

The WIP techniques are generally evaluated only with subjective questionnaires to evaluate presence or cybersickness. In our evaluation, we added new criteria based on the task performed by the participants. Thus, we measured for each participant the task completion time for each trial and the percentage of success for the different gates. A subjective questionnaire was also proposed.

## 2.2.2 Results

### 2.2.2.1 Task Completion Time

For each participant, the task completion time of each trial was measured for the different experimental conditions. An exploratory analysis was first performed. A Principal Component Analysis revealed the presence of one spurious individual who has been taken out from the analysis. A specific analysis was developed to study the learning effect of the two conditions (Joystick/Keyboard and WIP techniques). A linear model where all conditions are mixed was fitted to explain the relation between the task completion times and the trial number. It revealed that the slope of the linear regression was significantly lower than zero ( $p < 0.001$ ), reflecting a significant decrease in the task completion time as the number of trials increases. The same analysis, where the first trial was removed, showed that the slope was not significantly different from zero anymore. In the following paragraph, the first trial was removed from the analysis as it corresponds to a learning effect.

A two-way ANOVA was performed on the 2 different conditions (Joystick/Keyboard and WIP techniques) and the 2 different positions (Sit-Down and Stand-Up). A post-hoc analysis using Tukey's procedure was then performed. The ANOVA was achieved separately for the two different types of paths (normal/steeple).

Concerning the normal path, the two-way ANOVA accounting for the conditions and the positions revealed a significant dependency between the position and the task completion time ( $F(1, 11) = 32.00$ ,  $p < 0.001$ ) and between the condition and the task completion time ( $F(1, 11) = 6.05$ ,  $p = 0.014$ ). Interaction between condition and position was also considered as a significant factor to discriminate task completion time ( $F(1, 11) = 27.19$ ,  $p < 0.001$ ). Post-hoc analysis showed that the task completion time in the SD-WIP configuration ( $M = 55.67$  s) was significantly lower than in the SD-Ctrl configuration ( $M = 61.72$  s), adjusted  $p < 0.001$ , in the SU-Ctrl configuration ( $M = 62.06$  s), adjusted  $p < 0.001$ , and in the SU-WIP configuration ( $M = 64.23$  s), adjusted  $p < 0.001$ . The other pairs of effects did not give any significant adjusted p-values.

The results concerning the different conditions are represented in [Figure 2.7](#) for Sit-Down and Stand-Up experiments respectively, for the normal path only. The results are ordered in function of the trials. The first trial was kept to illustrate the learning effect.

For the steeple path, the pre-analysis suggested the presence of a spurious individual and the existence of one learning trial. The two-way ANOVA accounting for the conditions and positions revealed a significant dependency between the position and the task completion time ( $F(1, 11) = 8.57$ ,  $p < 0.005$ ), and the condition and the task completion time ( $F(1, 11) = 11.89$ ,  $p < 0.001$ ). Interaction between condition and position was also considered as a significant factor to discriminate task completion time ( $F(1, 11) = 8.77$ ,  $p < 0.005$ ). Post-hoc analysis showed that the task completion time in the SU-WIP configuration ( $M = 86.07$  s) was significantly higher than in the SD-Ctrl configuration ( $M = 74.78$  s), adjusted p-value  $< 0.001$ , in the SU-Ctrl configuration ( $M = 74.72$  s), adjusted p-values  $< 0.001$  and in the SD-WIP configuration ( $M = 75.64$  s), adjusted p-values  $< 0.001$ . The other pairs of effects did not give any significant adjusted p-values.

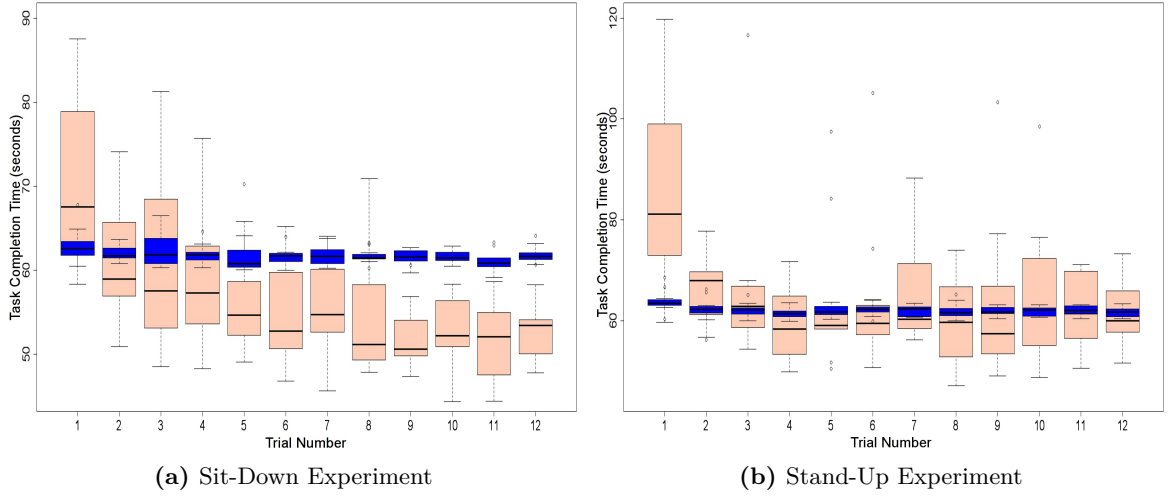


**Figure 2.7** – Task completion time for the two different techniques on normal paths for (a) SD experiments and (b) SU experiments. The blue and red light colors correspond to the Ctrl and WIP conditions respectively. Each boxplot is delimited by the quartile (25% quantile and 75% quantile) of the distribution of the condition over the individuals. The median is also represented for each condition.

### 2.2.2.2 Accuracy

For each participant and for each trial, the percentage of errors for the different paths was measured. The two types of path (Normal and Steeple) are separated. The resulting percentages are for the normal path: 0.61% of error for SD-WIP configuration, 0% of error for SD-Ctrl configuration, 1.39% of error for SU-WIP configuration, 0.09% of error for SU-Ctrl configuration.

The resulting percentages are for the steeple path: 20.49% of error for SD-WIP configuration, 7.81% of error for SD-Ctrl configuration, 27.28% of error for SU-WIP configuration, 13.19% of error for SU-Ctrl configuration. We found a significant effect between Ctrl and WIP techniques for the steeple path.

### 2.2.2.3 Subjective Questionnaire

After Sit-Down and Stand-Up configurations, a preference questionnaire was proposed in which participants had to grade from 1 (low appreciation) to 7 (high appreciation) the four different conditions (SD-Ctrl, SD-WIP, SU-Ctrl, SU-WIP) according to 9 subjective criteria: (a) Fun, (b) Easiness of Use, (c) Intuitive, (d) Accuracy, (e) Presence, (f) Walking realism, (g) Fatigue, (h) Cybersickness and (i) Global appreciation. [Figure 2.8](#) shows the results concerning the grades (Likert-scale) obtained by the two different techniques for each of the subjective criteria, for the two experimental conditions (SD and SU). The grade 7 for Fatigue and Cybersickness respectively means that the technique does not induce any fatigue and does not imply any cybersickness feeling.

Concerning SD configuration, no significant effect was found for the following criteria: Intuitive ( $p = 0.052$ ) and Cybersickness ( $p = 0.12$ ). Concerning SU configuration, no significant effect was found for the following criteria: Intuitive ( $p = 0.3$ ), Walking realism ( $p = 0.19$ ) and Cybersickness ( $p = 0.21$ ). We found a significant effect for all other criteria.



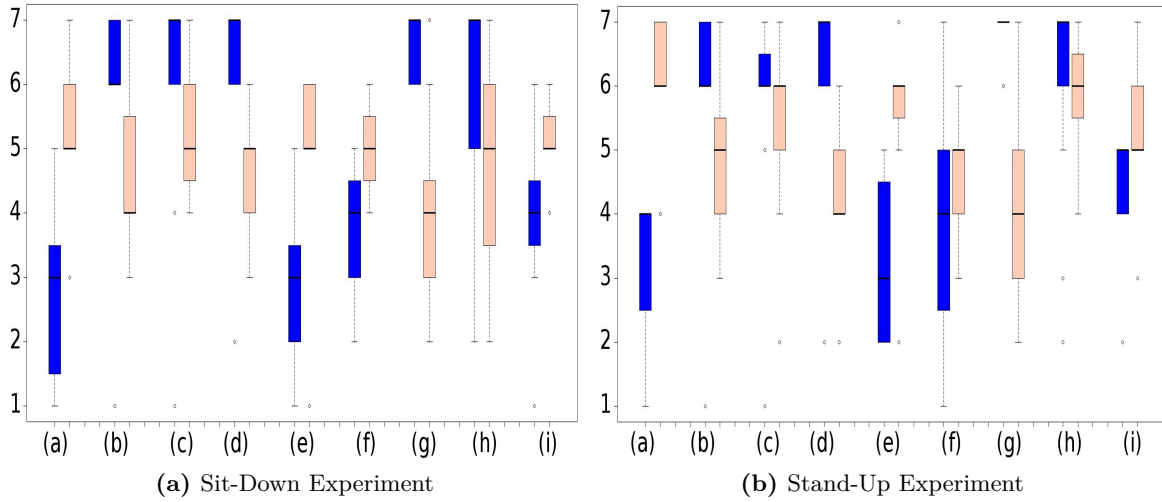


**Figure 2.8** – Results for subjective rating for the two different techniques for (a) SD experiments and (b) SU experiments. The blue and red light colors correspond to the Ctrl and WIP conditions respectively. The subjective criteria are (a) Fun, (b) Easiness of Use, (c) Intuitive, (d) Accuracy, (e) Presence, (f) Walking realism, (g) Fatigue, (h) Cybersickness and (i) Global appreciation. Each boxplot is delimited by the quartile (25% quantile and 75% quantile) of the distribution of the condition over the individuals. The median is also represented for each condition.

In particular, our technique was better ranked for Fun, Presence and Global Appreciation, for both configurations.

### 2.2.3 Discussion

Our results suggest that the Shake-Your-Head (SYH) technique can allow efficient navigation even compared with standard and well-known input devices such as keyboards and gamepads. The participants could sometimes go even faster with WIP, without any strong loss in precision. The WIP-based interaction seems also fast to learn, after only a couple of trials. The technique is well appreciated and perceived as more immersive and more fun than classical configurations.

The quick learning of our technique could be explained by the fact that interfaces based on webcam are generally intuitive and simple to learn [Polaine 05]. After the learning phase, WIP tends to become faster than the keyboard in sitting condition. One explanation could be that with our technique (but also with the joystick in the standing condition) we could observe that participants tended to turn without stopping their advance motion. On the contrary, with the keyboard condition, participants tended to walk and turn sequentially, which might have globally increased the task completion time. Another explanation could be that, in our implementation of WIP, the advance speed is influenced by the speed of lateral movements. The seated position allows the user to make faster oscillations than the standing position, and thus to accelerate the walking motion by making fast lateral oscillations. Interestingly, these faster motions did not impair the precision of users.

The longer task completion time observed for WIP in the steeple paths (involving jumping and crawling motions) could be due to unexpected behaviors which induced incorrect transitions in our locomotion automaton. Indeed, some participants acted as if they were

“anticipating” the jumps and bent down prior jumping. We could easily fix this problem in the future by using additional conditions in our automaton based on both speed and position.

Results from the questionnaire are very consistent with previous subjective evaluations of WIP [Usoh 99]. In our study, the WIP is more appreciated, and is perceived as more fun, and improving presence. As expected, more standard techniques (i.e. joystick and keyboard) are found easier to use, more precise, and less tiring (as they induce less physical movements). Interestingly, impression of cybersickness is not increased by WIP. This could be due to our desktop (and thus less immersive) configurations. Last, realism of walking in the VE was significantly improved only in the sitting condition. The perception of walking with WIP is actually quite complex, as participants wrote: “we have the impression to be a video game character”, “the motions are exaggerated”, or “we really have the sensation of walking, and not running”. In the standing condition, some participants found that the physical motions were closer to “skiing” or “skating”, as they noticed that they did not lift their feet from the ground but only oscillated their body. For these people we could further stress in the future that our implementation of WIP still works very well when lifting the feet and walking in place, as the oscillations of the head can be captured the same way in both situations (lifting the feet or not).

Taken together, our results suggest that our Shake-Your-Head technique could be used in a wide range of applications, when navigating in a 3D world, in sitting or standing configurations. It seems to be both a low-cost and an efficient paradigm that can match a lot of walking motions. It could thus be used for training in VR with more physical engagement (military infantry, vocational procedures), or more realistic virtual visits such as for project review in architecture or urban planning.

## 2.3 Analysis of the Virtual Trajectories Generated with the Shake-Your-Head

In this section, we propose to evaluate quantitatively the navigations produced with the SYH. We analyze and compare the trajectories produced by the SYH with ones produced by joystick on slalom paths.

This analysis is based on the experimental data collected in the experiment described in [section 2.2](#). However, we only conducted the analysis on the data corresponding to the standing position. Therefore, the trajectories produced by the SYH (WIP condition) are compared to trajectories produced by the joystick. Moreover, the steeple path was also removed from the analysis to remove any possible interference of the jumping and crawling commands.

### 2.3.1 Trajectories Analysis

The proposed evaluation is based on both spatial and temporal analysis. Moreover, the spatial analysis focuses on both macroscopic and microscopic aspects of trajectories.



### 2.3.1.1 Spatial Analysis

The produced trajectories are time parametric functions. However, some relevant information can be extracted from the shape of the trajectories, independently of time.

**Shape of the Trajectories.** To stress the differences of trajectories between the SYH and joystick conditions, we represented all the trajectories in accumulation buffers to produce graphical representations of the trajectories for each path. The results for the joystick and SYH conditions on the first normal path are displayed [Figure 2.9](#).

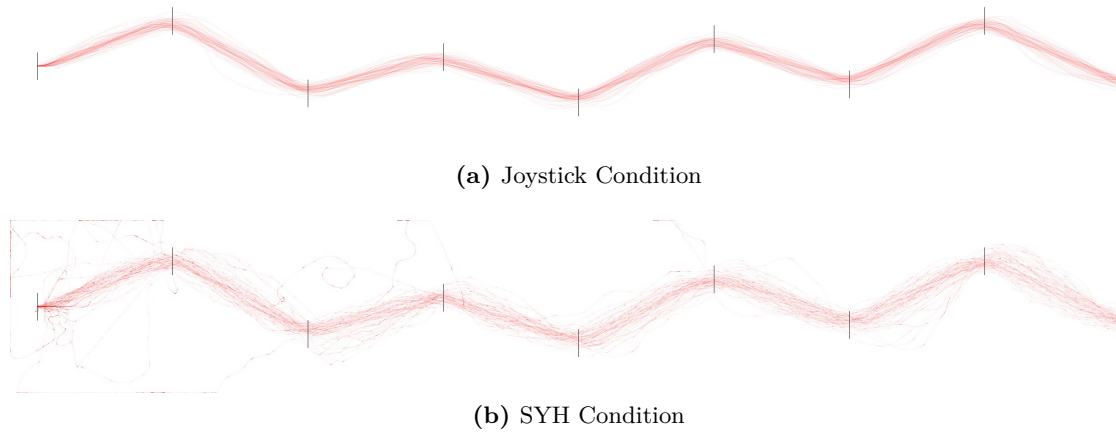


**Figure 2.9** – Accumulated trajectories for the first path. The gates are represented in black and the trajectories in red. The brighter red colors indicate more frequently crossed areas. The participants were traveling from the left to the right.

The graphs stress the differences between the two conditions. First, we can notice that the participants had two very different behaviors for the joystick condition. Indeed, a majority of them tried to get as close as possible from the shortest trajectory while others chose to do long regularly curved trajectories. However, in both cases, the trajectories seem smooth and regular. On the other hand, with the SYH condition, the trajectories seem more dispersed and do not follow the shortest trajectory. Moreover, the trajectories display more frequent and sudden turns.

**Distance to Shortest Trajectory.** To characterize the differences between the two conditions, we computed for each participant the mean difference between the produced trajectories and the shortest trajectory for each condition. The shortest trajectory was defined as the trajectory composed of straight lines between the inner post of each gate.

We conducted a one-way repeated measure ANOVA on the technique used (joystick and SYH). The ANOVA revealed a significant dependency between the distance to the shortest trajectory and the interaction technique used ( $F(1, 11) = 16.94$ ,  $p = 0.002$ ). The area between the trajectory and the shortest trajectory is significantly smaller with the joystick technique ( $M = 86.55 \text{ m}^2$ ) compared to the SYH technique ( $M = 110.93 \text{ m}^2$ ).

**Mean Trajectory.** To further stress the differences between the two techniques, we computed the mean trajectory for all participants for each set of conditions for the two paths. In order to be able to compute the mean trajectories, we re-sampled the trajectories with

samples every 1 m in the forward direction. The new samples were computed as the mean of all the values in the sample interval. A sample of the mean trajectories for the joystick and SYH conditions on the first path is displayed in Figure 2.10. The standard deviations of the mean trajectories represented in Figure 2.10 stress higher variability of the trajectories produced with the SYH technique. Moreover, the behavior during the crossing of the gates seems to be different.

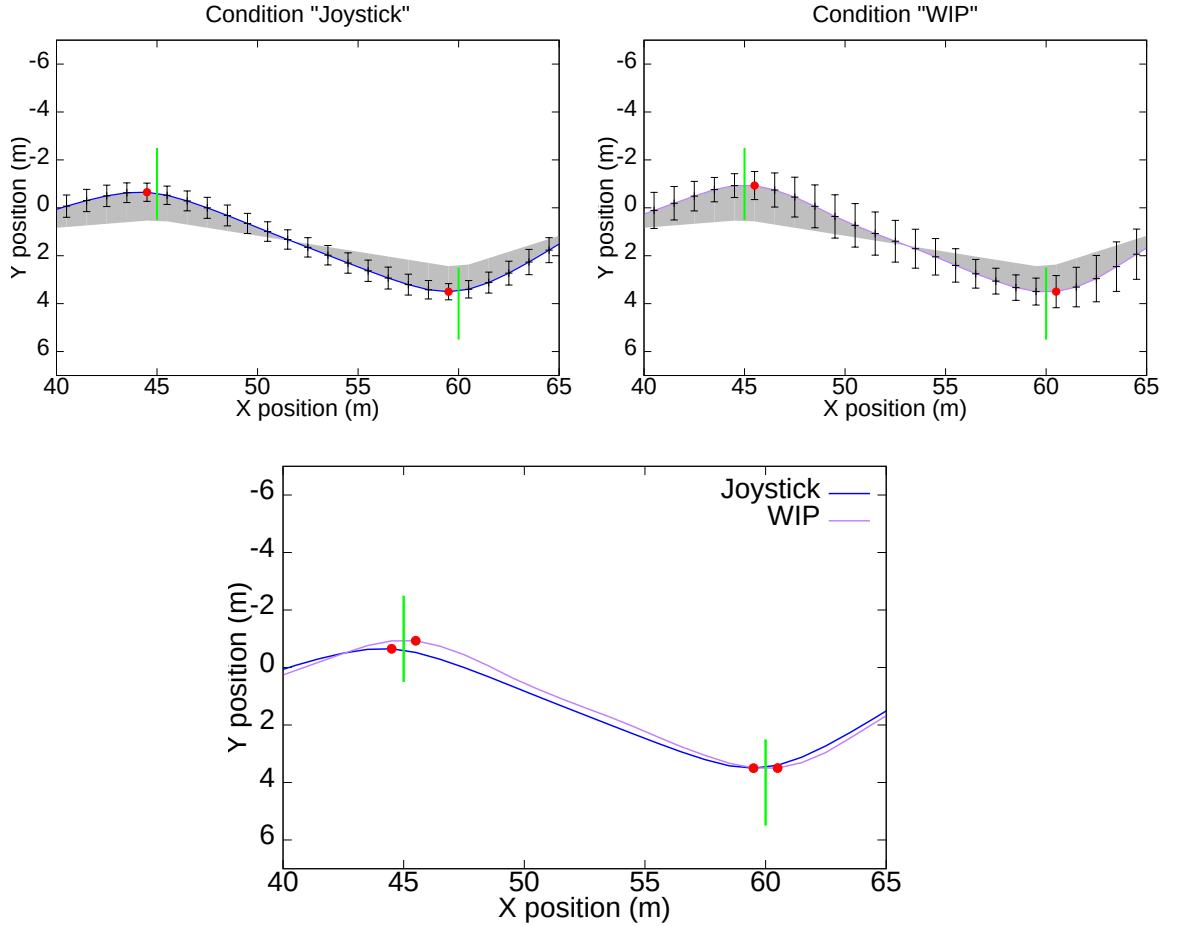


**Figure 2.10** – Samples of the mean trajectories of SYH and joystick. The error boxes represent the standard deviations. Gates are represented in green, the distance to the shortest trajectory in gray and the inflexion points in red.

For each gate of the 2 mean trajectories, we computed the signed distance of the inflexion point to the closest gate, as well as the distance to the center of the gate when the users crossed the gates. For both criteria, we conducted a one-way repeated measure ANOVA on the technique used (joystick and SYH). We found a significant effect of the technique on the position of the inflexion points ( $F(1, 13) = 17.33$ ,  $p = 0.001$ ). With the SYH technique the inflexion point is located after the gate ( $M = 0.14$  m), while it is located before with the joystick technique ( $M = -0.42$  m). We also found a significant effect of the technique on the distance to the center of the gate during the crossings ( $F(1, 13) = 34.75$ ,  $p < 0.001$ ). Thus, the user crossed the gates closer to their centers with the SYH technique ( $M = 0.38$  m) compared to the joystick ( $M = 0.63$  m). In other words, with the SYH technique, the participants turned after crossing the gates, while they turned before with the joystick.

**Curvature of the Trajectory.** In order to further stress the differences in the behavior during the turns, we focused our analysis on the curvature of the trajectories. We computed the curvature at a microscopic level of trajectories parametrically defined as plane curves over time. This elicits a high difference in magnitude of curvature peaks between SYH and joystick. The Figure 2.11 illustrates this difference for two trials of the 6<sup>th</sup> participant. The signal made of the curvatures of the trajectory over time is composed of impulses. In order to count and detect impulses, we used a first order continuous-time low-pass filter with a cut-off frequency of 10 Hz to filter the computed curvatures, and set a detection threshold for impulses at  $0.02 \text{ m}^{-1}$ .

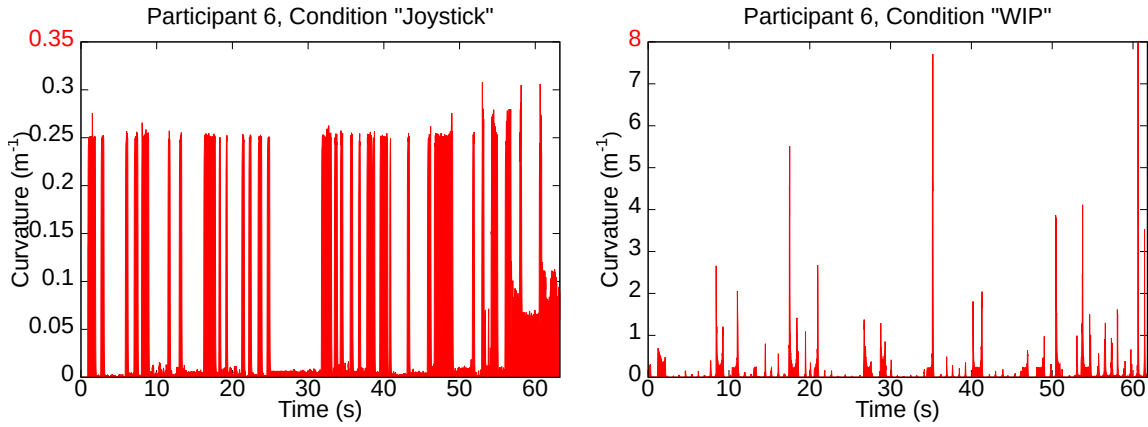


**Figure 2.11** – Curvatures of trajectories for two trials of the 6<sup>th</sup> participant.

To characterize the properties of the curvature for the different conditions, we computed 3 different criteria based on the detected impulses: (1) the number of impulses per trial, (2) the length of the impulses (in seconds) and (3) the area of each impulse. For each criterion, we computed the mean for each participant and we conducted a one-way repeated measure ANOVA on the technique used (joystick and SYH). The analysis revealed a significant dependency to the technique used for all 3 criteria. The results are summarized in Table 2.1.

Criterion	$F(1, 11)$	$p$
Number of impulses	30.27	< 0.001
Length of impulses	13.43	0.004
Area of impulses	6.77	0.025

**Table 2.1** – Results of the ANOVA on the curvature criteria.

The participants significantly turned more often with the SYH technique ( $M = 1108.9$ ,  $SD = 284.6$ ) than with the joystick ( $M = 608.9$ ,  $SD = 77.2$ ). However, they turned significantly for a shorter amount of time with the SYH ( $M = 0.33 \text{ s}$ ,  $SD = 0.08$  and  $M = 0.45 \text{ s}$ ,  $SD = 0.07$  respectively). Finally, the area of impulses revealed that the participants significantly turned more with the SYH technique ( $M = 0.19 \text{ s} \cdot \text{m}^{-1}$ ,  $SD = 0.14$ ) than with the joystick ( $M = 0.08 \text{ s} \cdot \text{m}^{-1}$ ,  $SD = 0.02$ ).

### 2.3.1.2 Temporal Analysis

**Speed.** We computed the advance speed of the participants depending on the experimental conditions. We filtered and re-sampled the data using the same method as with the computation of the mean trajectories. To characterize the speed behavior during the trajectories, we computed the average speed for all participants at each gate. We conducted a one-way repeated measure ANOVA on the technique used. We found a significant effect of the technique used on the speed at each gate ( $F(1, 13) = 195.46$ ,  $p < 0.001$ ). The users were faster with the SYH technique ( $M = 2.48 \text{ m} \cdot \text{s}^{-1}$ ,  $SD = 0.1$ ) compared to the joystick technique ( $M = 2.10 \text{ m} \cdot \text{s}^{-1}$ ,  $SD = 0.007$ ). These results suggest that participants tended to cross the gates at full speed with the SYH technique.

**Smoothness.** The maximum smoothness model [Pham 07] was used as another criterion. According to this model, natural motions tend to be as smooth as possible to minimize the energy involved. For each participant, we computed the mean value of the integrated absolute value of the jerk over the time for each trajectory. Greater jerk corresponds to a smaller smoothness of the trajectory and thus can be considered as less natural. A one-way repeated measure ANOVA on the technique used (joystick and SYH) revealed a significant dependency between the cumulated jerk and the technique used ( $F(1, 11) = 59.56$ ,  $p < 0.001$ ). The trajectories are smoother with the joystick technique ( $M = 10.7 \text{ m} \cdot \text{s}^{-2}$ ,  $SD = 1.6$ ) compared to the SYH technique ( $M = 197.5 \text{ m} \cdot \text{s}^{-2}$ ,  $SD = 84.0$ ). Thus, the trajectories produced by the joystick seem to be closer to realistic natural walking trajectories compared to SYH, according to the smoothness model [Pham 07].

### 2.3.2 Discussion

Our results show strong differences between trajectories produced by the SYH and the joystick, according to different criteria. The characteristics of the curvatures highlight more frequent and tighter changes in direction with the SYH technique. It seems that the users were not able to predict their future trajectory accurately with the SYH technique, resulting in a continuous adaptation of the advance direction. The position of the inflexion points and the distance to the center of the gates at each gate are consistent with this hypothesis. The implementation of the turns with the SYH might explain those results. Indeed, if the user's head oscillations were too important, turns could be triggered inappropriately.

Moreover, our results suggest that the trajectories produced with the SYH technique are less "efficient" in terms of traveled distances as well as naturalness compared to those made using the joystick. This difference could be explained by the difference in training of the participants. Indeed, all of them were proficient with the joystick but were using SYH for the first time. The control law for turns can be another reason, as the participants were apparently less able to choose their direction accurately with the SYH technique.

Finally, the curvature of the trajectories is clearly more important with the SYH technique. The participants tended to follow tighter turns. However, the underlying implementation of the turns for both joystick and SYH conditions were strictly identical. Thus, the participants decreased their speed during the turns with the SYH. The users seem more able to modulate their speed precisely with the SYH, which provided more varied navigation

patterns. These results could provide guidelines for future implementations of turns when designing a SYH technique.

### 2.3.3 Conclusion

In this section, we compared a SYH technique to the joystick interface. When observing slalom trajectories produced with both techniques, we found that the navigation strategy of the user was different with the SYH technique compared to the joystick. The participants had more difficulty to anticipate their trajectory with the SYH. We also found that the speed during the turns decreased and the user modulated their speed more precisely with the SYH technique. The trajectories produced by the SYH had more jerk than those produced by the joystick and thus were less likely to feel natural for the users. However, the SYH provided a better control of advance speed while the joystick was more precise for controlling direction.

## 2.4 Conclusion

This chapter presented a new interaction technique for navigation in VR. Our technique is designed for efficient and ecological navigations simulating the human walk. Moreover, our technique was designed to be affordable even for applications designed to large audiences, such as training simulations or video games for example.

We proposed to revisit the whole pipeline of the Walking-In-Place technique to match a larger set of configurations and apply it notably to the context of Desktop Virtual Reality. We have introduced the Shake-Your-Head (SYH) technique using as sole input the head movements of the user. It can be used in a desktop configuration with the possibility for the user to sit down and to navigate in the VE through small screens and standard input devices such as a basic webcam for tracking. We implemented various motions such as turning, jumping and crawling in the locomotion simulation. We also introduced the use of additional visual feedback based on camera motions to enhance the walking sensation.

We conducted an experiment in order to evaluate the SYH technique compared to standard techniques such as keyboard and joystick. In this experiment, participants had to walk through series of gates forming a slalom path. The evaluation was performed both in immersive and desktop configurations. We notably found that WIP technique only requires a small learning time to allow faster navigation in seated position compared to the keyboard. Moreover, our technique was more appreciated and considered as more fun and inducing more presence than the other classical techniques.

We also compared the trajectories produced by the SYH technique in standing position with similar trajectories produced using a standard joystick. We found that the users had different navigation strategies for each technique: the users exhibited a more precise control over their advance speed with the SYH technique, but anticipated the turns better with the joystick. Moreover, the trajectories were smoother with the joystick technique. Taken together, those results provide useful information that could be used to further improve the SYH technique, especially concerning the turns.

# King-Kong Effects: Improving Sensation of Walking with Visual and Tactile Vibrations at each Step 3

## Contents

<b>3.1 Concept of King Kong Effects</b> . . . . .	<b>70</b>
3.1.1 Step Simulator . . . . .	71
3.1.2 Visual King Kong Effects . . . . .	73
3.1.3 Tactile King Kong Effects . . . . .	74
3.1.4 Conclusion . . . . .	76
<b>3.2 Evaluations of the King Kong Effects</b> . . . . .	<b>76</b>
3.2.1 Method . . . . .	76
3.2.2 Experiment 1: Selecting the Best Visual Vibration Pattern for KKE . .	77
3.2.3 Experiment 2: Testing the Combination of Visual KKE and Oscillating Camera Motions . . . . .	79
3.2.4 Experiment 3: Selecting the Best Tactile Vibration Pattern for KKE . .	81
3.2.5 Experiment 4: Testing Participant Preference for Multimodal KKE . . .	82
<b>3.3 Discussion</b> . . . . .	<b>84</b>
<b>3.4 Conclusion</b> . . . . .	<b>85</b>

To improve immersion when navigating in Virtual Environments (VE), researchers have developed numerous kinds of sensory feedbacks. For example, Lécuyer et al. [Lécuyer 06] proposed to use Camera Motions (CM) to reproduce the walking oscillations of the user's point of view during navigation in VR. The point of view oscillates in the VE to generate the visual flow that would be produced by a real walk. They demonstrated that their approach not only improves the user's sensation of walking in VE, but also his immersion [Lécuyer 06].

Another solution to improve immersion in VR consists in cumulating different types of sensory feedback [Bowman 05]. Visual feedback can be combined with audio or haptic feedback, for example, resulting in a fully multimodal walking simulation [Visell 10b]. A typical example can be found in video games which provide not only visual feedback, but also auditory and sometimes vibrotactile modalities.

In this chapter, we propose a new technique to enhance the sensation of walking in VE inspired by special effects in Hollywood movies. The King Kong Effects (KKE) (Figure 3.1) provide a new kind of sensory feedback that simulates the feet touching the ground at each step by producing Visual and Tactile vibrations. The KKE can be used in a seated position,

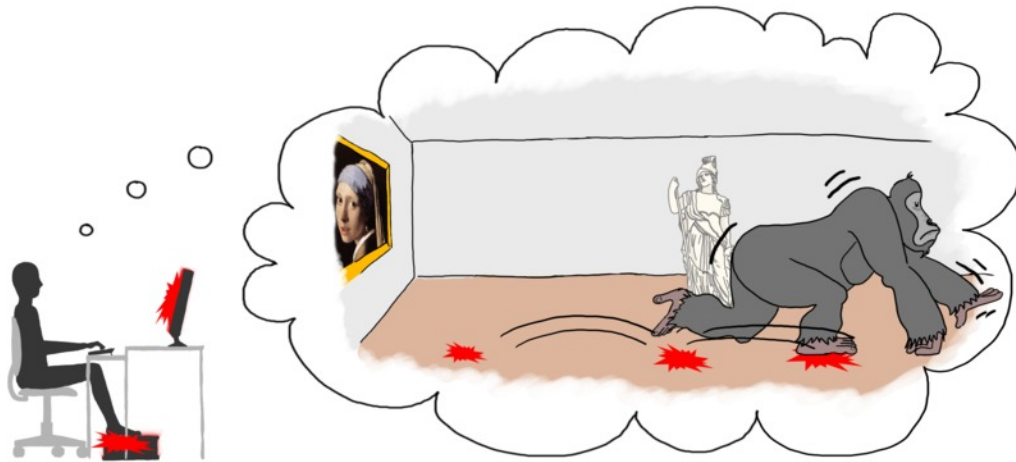


**Figure 3.1** – Concept of the King Kong Effects: Visual and Tactile vibrations inspired by special effects in movies enhance the sensation of walking in VE. Visual and Tactile feedbacks are generated at each step made in the VE.

and we designed different vibration patterns based on physical and metaphorical models. As a result, we propose a new concept of sensory feedback effects, which correspond to the four main innovations claimed in this chapter:

- **A step simulator.** We introduce a simple biomechanically-based model to compute the footstep events, and the different contacts of the feet with the ground.
- **New visual effects.** We introduce the use of visual vibration patterns which simulate the contact of the feet with the ground at each step. Moreover, we simulate both the contacts of heel and toe. We propose and study vibration patterns along either vertical or horizontal directions.
- **New vibrotactile effects.** We also introduce new vibrotactile feedbacks generated under the feet of the user to reproduce the step sensation. Again, we simulate both the contacts of the heel and toe. Moreover, we propose two different vibration pattern metaphors: (1) a physically based metaphor and (2) a metaphor where the stimulation is proportional to the force pressure applied by the feet on the ground.
- **Evaluation.** Finally, we evaluated the different vibration patterns for both modalities. We also investigated the influence on the Visual KKE of another visual technique, the Camera Motions [Lécuyer 06]. We also evaluated the KKE in a multi-modal context with the modalities taken individually or all together.

The remainder of this chapter is organized as follows: in [section 3.1](#) we introduce the King Kong Effects (KKE). We detail the Step Simulator used to generate the footstep events and we introduce our novel visual and vibrotactile patterns. In [section 3.2](#) we describe the results of a set of experiments conducted to identify the best parameters and best combinations of KKE.

### 3.1 Concept of King Kong Effects

We propose a new technique to enhance the sensation of walking in VE in desktop mode. The KKE is based on visual and tactile vibration patterns generated at each virtual step



to simulate the contacts of the feet with the ground. Our technique can be used in static position, such as when seated or standing, whereas the user controls the virtual walk with any input device (joystick, keyboard, etc.).

The KKE are inspired from famous Hollywood movies such as King Kong or Godzilla where the walk of gigantic creatures is emphasized to make the spectators “feel” the steps of the incoming creature. For instance, Jurassic Park’s T-Rex produces earth vibrations which generate waves in water, while Godzilla generates electrical disturbances. More recently, complex motions of the camera were used in movies like King Kong or Transformers to achieve the same goal. Our effects are, in a way, reproducing the special effects demonstrated in these movies for desktop VR technologies for the user himself, and are thus named “King Kong Effects” (KKE).

At each virtual step, the user can feel the sensation of hurting the ground with both visual vibration of the camera and vibrotactile feedback under his feet. For each modality, we propose a set of different vibration patterns. Visual and tactile vibrations can be used individually or together for a multimodal simulation. Moreover, existing auditory simulation of footstep sounds could be easily added to the KKE for even higher immersion.

The software architecture behind KKE is composed of three parts: the Step Simulator (1) is designed to compute footstep events based on a simple biomechanical model. Then, two different sensory feedback components corresponding to the visual (2) and vibrotactile (3) modalities have been developed to enhance the walk in the VE based on the generated footstep events ([Figure 3.2](#)).

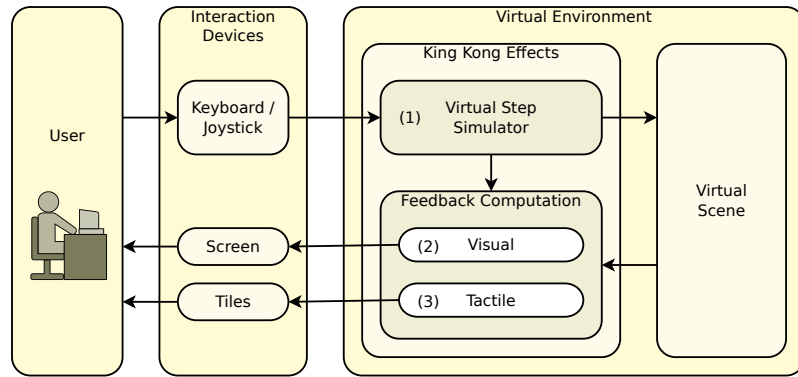


**Figure 3.2** – Architecture of the KKE. The user inputs are processed by the Step Simulator to generate footstep events. The events are used to generate visual and vibrotactile feedback.

### 3.1.1 Step Simulator

To compute the virtual footsteps events in the VE, we need a simple yet realistic biomechanical model. Contrarily to existing techniques, the KKE do not rely on force sensors to detect the footsteps. The users should have the possibility to use the KKE even when seated using desktop VR applications, in which case the force sensors would be ineffective. However, they must be generated in a realistic way accurately reflecting the different user’s interactions. Furthermore, the system must be compatible with different kinds of interaction devices, like a keyboard or a joystick for example.

To solve this problem, we propose a biomechanically inspired model that can generate

footstep events in real-time based on a given advance speed. First, we use the classical decomposition of the walking motion in events given by Vaughan [Vaughan 92]: (1) Heel Strike (HS), (2) Heel Off (HO), (3) Toe Strike (TS) and (4) Toe Off (TO). Using this formalism, most of the human walking gaits can be described as a succession of different events in a precise time and order. For example, walking, running, sprinting or even jumping can be described by such sequences associated with a global advance speed. The positions of these events during the walking cycle are shown in Figure 3.3.

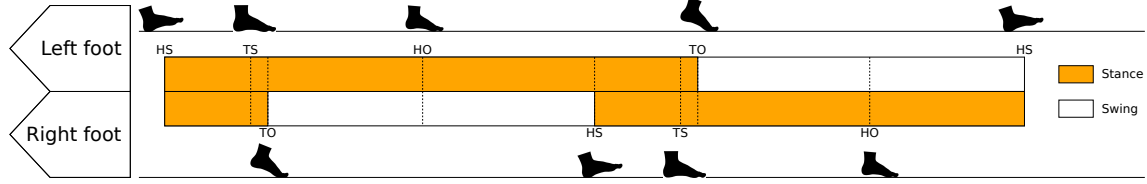


**Figure 3.3** – Walking cycle. The events of contact and separation of the heels and toes are placed accordingly to the position of the feet during the cycle. The parts of the cycle in orange correspond to the moments when the feet are in contact with the ground.

The position of each event in the gait cycle can be predicted. In our implementation, we used the data presented by Novacheck [Novacheck 98] for a regular walking motion, i.e. if the half-cycle is defined to start with HS, TS and HO will be at 21% and 60% of the half-cycle respectively, while TO and HS of the opposite foot will happen at 24% and 100% respectively (Figure 3.3).

To generate the events, we need to determine the gait half-cycle length  $T$ , to know the accomplished percentage of the cycle. For the walk, the advance speed is given by [Alexander 03]:

$$v = L * f \quad (3.1)$$

where  $v$  is the advance speed,  $L$  the step length and  $f$  the step frequency defined as  $\frac{1}{T}$ . Thus we have:

$$T = \frac{L}{v} \quad (3.2)$$

However, while  $v$  is obviously dependent on the users interactions, it can be easier to compute it from a factor of the interactions and the speed of comfort  $v_c$  for a given gait. For the walk, the speed of comfort can be estimated using a simple model interpolated from experimental data [Kuo 01]:

$$L \sim v_c^\beta \quad (3.3)$$

with  $\beta$  being a constant which equals to 0.42 for adults. With  $I$  the input speed in percentage of the comfort speed, such as  $v = I * v_c$ , we obtain:

$$T = \frac{L}{I * e^{\frac{\ln(L)}{\beta}}} \quad (3.4)$$

Thus,  $T$  depends on  $I$ : the gait cycle length can change in the middle of one step, which would be unrealistic and could induce implementation troubles. Thus, the value of  $T$  must be updated only at the beginning of each new step.

For example, for a step length  $L = 1$  m, at the comfort speed, the duration of one step  $T$  is 1 second, and thus the contact of the toe will happen 210 milliseconds after the contact of the heel of the same foot. Similarly, the heel will be off the ground 600 milliseconds after

its initial contact, and the toe of the opposite foot will leave the ground 240 milliseconds after the initial heel strike.

Finally, our Step Simulator can generate footstep events using only a percentage of the comfort advance speed and the virtual avatar size as input. The events are generated using a simple biomechanical model, and can be used to synchronize our KKE.

### 3.1.2 Visual King Kong Effects

Based on the generated events for the heels and toes contact, each step can be visually simulated using KKE: the technique is based on the metaphor of visual vibrations produced by each step.

A first metaphor considers the vibration from the point of view of the “creature” as a result of the feet hurting the ground and thus producing **Vertical (V)** vibrations. Moreover, a second metaphor emphasizes the point of view from the environment point of view, as each step produces **Horizontal (H)** seismic vibrations when the feet of a heavy virtual avatar hit the ground.

We simulated two types of vibration patterns with 1 and 2 successive contacts of the feet with the ground respectively: contact of the heel alone (**1 contact**) as used in most movies, and a combination of the heel and toe strike together (**2 contacts**) to provide a more realistic biomechanical simulation.

All different combinations were tested resulting in 4 different types of vibrations (Figure 3.4). Thus, the Visual KKE can be described by the function  $K_V(x, y)$  with  $x$  the direction of the vibrations ( $x \in \{V, H\}$ ) and  $y$  the number of contacts ( $y \in \{1, 2\}$ ).

The vibration model is based on a Rigid Contact Model (RCM) used in haptic simulations for the contact between two rigid objects [Okamura 98]. The vibrations of the camera are based on high frequency sinusoidal oscillations with an exponentially decaying envelope:

$$Q(t) = A(v)e^{-Bt}\sin(\omega t) \quad (3.5)$$

where  $Q(t)$  is the produced vibration,  $A(v)$  the attack depending of the starting velocity  $v$ ,  $\omega$  the frequency of the oscillations and for a given material  $B$  is the decay constant of the envelope.

Values of  $\omega$  and  $B$  can be found for different materials in the literature [Okamura 98]. However, the visual rendering strongly depends on the display device frame rate. If the frame rate is too low or the vibration frequency too fast, the user will not be able to perceive the vibration correctly. After preliminary testing, the decaying value  $B$  was set to be twice the interval between HS and TS, i.e. 0.3 s and we used a constant amplitude for the attack ( $A_{HS} = 7$  cm and  $A_{TS} = 3$  cm). Finally, our preliminary tests showed that the value of  $\omega$  should be inferior to twice the display frequency. In our implementation, we chose  $\omega = 67$  Hz corresponding to a ground made of wood.

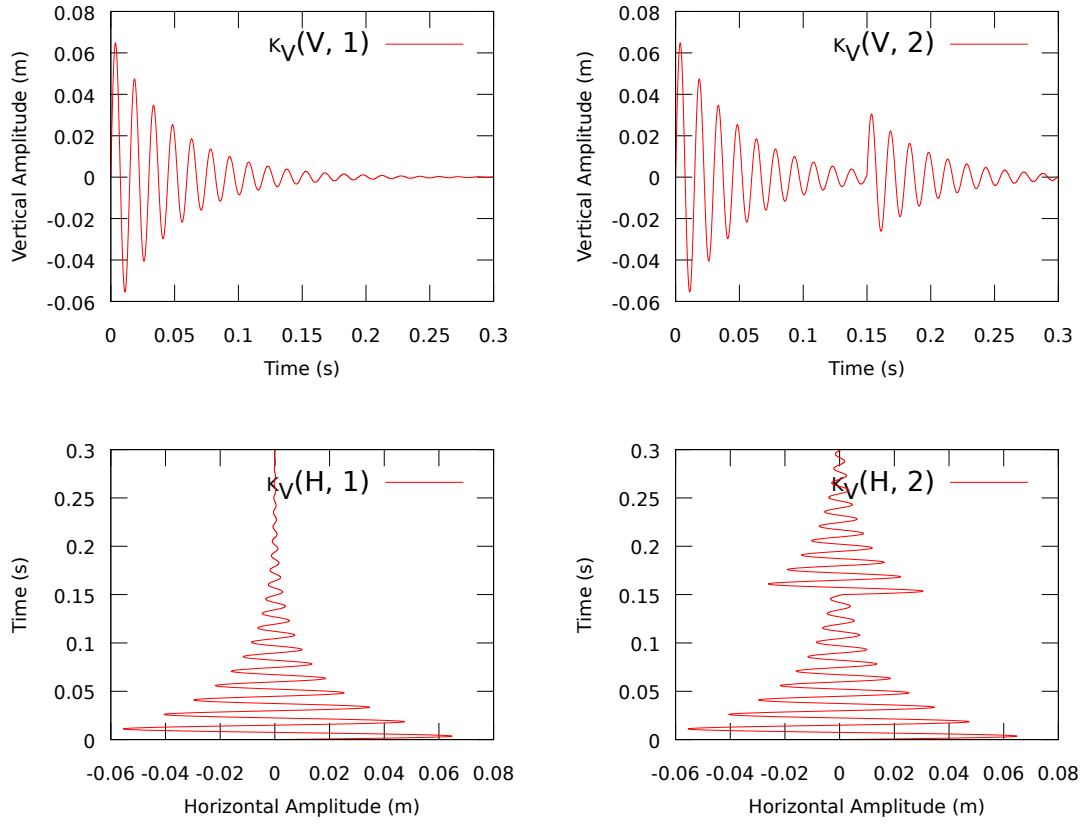


**Figure 3.4** – Vibration patterns for the Visual KKE. Amplitude (in meters) over Time (in seconds) of the vibration patterns used for the Visual KKE: 1 or 2 contacts in Vertical and Horizontal directions.

### 3.1.3 Tactile King Kong Effects

We also designed a set of vibrotactile techniques to stimulate the feet of the users. The vibrations were transmitted using low frequency loud speakers fixed on tiles under the users' feet [Visell 08] (Figure 3.5).

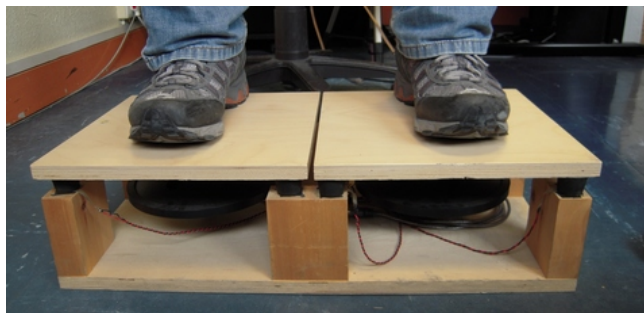


**Figure 3.5** – Vibrotactile tiles. The vibrations are produced by low frequency loud speakers fixed under the tiles [Visell 08].

Again, we simulated two types of contact of the feet with the ground: Heel Strike (**1 contact**) and both Heel Strike and Toe Strike (**2 contacts**). We also developed 2 different metaphors for the vibrations. The first metaphor is a physically-based simulation of the vibrations that would be produced in real life using a Rigid Contact Model (**RCM**) [Okamura 98] presented section 3.1.2. With this model, the user's feet are considered to be a rigid object colliding with a rigid surface. The resulting collision produces high frequency vibrations depending of the nature of the virtual ground. In the second metaphor, the vibrations are proportional to the forces applied on the ground by the feet: the Ground Reaction Forces Model (**GRFM**) simulates the force that is applied to the ground by each step [Novacheck 98]. We used the same vibration frequency as with the RCM model, but different envelopes are used for the signal. The envelopes reproduce the shape of the forces applied to the ground during each step [Novacheck 98]. For the heel contact only, only the beginning of the curve is interpolated from the data, while all the data is used otherwise. Thus, the Tactile KKE can be described by the function  $K_T(x, y)$  with  $x$  the model used ( $x \in \{RCM, GRFM\}$ ) and  $y$  the number of contacts ( $y \in \{1, 2\}$ ). The four resulting different vibration patterns are presented in Figure 3.6.

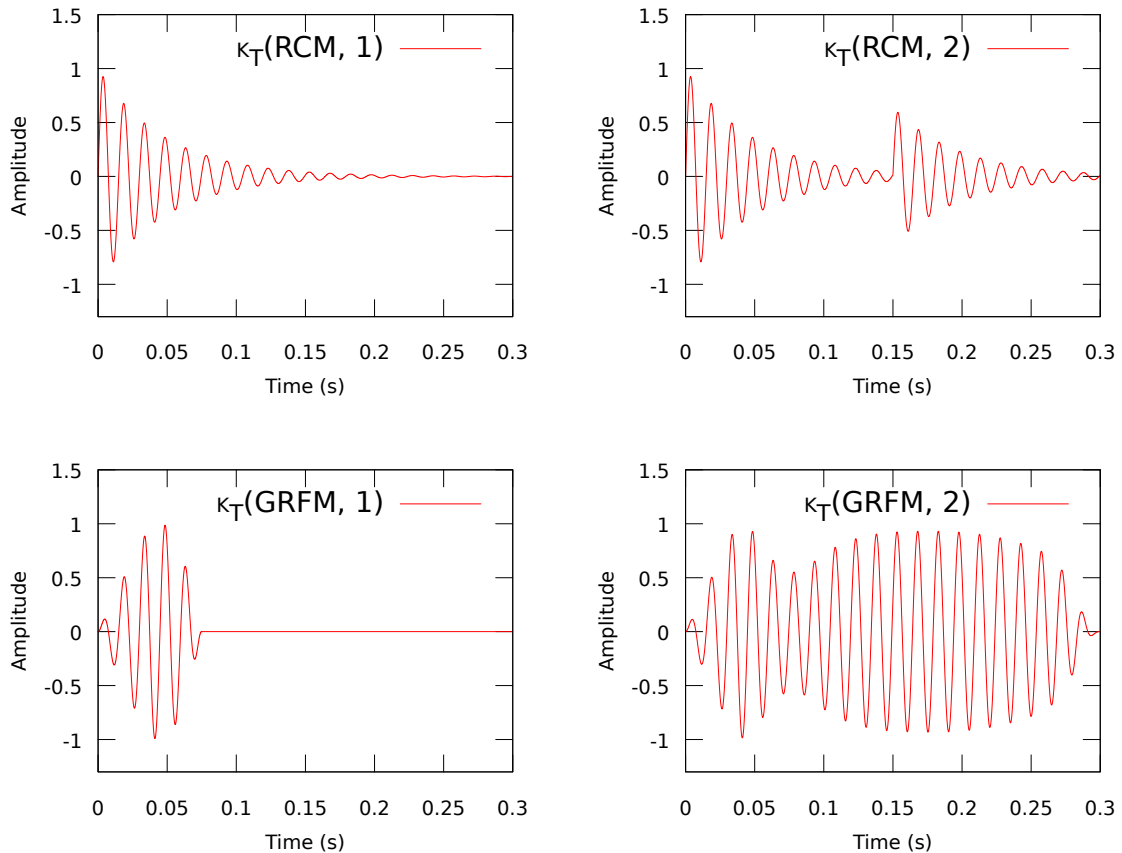


**Figure 3.6** – Vibration patterns for the tactile KKE. Amplitude over Time (in seconds) of the vibration patterns used for the Tactile KKE: Rigid Contact Model (RCM) and Ground Reaction Forces Model (GRFM) simulating 1 or 2 contacts.

### 3.1.4 Conclusion

To sum up, our approach is composed of (1) a Step Simulator which computes the foot-step events during the walk, (2) Visual vibration patterns based on vibrations along two different directions (vertical and horizontal) to produce different effects and (3) Tactile vibration patterns based on two different metaphors. Moreover, the different patterns can simulate both the heel and toe contacts with the ground. The KKE can be used in static position, such as when seated or standing, whereas the user controls the virtual walk with any input device (joystick, keyboard, etc.). Finally, the KKE can be implemented on any kind of computer, requiring only the tiles which are a low cost device.

## 3.2 Evaluations of the King Kong Effects

We conducted a set of experiments to evaluate the different components of the KKE and to determine the best combination among modalities and effects.

We conducted four different experiments. The first three experiments were based on the 2 Alternative Forced Choice (2AFC) paradigm. For each experiment, the participants were exposed to pairs of passive navigations in straight line using different conditions. At the end of each pair, the participants were asked which one of the two navigations gave them the *best sensation of walking*. In every case, the participants had to choose between the two navigations. The first experiment was designed to evaluate the optimal parameters for the Visual KKE. The second investigated the influence of Camera Motions on the appreciation of Visual KKE. The third experiment focused on the optimal parameters for the tactile KKE. Finally, the fourth experiment tested the preference for the KKE in a multimodal context.

### 3.2.1 Method

#### 3.2.1.1 Experimental Apparatus

The participants were seated at 1 m in front of a 24 inch widescreen monitor with a resolution of  $1920 \times 1200$  pixels (physical field of view of  $29^\circ$  horizontally and  $18^\circ$  vertically). The rendering was made at a refresh rate of 50 Hz. Their feet were placed on top of the vibrating tiles, with their shoes removed (Figure 3.7a). Users were wearing headphones filled with white noise to mask any sound produced by the vibrating tiles. At the end of each pair of navigations, the users had to select their preferred navigation in terms of “sensation of walking” using the keyboard keys “1” and “2”. The participants had the possibility to take breaks by pressing the “Space” key at any time.

#### 3.2.1.2 Virtual Environment

The Virtual Environment was composed of an empty room with textured walls (Figure 3.7b). The room depth was set to 15 m. At the end of the room, in the center of the

screen, a cardboard box regularly textured was placed to provide the participants with a point to focus their gaze (Figure 3.7b). The participants were exposed to pairs of passive navigations of 5.4 m.

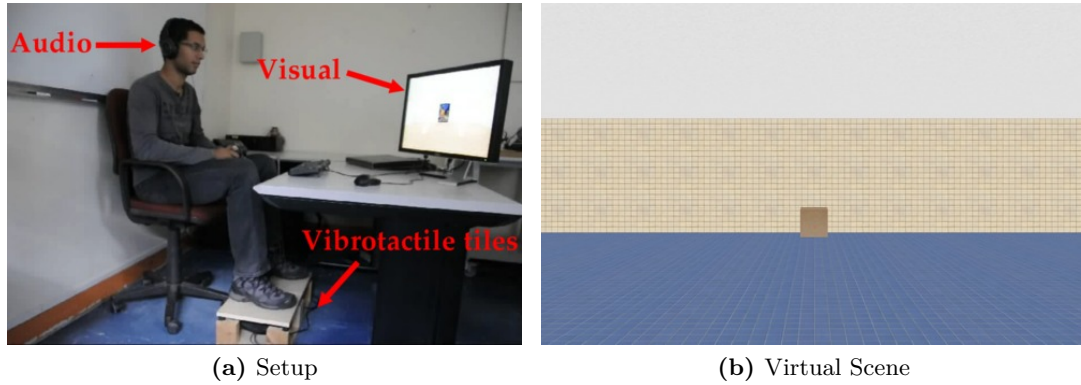


Figure 3.7 – Experimental apparatus.

### 3.2.1.3 Collected Data

For each pair of conditions, we recorded the choices of the participants. At the end of the experiment the participants had to complete a questionnaire in which they had to grade from 1 (very bad) to 7 (very good) the different techniques according to different criteria: (1) Presence, (2) Sensation of walking, (3) Realism of the walk, (4) Visual tiredness (5) Cybersickness and (6) Global appreciation. For the Visual tiredness and Cybersickness conditions, the grade 1 corresponded to “very tiresome” and “make sick” respectively, while the grade 7 was the opposite.

## 3.2.2 Experiment 1: Selecting the Best Visual Vibration Pattern for KKE

The first experiment was focused on Visual KKE. The goal was to find which set of parameters provides the best sensation of walking in the VE when the Visual KKE are used alone. The parameters were the number of contacts (1 contact versus 2 contacts) and the direction of oscillations (Vertical versus Horizontal).

### 3.2.2.1 Population

Twelve participants (10 males and 2 females) aged from 20 to 34 (Mean  $M = 23.8$ , Standard Deviation  $SD = 3.5$ ) performed the experiment. None of the participants had any known perception disorder. All participants were used to VEs but were naïve with respect to the proposed techniques, as well as to the experimental setup.

### 3.2.2.2 Experimental Conditions

We used a within subject design to evaluate five different Visual KKE conditions. The control condition *Ctrl* was composed of a linear camera motion without any Visual KKE. The four other conditions corresponded to: (1)  $K_V(V, 1)$ , (2)  $K_V(V, 2)$ , (3)  $K_V(H, 1)$  and



(4)  $K_V(H, 2)$ . All the possible combinations of the different conditions were tested 10 times in both orders. For each group of possible combinations, the order between the different pairs was randomized. The experiment lasted approximatively 25 min.

### 3.2.2.3 Results

We analyzed answers and preferences of participants for the different patterns in order to determine which condition provides the best sensation of walking in the VE. In particular, we analyzed the impact of the direction of the oscillations, as well as the effect of one contact versus two contacts.

For a given pair of conditions, each individual performed 20 comparisons. Under the null hypothesis of equal preference between the two conditions, the number of times an individual preferred the first condition follows a binomial distribution with parameters 10 and  $1/2$ . After standardization, such variable can be approximated by a standard normal random variable. Thus, for each pair of conditions, we tested the presence of a preferred condition using a Student's t-test. The p-values were adjusted with a Bonferroni correction. The analysis showed that  $K_V(V, 1)$  was more often significantly chosen than *Ctrl* ( $t(11) = 6.14$ ,  $p < 0.001$ ),  $K_V(H, 1)$  ( $t(11) = 11.49$ ,  $p < 0.001$ ) and  $K_V(H, 2)$  ( $t(11) = 7.58$ ,  $p < 0.001$ ). Moreover,  $K_V(V, 2)$  was more often significantly chosen than *Ctrl* ( $t(11) = 5.50$ ,  $p = 0.002$ ),  $K_V(H, 1)$  ( $t(11) = 9.57$ ,  $p < 0.001$ ) and  $K_V(H, 2)$  ( $t(11) = 5.45$ ,  $p = 0.002$ ). Our results suggest that for the Visual KKE, the Vertical vibrations are always preferred over the Horizontal ones. Moreover, the number of contacts with the ground does not change this result. However, the experiment failed to find any significant effect on the number of contacts of the feet (1 or 2 contacts) for the Visual vibrations.

Concerning the subjective questionnaires, we performed a Friedman test. The reported p-values were adjusted for multiple comparisons. We found a significant effect for 5 criteria: Global appreciation ( $\chi^2 = 3.6$ ,  $p = 0.003$ ), Presence ( $\chi^2 = 3.03$ ,  $p = 0.02$ ), Realism ( $\chi^2 = 4.27$ ,  $p < 0.001$ ), Walking sensation ( $\chi^2 = 3.96$ ,  $p < 0.001$ ) and Fatigue ( $\chi^2 = 4.91$ ,  $p < 0.001$ ). Post-hoc analysis showed that  $K_V(V, 1)$  was preferred to *Ctrl* for global appreciation ( $p = 0.01$ ), presence ( $p = 0.02$ ), realism ( $p < 0.001$ ) and walking sensation ( $p < 0.001$ ).  $K_V(V, 1)$  was also significantly better rated than  $K_V(H, 1)$  for global appreciation ( $p = 0.003$ ) and realism ( $p = 0.04$ ), and significantly better rated than  $K_V(H, 2)$  for global appreciation ( $p = 0.006$ ), walking sensation ( $p = 0.02$ ) and fatigue ( $p = 0.03$ ). Moreover,  $K_V(V, 2)$  was preferred to *Ctrl* for realism ( $p = 0.002$ ), walking sensation ( $p = 0.046$ ) and fatigue ( $p = 0.006$ ). Finally,  $K_V(H, 1)$  and  $K_V(H, 2)$  were significantly better rated than *Ctrl* for fatigue only ( $p < 0.001$  and  $p < 0.001$ ). The results of the questionnaires are displayed in [Figure 3.8](#).

The results of the subjective questionnaires confirm the results of the 2AFC. Indeed, the Vertical vibrations with 1 contact scored better than the other conditions with Horizontal vibrations in terms of global appreciation and either realism or walking sensation.

### 3.2.2.4 Conclusion

To sum up, for the Visual KKE the Vertical direction provides a better sensation of walking than the Horizontal direction. In particular, the Vertical Visual KKE with 1 contact was preferred by the participants over the other conditions.

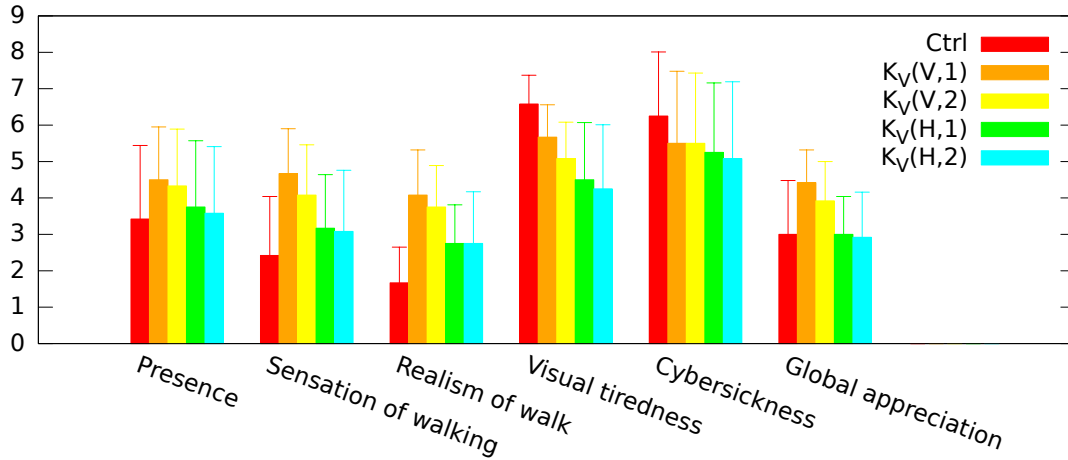


**Figure 3.8** – Results of the questionnaires for the first experiment. For each of the criteria, the mean and standard deviation for each condition are represented.

### 3.2.3 Experiment 2: Testing the Combination of Visual KKE and Oscillating Camera Motions

The second experiment tested the influence of standard oscillating Camera Motions on Visual KKE. The goal was to check if the preference for Visual KKE (number of contacts, direction of oscillations) would change when associated with another visual technique composed of standard camera motions.

#### 3.2.3.1 Population

The same twelve participants as the first experiment performed this experiment. However, to avoid any bias, half of the participants started with this experiment while the other half started with the first one.

#### 3.2.3.2 Experimental Conditions

We used a within subject design to evaluate five different Visual KKE when added to the regular Camera Motions proposed by Lécuyer et al. [Lécuyer 06]. The control condition *Ctrl* was made of classical camera motions composed of sinusoidal oscillations along the three axes, without any Visual KKE. The conditions were all composed of the camera motions combined respectively with: (1)  $K_V(V,1)$ , (2)  $K_V(V,2)$ , (3)  $K_V(H,1)$  and (4)  $K_V(H,2)$ . All the possible combinations of the different conditions were tested 10 times in both orders. For each group of possible combinations, the order between the different pairs was randomized. The experiment lasted approximatively 25 min.

#### 3.2.3.3 Results

We performed the same statistical analysis as for Experiment 1. The analysis showed that  $K_V(V,1)$  was more often significantly chosen than  $K_V(H,1)$  ( $t(11) = 4.99$ ,  $p = 0.004$ ).

Moreover,  $K_V(V,2)$  was more often significantly chosen than  $K_V(H,2)$  ( $t(11) = 4.17$ ,  $p = 0.016$ ). Our analysis suggest similar results to the first experiment: the Vertical vibrations are still preferred to the Horizontal ones. The presence and combination with Camera Motions do not change this result. Using the KKE in combination with standard Camera Motions does not modify the way users perceive the KKE, and the most efficient type of KKE remains the same. The analysis also failed to found any significant effect of the number of contacts of the feet (1 or 2 contacts) when combined with Camera Motions.

Concerning the subjective questionnaires, we performed a Friedman test. The reported p-values were adjusted for multiple comparisons. We found a significant effect for 5 criteria: Global appreciation ( $\chi^2 = 4.52$ ,  $p < 0.001$ ), Presence ( $\chi^2 = 3.14$ ,  $p = 0.01$ ), Realism ( $\chi^2 = 4.38$ ,  $p < 0.001$ ), Walking sensation ( $\chi^2 = 4.89$ ,  $p < 0.001$ ) and Fatigue ( $\chi^2 = 3.23$ ,  $p = 0.01$ ). Post-hoc analysis showed that  $K_V(V,1)$  was preferred to *Ctrl* for presence ( $p = 0.04$ ).  $K_V(V,1)$  was also significantly better rated than  $K_V(H,2)$  for presence ( $p = 0.02$ ) and fatigue ( $p = 0.01$ ). Moreover,  $K_V(V,2)$  was significantly better rated than  $K_V(V,1)$  for global appreciation ( $p < 0.001$ ), realism ( $p < 0.001$ ) and walking sensation ( $p < 0.001$ ).  $K_V(V,2)$  was also preferred to  $K_V(H,2)$  for global appreciation ( $p < 0.001$ ) and walking sensation ( $p = 0.01$ ). Finally,  $K_V(H,1)$  was significantly better rated than  $K_V(V,1)$  for global appreciation ( $p = 0.008$ ), realism ( $p = 0.01$ ) and walking sensation ( $p = 0.02$ ). The results of the questionnaires are displayed in Figure 3.9.

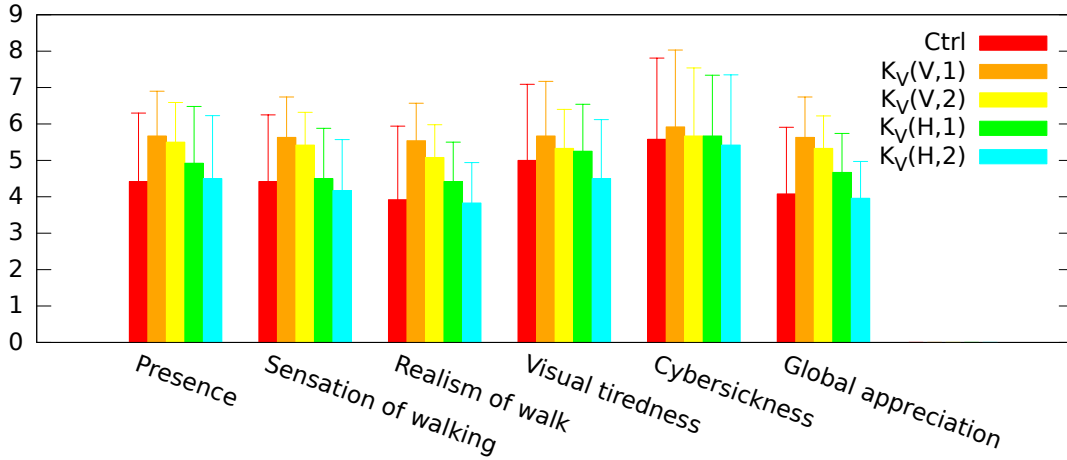


**Figure 3.9** – Results of the questionnaires for the second experiment. For each of the criteria, the mean and standard deviation for each condition are represented.

The results of the questionnaires are more contrasted. Indeed, Vertical vibrations scored better than Horizontal vibrations for walking sensation and global appreciation with 2 contacts, while it is the opposite for 1 contact.

### 3.2.3.4 Conclusion

To sum up, combined with CM, the Vertical direction of the Visual KKE is still preferred over the Horizontal direction.

### 3.2.4 Experiment 3: Selecting the Best Tactile Vibration Pattern for KKE

The third experiment focused on tactile KKE. The goal was to find which set of parameters provides the best sensation of walking in the VE when the tactile KKE are used alone. The parameters were the number of contacts (1 contact versus 2 contacts) and the model used (RCM versus GRFM).

#### 3.2.4.1 Population

Twelve participants different from the participants from the two previous experiments (8 males and 4 females) aged from 21 to 59 (Mean  $M = 30.1$ , Standard Deviation  $SD = 12.6$ ) performed the experiment. None of the participants had any known perception disorder. All participants were used to VEs but were naïve with respect to the proposed techniques, as well as to the experimental setup.

#### 3.2.4.2 Experimental Conditions

We used a within subject design to evaluate five different Tactile KKE conditions. The control condition *Ctrl* was composed of no Tactile KKE. The conditions were respectively: (1)  $K_T(RCM, 1)$ , (2)  $K_T(RCM, 2)$ , (3)  $K_T(GRFM, 1)$  and (4)  $K_T(GRFM, 2)$ . All the possible combinations of the different conditions were tested 10 times in both orders. For each group of possible combinations, the order between the different pairs was randomized. The experiment lasted approximatively 25 min.

#### 3.2.4.3 Results

We performed the same statistical analysis as in Experiment 1. The analysis showed that  $K_T(RCM, 1)$  was more often significantly chosen than *Ctrl* ( $t(11) = 36.38$ ,  $p < 0.001$ ),  $K_T(RCM, 2)$  ( $t(11) = 4.26$ ,  $p = 0.013$ ) and  $K_T(GRFM, 2)$  ( $t(11) = 4.64$ ,  $p = 0.007$ ). Moreover,  $K_T(GRFM, 1)$  was more often significantly chosen than  $K_T(RCM, 2)$  ( $t(11) = 5.46$ ,  $p = 0.002$ ) and  $K_T(GRFM, 2)$  ( $t(11) = 8.25$ ,  $p < 0.001$ ). Concerning the vibration patterns, no significant effect on the metaphor was found during the 2AFC analysis. Rigid Contact Model (RCM) with only heel strikes was preferred to the Ground Reaction Forces Model (GRFM) with heel and toe strikes. On the other hand, the GRFM with only heel strikes was also found significantly preferred to the RCM with heel and toe strikes. Thus, the number of contacts seems to be a more important criterion for the Tactile vibrations. Indeed, the Heel Strike alone simulation is preferred to the simulation of Heel Strike and Toe Strike. The metaphor used to design the vibration pattern does not influence these results. Thus, both metaphor can be used.

Concerning the subjective questionnaire, we performed a Friedman test. The reported p-values were adjusted for multiple comparisons. We found a significant effect for 4 criteria: Global appreciation ( $\chi^2 = 3.99$ ,  $p < 0.001$ ), Presence ( $\chi^2 = 4.2$ ,  $p < 0.001$ ), Realism ( $\chi^2 = 4.65$ ,  $p < 0.001$ ) and Walking sensation ( $\chi^2 = 4.83$ ,  $p < 0.001$ ). Post-hoc analysis showed that  $K_T(RCM, 1)$  was preferred to *Ctrl* for global appreciation ( $p = 0.001$ ), presence ( $p < 0.001$ ), realism ( $p < 0.001$ ) and walking sensation ( $p < 0.001$ ).  $K_T(RCM, 1)$  was

also significantly better rated than  $K_T(GRFM, 2)$  for realism ( $p = 0.009$ ). Moreover,  $K_T(RCM, 2)$  was significantly better rated than *Ctrl* for walking sensation ( $p = 0.01$ ). Finally,  $K_T(GRFM, 1)$  was preferred to *Ctrl* for global appreciation ( $p = 0.03$ ), presence ( $p < 0.001$ ), realism ( $p < 0.001$ ) and walking sensation ( $p < 0.001$ ).  $K_T(RCM, 1)$  was also significantly better rated than  $K_T(RCM, 2)$  for global appreciation ( $p = 0.03$ ). The results of the questionnaires are displayed in Figure 3.10.

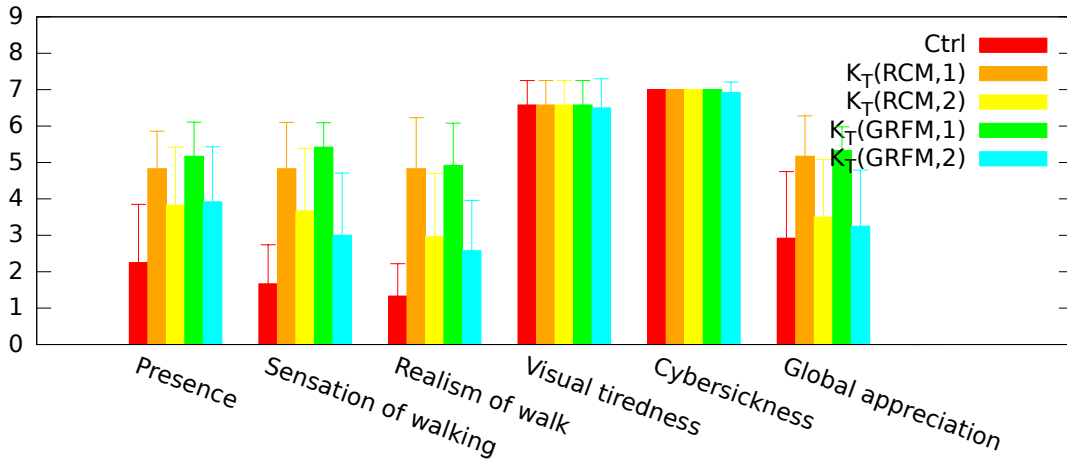


**Figure 3.10** – Results of the questionnaires for the third experiment. For each of the criteria, the mean and standard deviation for each condition are represented.

The subjective questionnaires did not reveal any clear significant preference on the number of contacts for any of the experiments. The results suggest a small preference for 1 contact over 2 contacts, only for the Tactile vibrations.

#### 3.2.4.4 Conclusion

To sum up, the Tactile KKE provide a better sensation of walking when only 1 contact of the foot with the ground is simulated. More complex simulations are perceived as less natural for the users.

### 3.2.5 Experiment 4: Testing Participant Preference for Multimodal KKE

This last experiment focused on multimodal rendering of KKE. For this experiment, we introduced audio feedback of prerecorded footsteps to the KKE. The footstep sounds were synchronized with the other KKE by the Step Simulator. We used audio, visual and vibrotactile modalities individually or all together. For each modality, we selected the best components found in the previous experiments to yield the best sensation of walking in the VE and we tested every possible combinations of modalities.

Taken together, our previous results suggest guidelines for the best Visual and Tactile KKE. Heel strikes (1 contact) only should be used for the Tactile vibrations. Moreover, Vertical oscillations should be used for the Visual vibrations. Because the metaphor used has no clear significant effect on the Tactile vibrations, we chose to use the Rigid Contact Model for both modalities to simplify our model. Moreover, to keep the model as simple as possible, we chose to use only heels strikes for the Visual Vibrations as well.

### 3.2.5.1 Population

Ten new participants (9 males and 1 female) aged from 21 to 27 (Mean  $M = 24.1$ , Standard Deviation  $SD = 2.2$ ) performed the experiment. None of the participants had any known perception disorder. All participants were used to VEs but were naïve with respect to the proposed techniques, as well as to the experimental setup.

### 3.2.5.2 Experimental Conditions

We used a within subject design where the participants could freely navigate on a museum scene (Figure 3.11). They had the possibility to switch at will from one condition to the others. The visual ( $V$ ) modality was composed of  $K_V(V, 1)$ , the haptic (vibrotactile) ( $H$ ) modality was composed of  $K_T(RCM, 1)$ , and the audio ( $A$ ) modality was rendered using recorded playback of a wooden floor. All the possible combinations of these 3 modalities were available, from one modality alone to the 3 combined together, resulting in the following conditions:  $V$ ,  $H$ ,  $A$ ,  $VH$ ,  $VA$ ,  $HA$  and  $VHA$ . The experiment lasted approximatively 15 min.



Figure 3.11 – Museum scene of the 5th experiment.

### 3.2.5.3 Collected Data

The participants had to grade from 1 (very bad) to 7 (very good) the different conditions based on the following criteria: (1) Presence, (2) Sensation of walking, (3) Realism of the walk, (4) Fun and (5) Global appreciation.

### 3.2.5.4 Results

Concerning the subjective questionnaires, we performed a Friedman test. The reported p-values were adjusted for multiple comparisons. We found a significant effect for all criteria: Fun ( $\chi^2 = 4.49$ ,  $p < 0.001$ ), Global appreciation ( $\chi^2 = 2.97$ ,  $p = 0.047$ ), Presence ( $\chi^2 = 4.90$ ,  $p < 0.001$ ), Realism ( $\chi^2 = 5.29$ ,  $p < 0.001$ ) and Walking sensation ( $\chi^2 = 4.90$ ,  $p < 0.001$ ). Post-hoc analysis showed that  $H$  was preferred to  $V$  for fun ( $p = 0.02$ ).  $VA$  was preferred to  $V$  for fun ( $p = 0.03$ ), global appreciation ( $p = 0.047$ ), and walking sensation ( $p = 0.04$ ).  $HA$  was preferred to  $V$  for fun ( $p < 0.001$ ), presence ( $p = 0.007$ ), realism

( $p < 0.001$ ), and walking sensation ( $p = 0.001$ ). *HA* was also significantly better rated than *VH* for fun ( $p = 0.008$ ). *VHA* was preferred to *V* for presence ( $p < 0.001$ ), realism ( $p < 0.001$ ), and walking sensation ( $p < 0.001$ ). *VHA* was significantly better rated than *H* for presence ( $p = 0.01$ ), realism ( $p = 0.03$ ), and walking sensation ( $p = 0.04$ ). *VHA* was significantly better rated than *A* for presence ( $p = 0.03$ ), realism ( $p = 0.01$ ), and walking sensation ( $p = 0.009$ ). *VHA* was significantly better rated than *VH* for realism ( $p = 0.04$ ) and walking sensation ( $p = 0.02$ ). *VHA* was significantly better rated than *VA* for realism ( $p = 0.002$ ). *VHA* was significantly better rated than *HA* for fun ( $p = 0.003$ ).

The multimodal evaluation of the KKE showed that the effects produced by each modality are reinforced when used in conjunction with the other modalities. In particular, conjunctions of two modalities scored higher on the fun criteria. Finally, the combination of the three modalities resulted in higher grades for presence, realism and walking sensation compared to each modalities taken alone or by two. Thus, our results suggest that a multimodal approach for the perception of the walk in the VE is preferred by the participants. The results of the questionnaires are displayed in [Figure 3.12](#).

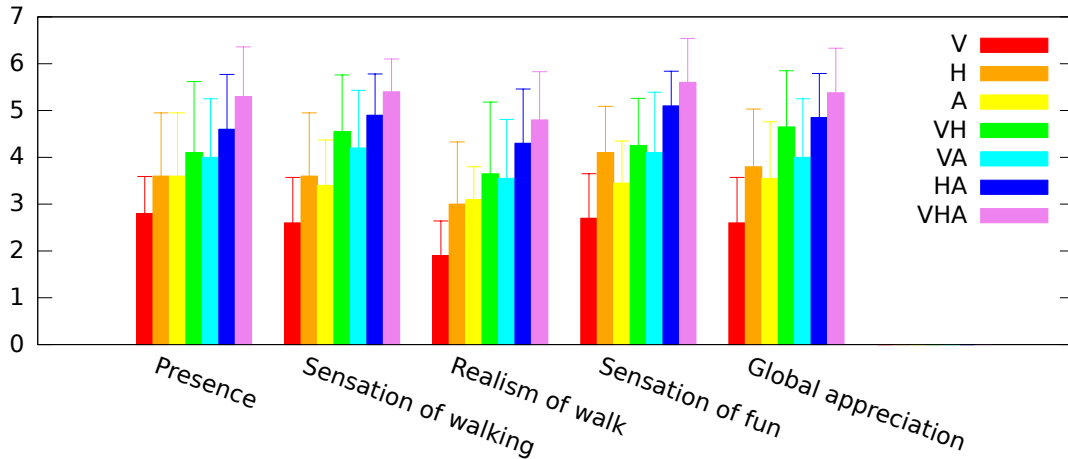


**Figure 3.12** – Results of the questionnaires for the fourth experiment. For each of the criteria, the mean and standard deviation for each condition are represented.

### 3.2.5.5 Conclusion

To sum up, the sensation of walking is increased when the different modalities of the KKE are taken together. A multimodal simulation is not only possible but is also recommended.

## 3.3 Discussion

Our results suggest that the KKE allow more immersive and more enjoyable navigation compared to the classic FPS paradigm. Moreover, it clearly increases the sensation of actually walking inside the VE, while only using low cost devices. Finally, the KKE can be used to simulate different morphologies of virtual avatars, like height or weight, while still using the FPS paradigm.

The results of the experiments show that for the Visual KKE, the Vertical vibrations are always preferred to the Horizontal ones, and the type of contact of the feet with the



ground does not change this result. Indeed, with Heel Strike only or with both Heel Strike and Toe Strike simulations, the Vertical is always preferred. The Vertical vibrations were designed to reproduce the point of view of a big creature walking like King Kong, while the Horizontal vibrations are more related to an external point of view. Thus, it seems that the Vertical vibrations are more immersive and thus provide a better sensation of walking in the VE.

Moreover, the standard Camera Motions do not change this result. Using the KKE in combination with standard Camera Motions does not modify the way a user perceives the KKE, and the most efficient type of KKE remains the same. This result gives a good hope that the KKE could be associated with many other techniques while keeping its properties. In particular, the best type of Visual KKE can probably be used safely in most situations.

Concerning the Tactile vibrations, the number of contacts was significant but the model used was not found to be significant. Thus, it seems that the simplicity of the model is a key to provide the best sensation of walking. However, some more complex models could be tested to simulate more complex virtual grounds, such as aggregate grounds made of sand or gravel for example [Nordahl 10]. The model of vibration could also be adapted dynamically to reproduce more accurately all the changes of the properties of the virtual ground during the navigation.

Interestingly, for some participants, the KKE modified their self perception inside the VE. Some participants quoted that they "felt like if they were heavier", or "like if they were a big creature like a troll". One of the women who participated also quoted that the double contact felt "as if walking with high heels".

Finally, our results clearly suggest the importance of a multimodal approach. In this chapter we did not focus on the auditory modality. However, further integration of this modality would be highly interesting. Indeed, this modality fits particularly well into the scope of a desktop VR, and can provide a lot of useful information about the footsteps and the virtual ground properties.

## 3.4 Conclusion

In this chapter, we proposed a novel sensory feedback technique inspired from movies to increase the sensation of walking in a VE. Our technique simulates each virtual step made in the VE by producing a visual and/or tactile vibration. The KKE simulates the contact of the feet with the ground.

We proposed two different directions for the Visual vibrations corresponding to different points of view. The vertical vibrations correspond to a view at the first-person, while horizontal vibrations emphasize on an external view. We also proposed two different models for the Tactile vibration patterns. The first model simulates vibrations produced by rigid contacts between the feet and the ground. On the other hand, the second model uses vibrations as a metaphor of the forces applied to the ground at each step. For both visual and tactile modalities, we simulated the contact of the heel alone or accompanied by the contact of the toes.

We conducted an evaluation of each of the components of the KKE, as well as a multimodal evaluation in order to determine which components and parameters provide the

best sensation of walking in VE. We found that vertical visual vibration simulating only heel contact were preferred by the participants. We also found that the Rigid Contact Model with only Heel Strike simulation was also preferred for the vibrotactile pattern. Finally, the participants showed that using the best patterns for each modality, multimodal feedback was preferred to navigations using only one modality.

Taken together, our results show that the KKE can be used to improve the sensation of walking in VE using multimodal simulation of the virtual footsteps during the navigation.

# Personified and Multi-States Camera Motions for First-Person Navigation in Virtual Reality 4

## Contents

<b>4.1 Multi-States and Personified Camera Motions</b>	<b>88</b>
4.1.1 Approach	89
4.1.2 Existing Models of Camera Motions	89
4.1.3 Our Novel Model of Camera Motions	90
4.1.4 Personified Camera Motions	90
4.1.5 Multi-states Camera Motions	93
4.1.6 Advance Speed of Camera Motions	95
4.1.7 Results and Performance	97
4.1.8 Conclusion	99
<b>4.2 Perceptual Evaluation of Personified and Multi-States Camera Motions</b>	<b>101</b>
4.2.1 Method	101
4.2.2 Experiment 1: Detection of the Locomotion Modes	102
4.2.3 Experiment 2: Detection of the Transitions Between Locomotion Modes	103
4.2.4 Experiment 3: Perception of the Virtual Human Properties	104
4.2.5 Experiment 4: Influence of VR on the Detection of the Locomotion Modes	105
4.2.6 Discussion	106
4.2.7 Conclusion	108
<b>4.3 Influence of Camera Motions on Perception of Traveled Distances in Virtual Environments</b>	<b>108</b>
4.3.1 Method	109
4.3.2 Collected Data	111
4.3.3 Results	111
4.3.4 Discussion	113
4.3.5 Conclusion	115
<b>4.4 Conclusion</b>	<b>115</b>

In order to improve the immersion of the user during a navigation in a virtual environment, different techniques can be used. For example, the King-Kong Effects (KKE) presented in [chapter 3](#) can simulate the contact of the feet with the ground using both visual and tactile modalities.

The Camera Motions (CM) introduced by Lécuyer et al. [Lécuyer 06] are another sensory feedback technique that can be used to improve the immersion in the VE. The CM simulate and reproduce the oscillations of the eyes and head motions during the walk. The motion of virtual camera (point of view) in the VE during the navigation generates a visual flow similar than that produced by a real walk. Researchers notably showed that such visual effect improve the sensation of walking.

However, the existing CM models are rather limited. They were exclusively designed for simulating the walk [Lécuyer 06] on flat surfaces. They have not been applied to other locomotion modes such as for running or sprinting for example. The current CM do not take into account information related to the physiology of the virtual human (avatar). Indeed, the user would probably expect different CM depending for instance on the size, age or fitness of the avatar.

Therefore, in this chapter, we study and introduce a new approach which revisits and drastically improves the possibilities offered by Camera Motions in virtual environments. This approach enables to display the multiple modes of locomotion, and can take into account the properties of the avatar or the topography of the virtual environment. It is based on a locomotion simulator which notably simulates the fatigue and recuperation of the avatar, and handles the synchronization and updates of the camera motions. The three main contributions in this chapter are thus:

- A new approach for Camera Motions. We have introduced a generic approach for multi-states, personified, and topography-dependent Camera Motion in virtual environments.
- Series of experiments. We have conducted a series of experiments to evaluate the perception of our new multi-states and personified CM by naive participants when navigating in VE in a first-person mode.
- A second experiment to evaluate the influence of Camera Motions in the perception of traveled distances in the VE.

The remainder of this chapter is organized as follows: In [section 4.1](#) we present our novel approach for multi-states and personified camera motions. In [section 4.2](#), we present the evaluation of our new multi-states and personified CM. In [section 4.3](#), we conduct another experiment designed to evaluate the influence of camera motions on traveled distances. The chapter ends with a general conclusion.

## 4.1 Multi-States and Personified Camera Motions

In order to improve the sensation of walking of the users in the VE, we introduce a new approach of Camera Motions (CM).

Our CM are adapted to the different modes of the human locomotion. In particular, our new camera motions render the walk, run and sprint. Moreover, we propose new CM adapted to the physiology of the virtual human. Indeed, the visual feedback of CM is different if the virtual human is heavier or is in a better physical condition for example. Finally, our CM are adapted to the slope of the VE.

In this section, we will recall the basic principles and components of CM. We will describe

next our new CM. Finally, we will detail the improvement made to the CM to allow multi-state, personified and slope dependent simulation.

#### 4.1.1 Approach

The CM are defined as motions of the virtual camera in the VE used to simulate and enhance the sensation of walking. Those motions can be described as a combination of translations  $T$  and rotations  $R$  around the three different axes of space. The translations can be composed of oscillations  $O$  (standard CM [Lécuyer 06]), or vibrations  $Vib$  (King-Kong Effects, chapter 3). Therefore, if the advance speed over time is defined as  $v(t)$  and  $H_{eyes}$  is the height of the eyes of the virtual human, the global equation of CM is described Equation 4.1.

$$\begin{cases} T_x = O_x \\ T_y = O_y + Vib + H_{eyes} \\ T_z = O_z + v(t) \end{cases} \quad and \quad \begin{cases} R_x \\ R_y \\ R_z \end{cases} \quad (4.1)$$

#### 4.1.2 Existing Models of Camera Motions

Previous Camera Motions (CM)[Lécuyer 06] simulate the movements of the user's head during a locomotion in first person mode by oscillating the position of the camera. The motions of the virtual camera along the three different axes simulate the motions of the viewpoint of the user during the navigation. Previous models of CM[Lécuyer 06] propose oscillating the camera along the three different axes, producing a complex trajectory. These oscillating motions correspond to the mathematical description of Equation 4.2, where  $T$  is a constant period for the oscillations,  $t$  is the current simulation time and  $A_x$ ,  $A_y$  and  $A_z$  are constant amplitudes for each axis.

$$\begin{cases} O_x = A_x \cdot \cos(\frac{\pi}{T}t + \frac{\pi}{2}) \\ O_y = A_y \cdot \cos(\frac{2\pi}{T}t) \\ O_z = A_z \cdot \cos(\frac{2\pi}{T}t + \frac{\pi}{2}) \end{cases} \quad (4.2)$$

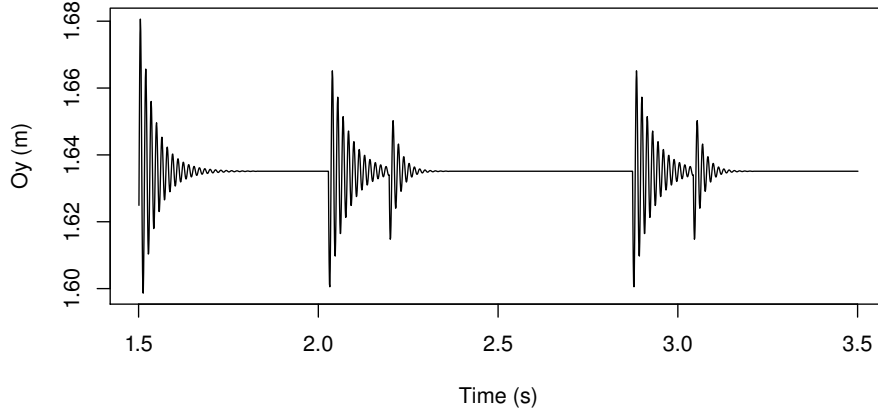
A recent technique introduced in chapter 3 considers other motions of the camera to simulate the impact of the feet with the ground at each step. This technique, also called the “King-Kong Effects”, uses high frequency vibrations of the camera (Equation 4.5) to simulate the contact of the heels and toes of the virtual human with the ground in the VE (Figure 4.1).

$$Vib = A_{event} \cdot e^{-T_{event} \cdot \Delta t} \sin(\omega t) \quad (4.3)$$

$\Delta t$  is the time between the contact of the heel and toes and  $\omega t$  is the frequency of the vibrations.  $A_{event}$  and  $T_{event}$  depend of the type of event (Table 4.1).

As found in chapter 3, the two CM techniques can be combined to further improve immersion and self-motion sensation.

Parameters	Heel contact	Toes contact
$A_{event}$	0.05	0.03
$T_{event}$	2.0	1.0

**Table 4.1** – Parameters of the vibration model.**Figure 4.1** – Vibrations applied to the virtual camera at each step to simulate contacts of the feet with the ground.

### 4.1.3 Our Novel Model of Camera Motions

We propose a new model for multi-states and personified CM. The new equations of the proposed Camera Motions are detailed [Equation 4.4](#) and [Equation 4.5](#).

$$\begin{cases} O_x = A_x * A_{state_x} \cdot A_{VH_x} \cdot \sin(\pi P_{step} + \pi\varphi) \\ O_y = A_y * A_{state_y} \cdot A_{VH_y} \cdot \sin(2\pi P_{step} - \frac{\pi}{2}) \\ O_z = A_z * A_{state_z} \cdot A_{VH_z} \cdot \sin(2\pi P_{step}) \end{cases} \quad (4.4)$$

$$Vib = A_{vib} \cdot A_{event} \cdot e^{-T_{event} \cdot \Delta t} \sin(\omega t) \quad (4.5)$$

To produce multi-states CM, the  $A_{state}$  and  $A_{event}$  parameters are used. Moreover, the personified component of our CM is defined by the  $A_{VH}$  and  $A_{vib}$  factors. The phase  $\varphi$  is introduced for the lateral synchronization of the CM with the correct foot (left or right). Finally, the previous  $T$  and  $t$  parameters of the CM are replaced to synchronize the visual feedbacks with the steps of the virtual human  $P_{step}$ . Therefore, the new CM are synchronized with the advance speed  $v(t)$ .

### 4.1.4 Personified Camera Motions

CM are adapted to the physiology of the virtual human. The feedback depends on both the physical properties of the virtual human, such as its size or weight, as well the physical condition of the virtual human. Moreover, the fatigue of the virtual human also influences the visual feedback produced.

#### 4.1.4.1 Influence of the Physical Condition of the Virtual Human

Trained athletes learn to stabilize their head during the run or sprint in order to minimize the energy loss at each step. This effect was simulated by applying coefficients to the amplitude depending on the fitness ( $A_{fitness}$ ) of the virtual human. Moreover, the amplitude of the oscillation also depends on the fatigue of the virtual human  $P_{energy}$ , defined as a percentage of the maximal energy. Therefore, when the virtual human gets tired, its performances are reduced and the visual feedback is adapted accordingly. To keep the model as simple as possible, we chose to use the same factors on each axis, i.e.  $A_{VH_x} = A_{VH_y} = A_{VH_z} = A_{VH}$ .

$$A_{VH} = A_{fitness} \cdot \left( \frac{1}{2} P_{energy} + 1 \right) \quad (4.6)$$

Fitness	Poor	Fair	Good	Excellent	Superior
$A_{fitness}$	1.0	0.8	0.6	0.4	0.2

**Table 4.2** – Amplitude factors depending on virtual human fitness.

To render fatigue we introduced a new visual effect. A roll effect  $R_z$  is applied on the camera depending on the level of fatigue. The roll is synchronized to locomotion using the phase  $\varphi$ . The roll of the camera in degree is given by:

$$R_z = \frac{1}{2} P_{energy} \cdot \sin(\pi P_{step} + \pi \varphi + \frac{\pi}{2}) \quad (4.7)$$

Thus, the physical condition of the virtual human is rendered by the CM, depending on its general fitness, as well as its level of fatigue  $P_{energy}$  (subsubsection 4.1.4.3). Moreover, the CM also depends on the physical properties of the virtual human.

#### 4.1.4.2 Influence of the Physical Properties of the Virtual Human

Our visual feedback also depends on the physical properties of the virtual human. Currently, our feedbacks render the age, gender, weight and size of the virtual human. All those parameters are used to render a locomotion that depends on the virtual human physiology.

**Size.** The position of the point of view depends directly from the size of the virtual human. The average height of the eyes was set using anthropometric tables [Motmans 05]. Moreover, the size is also used in the locomotion simulation to determine the maximal step length. Hence the virtual human size can also be perceived through the length of the oscillations of the camera. The height of the camera was set to  $H_{eyes} = 0.934 * Size$ .

**Weight.** The weight of the virtual human has an important impact on the perception of the steps. Indeed, the weight can be perceived through the gait of the virtual human. Thus, a heavier virtual human will produce more intense vibrations of the camera when its feet touch the ground. Therefore, the visual vibration of the camera is adapted based



on the weight of the virtual human. Indeed, a coefficient  $A_{vib}$  is applied to the amplitude of the vibration such as:

$$A_{vib} = weight/100 \quad (4.8)$$

**Age and Gender.** Age and gender are displayed through the physical capacity of the virtual human  $C_{VH}$  and thus those parameters strongly influence the determination of the advance speed and fatigue. Therefore, the age and gender are also rendered by our new CM. For example, the gait of an athlete is very different from the one of an old lady: the steps are longer and faster.

The physical capacity of the virtual human  $C_{VH}$  is inspired from the maximal oxygen consumption  $VO_2max$  model.

The value of  $VO_2max$  can be estimated using tables designed to classified participants in different classes of physical fitness based on their gender, age, weight and  $VO_2max$  [Heyward 06]. Therefore, our estimation of  $C_{VH}$  depends on the gender, age, weight and physical fitness of the simulated virtual human.

#### 4.1.4.3 Energy Expenditure Estimation

The fatigue of the virtual human is also an important factor to render personified CM. The variation of the energy available  $P_{energy}$  over time simulates the amount of energy spent or recuperated during locomotion or rest.  $P_{energy}$  is the inverse of fatigue and is defined in Equation 4.9, with  $E_{max}$  the maximal amount of energy available after rest.

$$P_{energy} = \frac{E_{max} - E(t_n)}{E_{max}} \quad (4.9)$$

Therefore we propose the simple following model in which the variation of energy is function of time:

$$E(t_n) = E(t_{n-1}) + \alpha(P_{C_{VH}})\Delta t \quad (4.10)$$

where  $E(t_n)$  is the energy available at the time  $t_n$  and  $\Delta t$  is the time interval between  $t_n$  and  $t_{n-1}$ .  $P_{C_{VH}}$  is the user input corresponding to the required advance speed.  $P_{C_{VH}}$  is defined as a percentage of the physical capacity of the virtual human  $C_{VH}$ .  $\alpha(P_{C_{VH}})$  is a function to be determined.

The function  $\alpha(P_{C_{VH}})$  must simulate fast losses of energy at high speeds, but it must also allow recuperation during rest or slow walks. Therefore, we propose two different models for  $\alpha(P_{C_{VH}})$  depending on the range of  $P_{C_{VH}}$ . If  $P_{C_{VH}} > 0.8$  the model simulates the fatigue of the virtual human, and for  $P_{C_{VH}} < 0.8$  it simulates the recuperation.

**Fatigue of the Virtual Human.** For high speeds, i.e. for values of  $P_{C_{VH}} > 0.8$ , the virtual human spends a lot of energy and therefore get tired. The time to exhaustion  $t_{lim}$  parameter is used to quantify the amount of energy used for a locomotion at a given speed, depending on the capacity of the virtual human. The experimental results presented by Blondel et al. [Blondel 01] exhibited a trend which can be modeled by a generalized linear model.  $C_{VH}$  was chosen to match the properties of  $VO_2max$  (maximal oxygen consumption model).

First, a Box-Cox transformation showed that the data should be transformed with a logarithm. Therefore,  $\log(t_{lim})$  was analyzed depending on  $P_{CVH}$ :

$$\log(t_{lim}) = a.P_{CVH} + b \quad (4.11)$$

where  $a = -5.01$  and  $b = 10.99$ . Thus, if  $P_{CVH} \geq 0.8$ :

$$\alpha(P_{CVH}) = -E_{max}.e^{-a.P_{CVH}-b}, \text{ for } P_{CVH} > 0.8 \quad (4.12)$$

After a leave-one-out cross validation on the subject, the adjusted coefficient of determination was  $R^2 = 0.85$ .

**Recuperation of the Virtual Human.** For values of  $P_{CVH} < 0.8$ , the simulator must also simulate the energy recuperation during rest and slow walks. To complete the energy consumption simulator, we propose a recuperation model for lower values of  $P_{CVH}$  similar to the model used at high speeds. Indeed, our simulator must allow energy recuperation at rest and  $\alpha(P_{CVH})$  must be strictly decreasing. The simulator is the following:

$$\alpha(P_{CVH}) = X_1.e^{-X_2.P_{CVH}} + X_3, \text{ for } P_{CVH} < 0.8 \quad (4.13)$$

$$\left\{ \begin{array}{l} X_1 = \frac{E_{max}(\frac{1}{T_{recup}} + e^{-a.P_{CVH}-b})}{1 - e^{-R_{recup}.P_{CVH}}} \\ X_2 = R_{recup} \\ X_3 = \frac{E_{max}}{T_{recup}} - X_1 \end{array} \right. \quad (4.14)$$

where  $X_1$ ,  $X_2$  and  $X_3$  are determined by the time to fully regain all the energy at rest  $T_{recup}$  should be a parameter. Moreover, the continuity of the function  $\alpha(P_{CVH})$  must be assured for  $P_{CVH} = 0.8$ . However, it is mathematically impossible to also assure the continuity of the first derivative, thus one constraint is lacking to be able to solve this system. To avoid this problem, the value of the recuperation rate  $R_{recup}$  was chosen manually.

For the evaluation of the simulator, we used  $T_{recup} = 10$  s and  $R_{recup} = 10$ . Those values of the parameters provide a good compromise between a realistic behavior and a relatively short recuperation time.

#### 4.1.5 Multi-states Camera Motions

We propose new CM to render different modes of locomotion. In particular, our model renders an adapted feedback for the walking, running and sprinting modes. The feedback of the locomotion modes is improved using different parameters. Indeed, the locomotion modes are simulated using the amplitude of the oscillations and the type of vibrations produced at each step.

##### 4.1.5.1 Oscillations Amplitude

The amplitude of the oscillations depends on the type of locomotion. The amplitude tends to decrease while running and sprinting. This effect was modeled by applying coefficients

to the amplitude depending on the locomotion mode ( $A_{state}$ ). However, after preliminary testings, we increased slightly the coefficient for the sprint, otherwise the oscillations would not be perceived anymore. The same factors are used on the three different axes to reduce the complexity of the model. Therefore,  $A_{state_x} = A_{state_y} = A_{state_z} = A_{state}$ . The values used for  $A_{state}$  are presented [Table 4.3](#).

State	Stop	Walking	Running	Sprinting
$A_{state}$	0.0	1.0	0.5	0.8

**Table 4.3** – Amplitude factors of oscillating CM depending on the locomotion mode.

#### 4.1.5.2 Vibrations

The type and timing between the different contact events of the feet with the ground provide useful information on the locomotion mode. For example, the difference between the run and sprint is defined as the moment when the foot heels stop touching the ground at each step [[Novacheck 98](#)]. Therefore, for sprinting the vibration model will only simulates the contact of the toes with the ground, while it also simulates the contact of the heels for the walk and run. Therefore, for the heel contact events,  $A_{event} = 0$  if the locomotion mode is running. Moreover, the timings between events are also affected. During the walk the feet are in contact with the ground approximately 60% of the gait cycle [[Novacheck 98](#)]. However, for the run the feet are in contact only 40% of the cycle. Thus, the events are generated accordingly to the locomotion mode.

#### 4.1.5.3 Locomotion Modes

Different locomotion modes can be simulated with our model. In particular, the simulation can control the three following classical modes: (1) walking, (2) running and (3) sprinting [[Novacheck 98](#)]. Based on the user inputs, as well as the energy expenditure estimation, the current and appropriate locomotion mode for the navigation can be identified automatically. If the energy available  $E(t_n)$  is too low for the requested locomotion mode, our simulator will automatically stops the locomotion to allow the virtual human to rest. Therefore, in addition to the three walking, running and sprinting modes, a stopped mode was introduced. Each of the different modes have different biomechanical properties that are simulated.

Moreover, only correct transitions between locomotion modes are allowed. Therefore, we defined a state automaton to manage the transitions and maintain the simulation in a coherent state ([Figure 4.2](#)). Our simulator selects the type of each new step to minimize the transition time using the breadth first algorithm to find the shortest path between the current state and the requested state.

Finally, the contact events for the heel and toes with the ground are generated depending on the current mode. Therefore, the vibration model is always synchronized with the locomotion.

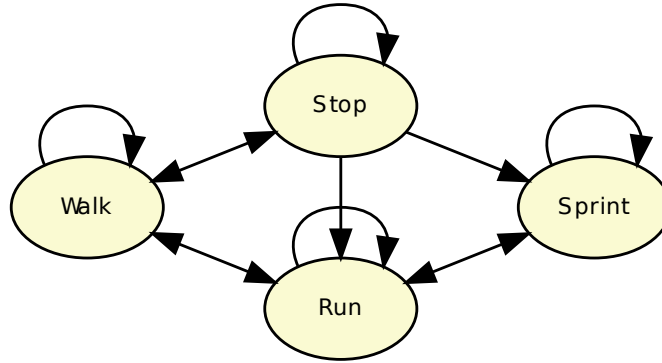


**Figure 4.2** – State Automaton for the transitions between locomotion types.

#### 4.1.6 Advance Speed of Camera Motions

To further increase the personified and multi-states characteristics of our new CM, we propose to modulate the advance speed  $v(t)$  to simulate more accurately the locomotion.

##### 4.1.6.1 Advance Speed

One major difference between the different locomotion modes is the differences in advance speed. Therefore, the advance speed can be used to render the different locomotion modes. Synchronized CM match the advance speed produced by the locomotion simulator. Thus, the visual flow is different depending on the locomotion mode. Locomotion modes are defined on non-overlapping speed ranges of user inputs in percentage of the virtual human physical capacity  $C_{VH}$ . For example, for a 35 years old male of 1.75 m high and 70 kg with a good fitness, the maximal advance speed for the different locomotion modes on flat ground is summarized [Table 4.4](#).

Stop	Walking	Running	Sprinting
$0 \text{ m} \cdot \text{s}^{-1}$	$1.16 \text{ m} \cdot \text{s}^{-1}$	$2.79 \text{ m} \cdot \text{s}^{-1}$	$6.22 \text{ m} \cdot \text{s}^{-1}$

**Table 4.4** – Maximal advance speeds set in our implementation for the different locomotion modes for a 35 years old male of 1.75 m high and 70 kg with a good fitness.

##### 4.1.6.2 Oscillations Phase and Frequency

The generated steps provide information on the locomotion mode used and the transitions between steps. Indeed, step length and duration depend of the locomotion mode. Therefore, synchronization of the CM with the steps generated by the locomotion simulator improves the rendering of the different modes. The oscillation frequency was set to match the current step duration, and incidentally the percentage of completion of the current step  $P_{step}$  ([Equation 4.15](#)). Moreover, the phase of the lateral oscillations  $\varphi$  was set depending on the current foot ( $\varphi = 0.5$  for the left foot and  $\phi = -0.5$  for the right foot).

$$P_{step} = \frac{t_{step}}{d_{step}} \quad (4.15)$$

where  $d_{step}$  is the duration of the current step and  $t_{step}$  the duration since the beginning of the step.

#### 4.1.6.3 Slope-Dependant Camera Motions

Interestingly enough our new CM can also take into account the geometry of the VE. Indeed, the slope has an important impact on the locomotion: the advance speed  $v(t)$  directly depends of the slope. When the virtual human navigates down a hill, the advance speed increases, and thus the oscillations of the CM are also adapted. The inverse is also true when the virtual human climbs a hill.

Moreover, the orientation of the camera also reflects the differences of the slope of the ground. A pitch component  $R_x$  is introduced in our CM to improve the perception of the slope. Indeed, the orientation of the camera can also be used to improve the perception of the slope [Marchal 10]. The camera is oriented to look on the ground in front of the user while climbing or going down a slope. Finally, to avoid jitter on the camera, a low-pass filter is used on the pitch component of the camera with a cut-off frequency of 0.1 Hz.

#### 4.1.6.4 Speed Computation

The navigation in the VE depends actually on the advance speed  $v(t)$ . The navigation speed is different between walking and running locomotion for example.

Our simulator provides a new method to evaluate the advance speed in the VE. The advance speed in VE depends on the speed required by the user  $P_{C_{VH}}$ , defined in percentage of the physical capacity of the virtual human  $C_{VH}$ . Therefore, the advance speed also depends on the characteristics of the virtual human. For example, a trained athlete will run faster than a man who does not make any exercise. However, the user would also expect a decrease in velocity when climbing a slope.

The variation of the sum of energies involved during the locomotion  $\Delta E_{tot}$  is null (principle of conservation of the energy):

$$\Delta E_{tot} = \Delta E_c + \Delta E_p + \Delta E_{loc} + \Delta \epsilon = 0 \quad (4.16)$$

where  $E_c$  is the kinetic energy,  $E_p$  the potential energy,  $E_{loc}$  the energy spent for the locomotion and  $\epsilon$  the sum of the energy losses of the system.

Therefor  $\Delta E_{loc}$  is defined such as:

$$\Delta E_{loc} = C.m.P_{C_{VH}}.C_{VH}\Delta t \quad (4.17)$$

with  $m$  the weight of the Virtual Human in kg and  $C = 0.336$  a constant required to maintain the compatibility between  $C_{VH}$  and the maximal oxygen consumption model.

The speed is directly correlated to the kinetic and potential energy and therefore to the variation of the altitude (i.e. to the slope) and the mass of the virtual human. Moreover, for aerobic locomotions, the advance speed and the oxygen consumption have a direct relation. Our locomotion simulator extrapolates this relation to estimate the advance speed for all the possible locomotions:

$$P_{C_{VH}}.C_{VH} = 3.5.v(t_n) + V_{rest} \quad (4.18)$$

where  $V_{rest} = 3.5$  is the energy cost associated to the stopped mode.

However,  $\Delta\epsilon$  is much more complex to evaluate, as it depends of the energy lost in heat or lost during the impacts of the feet with the ground for example. To simplify this problem, the variation of the energy loss was considered to remain approximately constant independently of the slope of the ground.

Finally, the value of the advance speed depends of the slope, the weight of the virtual human, but also all the other physiological parameters used to determine  $C_{VH}$ . Therefore, the advance speed for the navigation becomes multi-states and personified.

### 4.1.7 Results and Performance

To evaluate the behavior and performances of our CM, we generated test cases to exhibit the evolution of the different components of our simulator for various scenarios. For all the test cases, we simulated a 35 years old male of 1.75 m high and 70 kg with a good fitness.

#### 4.1.7.1 Benchmark

Our simulator is designed to have an algorithm complexity as small as possible. Indeed, our simulator must be able to run in real time on any kind of platform. Therefore, we need to evaluate the real performances of our simulator in term of execution time.

In this scenario, the advance speed was increased linearly from the rest position to the maximal sprint. The navigation was in straight line in a flat VE. The execution time of the CM feedbacks was measured at each frame. On a second time, the vibration component of the CM produced was deactivated. During the two benchmarks, the rendering was set at 50 Hz. The processor used was an Intel Quad Core Extreme Q9300 running at 2.53 GHz.

First, we observed that the Mean (M) and Standard Deviation (SD) of the frames execution time was low ( $M = 144 \mu s$  and  $SD = 594 \mu s$ ). However, the maximal frame execution time was significantly higher ( $4627 \mu s$ ). The high execution time frames corresponded to the contact of the heel and toes with the ground (Figure 4.3). We can observe that the time between contacts gets shorter when the speed increases. We also validated that only one event is generated for the sprint.

The first benchmark illustrated that the performances of our simulator depend only on the vibration visual feedbacks. Therefore, to get a better idea of the performances for other frames, we run a second benchmark without the vibration component activated (Figure 4.3). We found that the average execution time is indeed much lower ( $M = 4.87 \mu s$  and  $SD = 1.74 \mu s$ ).

#### 4.1.7.2 Influence of Slope

The slope has a direct impact on the advance speed. Indeed, the advance speed is computed using the variation of potential energy during the step. Therefore, the variations of the speed should follow the inverse of the slope.

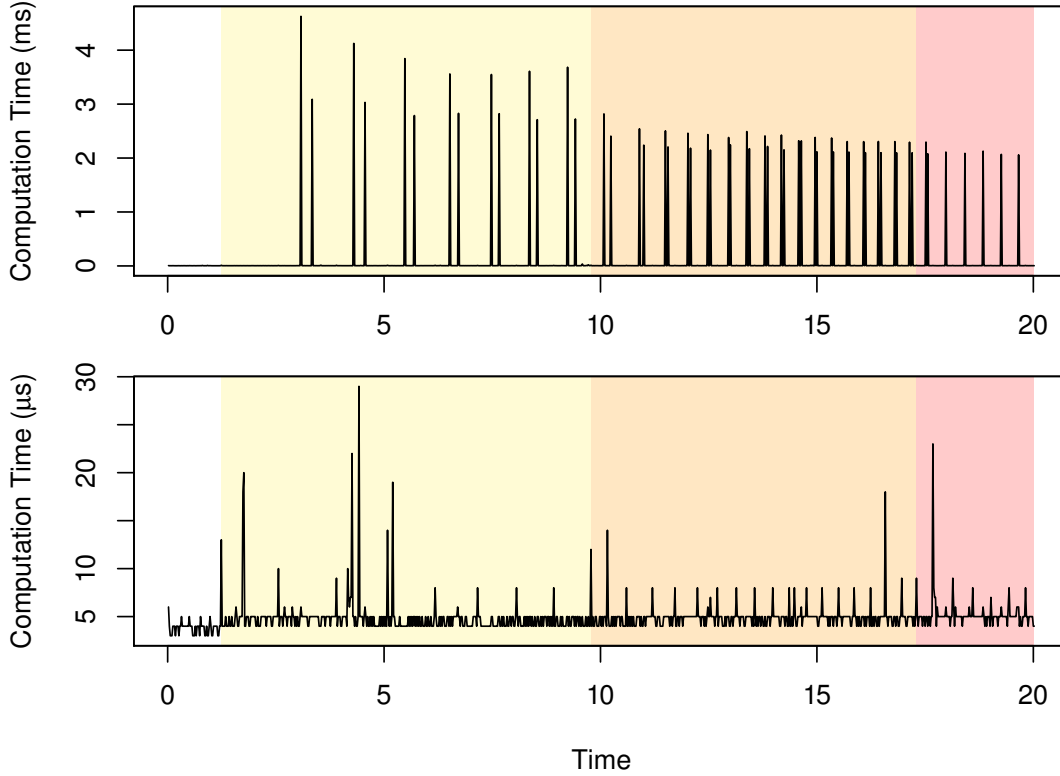


**Figure 4.3** – Benchmark of the locomotion simulator. The computation time of the simulator is measured for each frame with: (a) all feedbacks enabled and (b) without the vibration component. The benchmark is made for a graphical rendering at 50 Hz. The locomotion modes are represented as the background colors, yellow for walking, orange for running and red for sprinting.

The navigation was in straight line, with a constant user input corresponding to a moderate walk (Figure 4.4a). During the navigation, the virtual human crossed a regular 1 m high and 10 m wide bump. The advance speed was monitored step-by-step during all the navigation.

During the first flat section, the advance speed remained constant. However, when climbing the bump, the speed decreased proportionally to the slope (Figure 4.4a). On the other hand, when the virtual human started to go down the bump, the speed started to increase proportionally to the slope. Moreover, the speed during this phase was higher than the speed on flat ground.

#### 4.1.7.3 Influence of Virtual Human Morphology

The virtual human age, gender, weight and fitness have an important impact on many factors of the locomotion simulator. Indeed, those parameters are used to evaluate the fatigue as well as the advance speed. We propose to consider here the influence of the fitness on the advance speed. Similar evaluations for the other parameters and/or for the



fatigue were done similarly.

The advance speed increased gradually from the rest position to the maximal sprint (Figure 4.4b). The navigation was in straight lines in a flat VE. Finally, the value of the advance speed was monitored for different values of fitness: fair, good and superior.

First, we observed a correct transition between the different locomotion modes from walking to running and finally sprinting. The advance speed strictly increases with the user input (Figure 4.4b). As our simulator produces each step independently, the speed remains strictly constant during a given step. Therefore, the advance speed output is aliased: each level corresponds to a particular step during which the speed remained constant. The speed is lower for the fair fitness and greater for the superior fitness compared to the good fitness. Moreover, the difference between the three values of fitness increases with the speed. Indeed, the speed computation is quadratic and not linear. Finally, the step length is not impacted by the different values of fitness.

#### 4.1.7.4 Influence of Virtual Human Fatigue

The fatigue parameter is essential to the locomotion simulator. Indeed, not only the fatigue is a crucial parameter for our new Camera Motions, but it also controls the navigation directly when the energy reserves are depleted.

The user inputs were modulated precisely to exhibit different aspects of the energy expenditure estimation simulator (Figure 4.4c). The simulated navigation was in straight lines on a flat VE. The user inputs consisted in a phase of sprint, followed by a phase of rest. The user then walked at a slow pace and finally run at a high pace.

During the sprinting phase, the energy decreased very fast, but in a constant manner because the user input were constant (Figure 4.4c). When the energy was completely depleted, the virtual human stopped automatically (even when the user continued to ask for sprint), and transition steps were made from sprint to run and then walk. During the resting phase, the energy increased constantly and rapidly. During the slow walk, the energy continued to increase slowly. Finally, during fast running (marathon speed), the energy started to decrease again, but much more slowly than during the sprint. Indeed, the user should be able to run a long time at marathon speed.

#### 4.1.8 Conclusion

We proposed a new CM model to render multi-states and personified locomotion. Our model provides a feedback adapted for the walking, running and sprinting modes. Moreover, our new CM provides a personified rendering which depends on the simulated virtual human. Therefore, physical properties of the virtual human can be perceived visually, through the CM, during a first person navigation. Moreover, the physical condition of the virtual human is also rendered. Therefore, our CM can simulate different configurations of virtual human, ranging for instance from trained athletes to old ladies. An example of vertical oscillations produced by our CM is represented Figure 4.5.

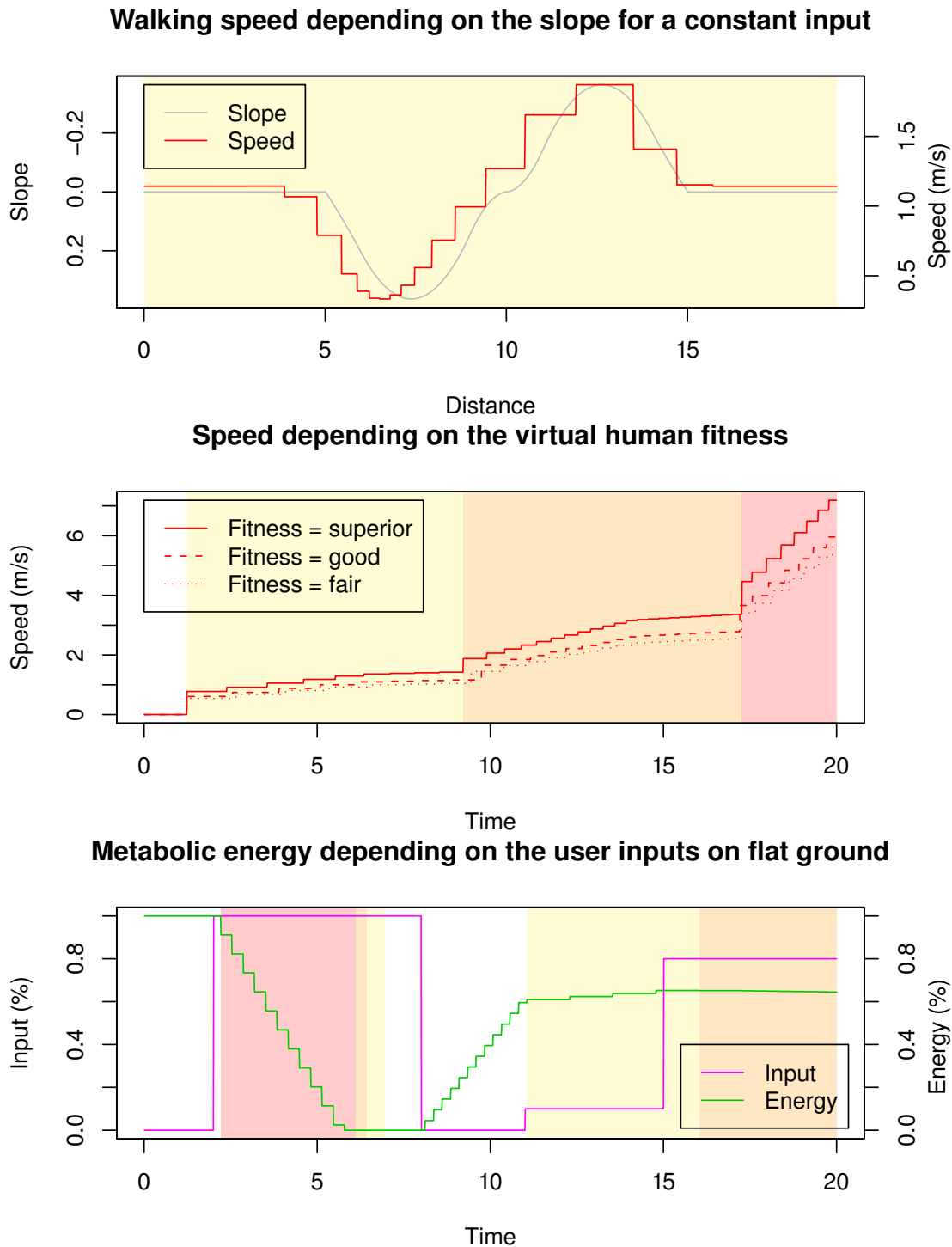


**Figure 4.4** – Influence of the slope and virtual human fitness and fatigue. The locomotion modes are represented as the background colors, yellow for walking, orange for running and red for sprinting. When walking up and down a small hill, the Speed depends on the inverse of slope.

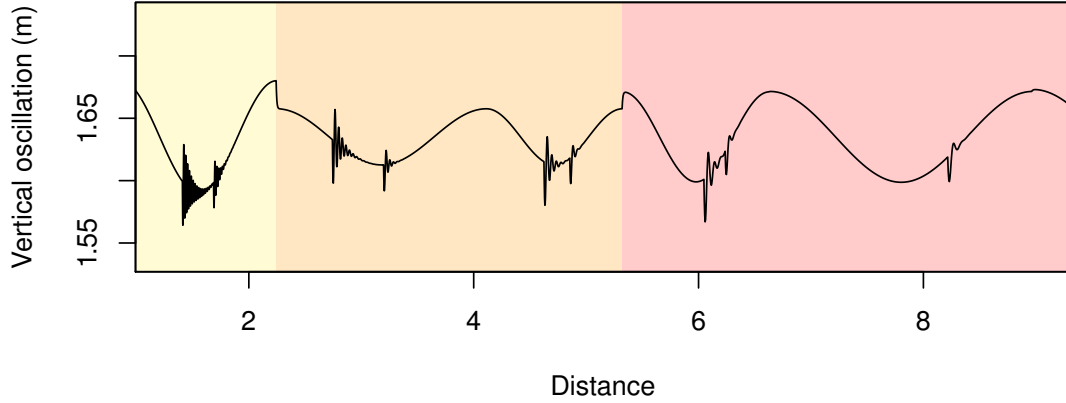


**Figure 4.5** – Vertical oscillations for a 35 years old male of 1.75 m, 70 kg with a good fitness. The amplitude and frequency of oscillations, as well as the amplitude of vibrations depends on the locomotion mode. The locomotion modes are represented as the background colors, yellow for walking, orange for running and red for sprinting.

## 4.2 Perceptual Evaluation of Personified and Multi-States Camera Motions

We conducted a perceptual study of the proposed multi-states and personified CM. Our objective was to demonstrate the value of CM to perceive the locomotions modes, as well as the characteristics of the virtual human. Our study is composed of four different experiments.

The first experiment is designed to evaluate whether the participants are able to correctly detect the locomotion mode used for the navigation. The second experiment focused on determining whether the transitions between different locomotions modes are perceived correctly. The third experiment seeks to determine if the participants perceive well the properties of the virtual human, such as its fitness, weight and age. Finally, the fourth experiment is designed to evaluate the influence of the advance speed on the detection of the locomotion mode.

### 4.2.1 Method

#### 4.2.1.1 Population

Twelve participants (10 males and 2 females) aged from 20 to 31 (Mean  $M = 25.75$ , Standard Deviation  $SD = 2.93$ ) performed the three first experiments. Moreover, twelve new participants (11 males and 1 female) aged from 15 to 34 (Mean  $M = 25.83$ , Standard Deviation  $SD = 5.1$ ) performed the fourth experiment. None of the participants had any

known perception disorder. All participants were used to VEs but were naïve with respect to the proposed techniques, as well as to the experimental setup.

#### 4.2.1.2 Virtual Environment

The Virtual Environment was composed of closed room representing a virtual museum with paintings and statues (Figure 4.6). The room depth was set to 15 m (Figure 4.6). Moreover, statues were placed along the advance path to improve the visual flow and perception of proportion in the VE. Finally, during the active navigations (third experiment), a bump on the ground was produced using the top of a 10 m radius sphere. The resulting bump was 1 m high and 8.7 m long (Figure 4.6). The participants were always exposed to navigations of 10 m.

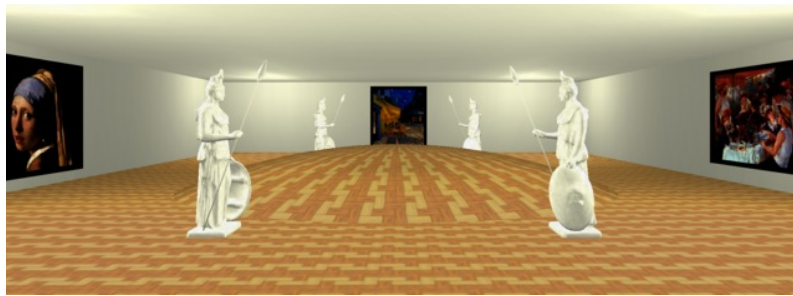


Figure 4.6 – Virtual Environment.

#### 4.2.1.3 Experimental Apparatus

The participants were seated at 1 m in front of a 24 inch widescreen monitor with a resolution of  $1920 \times 1200$  pixels (physical field of view of  $29^\circ$  horizontally and  $18^\circ$  vertically). The rendering was made at a refresh rate of 50 Hz. The participants had the possibility to take breaks by pressing the “Space” key at any time.

#### 4.2.1.4 Collected Data

For the first and fourth experiment, the answers of the participants were recorded at the end of each trial with the answer time. For the second experiment, a boolean was recorded for each trial if the participant detected a transition, as well as the time between the transition and the answer of the participant. Finally, for the third experiment, the preferred trial was recorded.

The participants were also asked to fill a questionnaire at the end of the experiment where they were free to detail their impressions on the different conditions they were exposed to.

### 4.2.2 Experiment 1: Detection of the Locomotion Modes

In this experiment, the participants had to detect the locomotion mode used for the navigation (walking, running or sprinting) at various constant advance speeds. The participant were exposed to passive navigation in straight line. At the end of each navigation, they had to choose which locomotion mode was presented.

#### 4.2.2.1 Experimental Conditions

For each of the possible locomotion modes (Walking, Running, Sprinting), we selected three different speeds corresponding to inputs of 0.25, 0.5 and 0.75 percents. It resulted in 9 different possible locomotions. The locomotions were presented randomly by block, each of the condition presented the same number of time than the others. The participants had to choose the correct locomotion mode at the end of the navigation using the keyboard keys “1”, “2” and “3” and then validate their choice with the “Enter” key.

#### 4.2.2.2 Results

We analyzed the Mean ( $M$ ) and standard deviation ( $SD$ ) of the percentages of correct answer for each locomotion mode. We found that walking was correctly detected ( $M = 0.95$ ,  $SD = 0.11$ ). However, the running and sprinting obtained poor global results ( $M = 0.26$ ,  $SD = 0.20$  and  $M = 0.34$ ,  $SD = 0.23$  respectively). In order to understand those results, we plotted the mean percentage for each condition (Figure 4.7). We found that the locomotion modes are largely underestimated. Indeed, the running locomotions are detected as walking, and the sprinting as running.

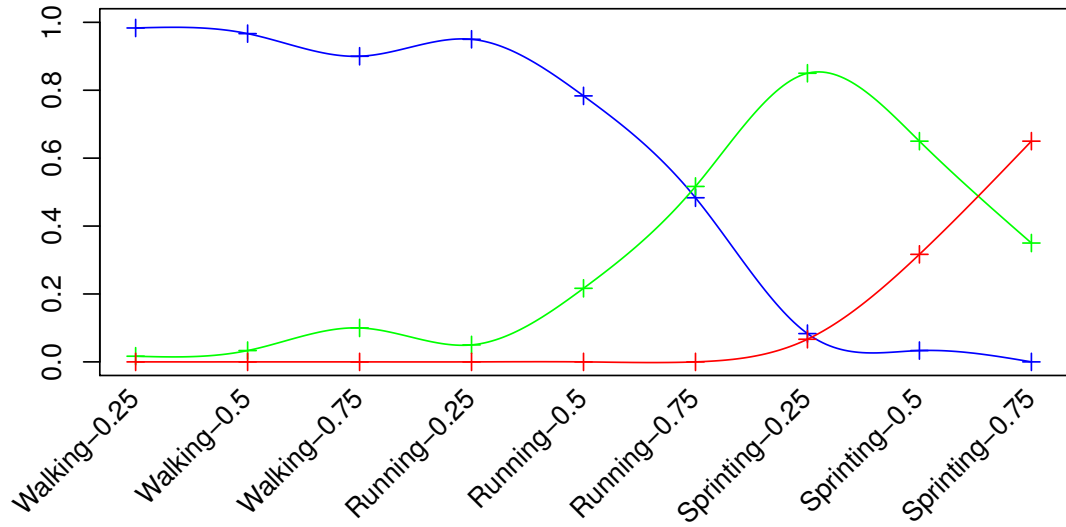


**Figure 4.7** – Detection rates for the three locomotion modes (walking in blue, running in green and sprinting in red).

#### 4.2.3 Experiment 2: Detection of the Transitions Between Locomotion Modes

During the second experiment, the participants were asked to detect the possible transitions between two locomotion modes for given variations in the advance speed.

##### 4.2.3.1 Experimental Conditions

For each of the possible locomotion modes (Walking, Running, Sprinting), we selected two different speeds corresponding to inputs of 0.4 and 0.8 percents. We tested all the

possible combinations between speeds, resulting in 22 different possible locomotions. The locomotions were presented randomly by block, each of the condition presented the same number of time than the others. The participants had to press the “Enter” key at the moment they detected the transition between two locomotion modes.

#### 4.2.3.2 Results

We analyzed the Mean (M) and standard deviation (SD) of the percentages of correct answer for each couple of locomotion mode (Table 4.5). We found that changes of speed without changing the locomotion mode are correctly detected ( $M = 92\%$ ,  $81\%$  and  $69\%$ ). However, the percentage of correct detection tends to decrease when the speed increases. The transitions between running and sprinting modes are also correctly detected ( $M = 71\%$  and  $M = 86\%$ ). However, the transitions between the walking and running modes are not detected by the participants: half of the transitions were not detected ( $M = 45\%$  and  $M = 45\%$ ).

	Walking	Running	Sprinting
Walking	0.92 (0.12)	0.45 (0.30)	-
Running	0.45 (0.27)	0.81 (0.26)	0.86 (0.15)
Sprinting	-	0.71 (0.22)	0.69 (0.30)

**Table 4.5** – Mean and standard deviation of the percentages of correct answers. The first locomotion modes are represented in row and second in column. Direct transitions from walking to sprinting are not allowed by the CM.

#### 4.2.4 Experiment 3: Perception of the Virtual Human Properties

The third experiment was based on a 2 Alternative Forced Choice (2AFC) paradigm. The participants were exposed to pairs of active navigations in straight line using different conditions. At the end of each pair, the participants were asked to chose one navigation between two depending on the parameters of the virtual human. In every case, the participants had to choose between the two navigations. The first criterion was designed to evaluate the perception of the virtual human fitness. Finally, the second investigated the influence of the age of the virtual human.

##### 4.2.4.1 Experimental Conditions

We tested two different parameters for the virtual human: (1) the fitness and (2) the age of the virtual human. All the other parameters were set to simulate a 35 years old male virtual human of 70 kg and 1.7 m height with a good fitness. We counter balanced the order of presentation of the different conditions. For each condition, we tested three different values. The pair of values were presented in random order by block, each of the pair presented the same number of time than the others.

The users used a joystick to control their advance speed. At the end of each pair of navigations, they had to select their preferred navigation using two joystick buttons and then validate their choice with the joystick trigger.

#### 4.2.4.2 Results

For a given pair of conditions, each individual performed 6 comparisons. Under the null hypothesis of equal preference between the two conditions, the number of times an individual preferred the first condition follows a binomial distribution with parameters 10 and  $1/2$ . After standardization, such variable can be approximated by a standard normal random variable. Thus, for each pair of conditions, we tested the presence of a preferred condition using a Student's t-test. The p-values were adjusted with a Bonferroni correction.

**Influence of the Virtual Human Fitness.** The different values of virtual human fitness were: (1) fair  $F_{fair}$ , (2) good  $F_{good}$  and (3) superior  $F_{sup}$ . The participants had to select the navigation where the virtual human had the best fitness. We analyzed the answers of participants for the different fitness in order to determine if the fitness of the virtual human is correctly perceived by the participants.

The analysis showed that  $F_{sup}$  was more often significantly chosen than  $F_{good}$  ( $t(11) = 21.06$ ,  $p < 0.001$ ) and  $F_{fair}$  ( $t(11) = 9.94$ ,  $p < 0.001$ ). Moreover,  $F_{good}$  was more often significantly chosen than  $F_{fair}$  ( $t(11) = 4.21$ ,  $p = 0.002$ ). Our results suggest that our personified CM provide enough feedback to always detect the fitness of the virtual human correctly.

**Influence of the Virtual Human Age.** The different values of virtual human age were: (1) 25 years old  $A_{25}$ , (2) 35 years old  $A_{35}$  and (3) 55 years old  $A_{55}$ . The participants had to select the navigation where the virtual human was older.

The analysis showed that  $A_{55}$  was more often significantly chosen than  $A_{35}$  ( $t(11) = 8.40$ ,  $p < 0.001$ ) and  $A_{25}$  ( $t(11) = 8.40$ ,  $p < 0.001$ ). Moreover,  $A_{35}$  was almost significantly more often chosen than  $A_{25}$  ( $t(11) = 3.63$ ,  $p = 0.006$ ). Our results suggest that our personified CM provide enough feedback to detect the age of the virtual human correctly.

### 4.2.5 Experiment 4: Influence of VR on the Detection of the Locomotion Modes

The fourth experiment was similar to the first one. However, for the tested navigation, the advance speed was multiplied by various factors  $SF$  in order to determine the impact of the VE on the perception of first person locomotions.

#### 4.2.5.1 Experimental Conditions

Contrary to the first experiment, we added a constant factor to the advance speed to increase the locomotion speed in the VE and improve the perception of the different locomotion modes. Moreover, we also modified the algorithm used to compute the step length for the sprint in order to keep a constant step length independent of the speed factor. Thus the frequency of the steps during the sprint was decreased to be inversely proportional to the speed factor  $SF$ .

We tested three different speed factors  $SF$  of 1, 2 and 3. For each speed factor we counter-balanced the order of presentation. Moreover, for each of the possible locomotion



modes (Walking, Running, Sprinting), we selected three different speeds corresponding to inputs of 0.25, 0.5 and 0.75 percents. It resulted in 9 different possible locomotions. The locomotions were presented randomly by block, each of the condition presented the same number of time than the others.

#### 4.2.5.2 Results

We analyzed the Mean (M) and standard deviation (SD) of the percentages of correct answer for each locomotion mode. We found that walking was correctly detected independently of the speed factor (Table 4.6). For  $SF = 1$ , the results for the running and sprinting modes are consistent with the first experiment. However, the percentage of correct answer gradually increase with the speed factor. Indeed, the running and sprinting detection are superior with  $SF = 2$  ( $M = 36\%$   $SD = 0.31$  and  $M = 49\%$ ,  $SD = 0.3$  respectively). Finally, the best results were obtained for  $SF = 3$  with  $M = 50\%$ ,  $SD = 0.27$  for the run and  $M = 79\%$ ,  $SD = 0.23$  for the sprint. For each condition we plotted the mean percentage of correct answer (Figure 4.8). We found that the locomotion modes are largely underestimated. Indeed, the running locomotions are detected as walking, and the sprinting as running. However, the underestimation of the locomotion mode clearly decreases when the speed factor  $SF$  is increased.

Speed Factor	1	2	3
Walking	0.99 (0.02)	1.0 (0.0)	0.93 (0.12)
Running	0.22 (0.22)	0.36 (0.31)	0.50 (0.27)
Sprinting	0.16 (0.17)	0.49 (0.30)	0.79 (0.23)

**Table 4.6** – Mean and standard deviation of the percentages of correct answers depending on the speed factor.

#### 4.2.6 Discussion

Our results suggest that our novel camera motion model, associated with our locomotion simulator, can provide meaningful visual feedback which can be successfully exploited by users to identify either: the locomotion mode, the transitions between the locomotion modes, and at least two parameters of the virtual human (age and fitness of the avatar).

Interestingly, we have found that the participants globally underestimated the advance speed in the VE. Indeed, running motions were often classified as walking ones, or sprinting motions were classified as running ones. For a “normal” speed factor (of 1), some participants explicitly notified or stressed this effect: “*I think the speed should be increased because for me it felt more like slow walk, normal walk and run*”. Scaling up the advance speed parameter seems to improve the detection rates and reduce the shift. We found that the best detection rates, closest to what would be expected, were achieved for a speed amplification factor of 3. This underestimation might be related to the well-known underestimation of (traveled) distances in virtual environments, which would here straightforwardly influence the speed estimation.

We also found that participants were able to correctly discriminate the motions corresponding to different values of age or fitness of the virtual humans used. To do so, participants

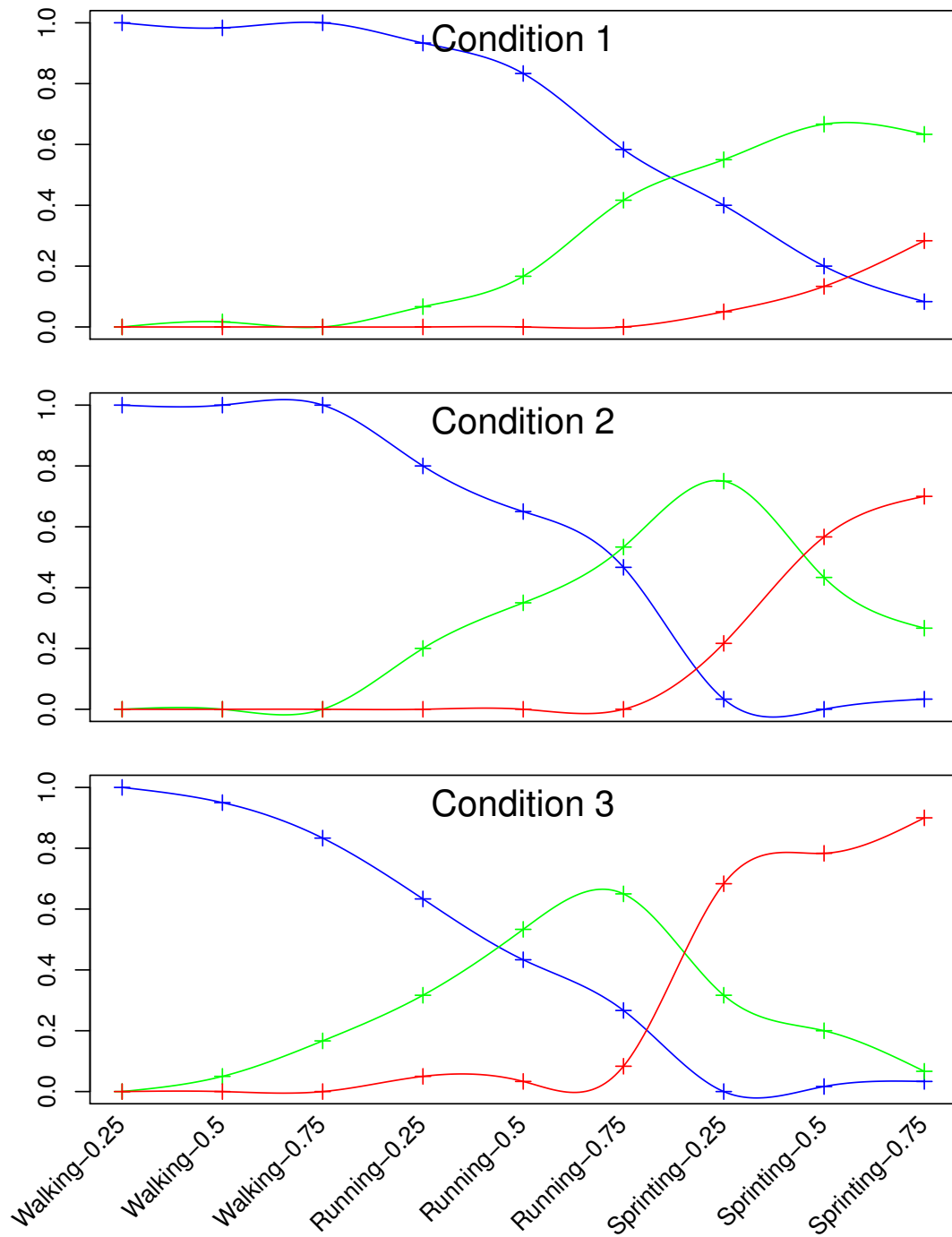


**Figure 4.8** – Detection rates for the first, second and third conditions for the three locomotion modes (walking in blue, running in green and sprinting in red).

could rely on the advance speed but also on numerous other visual cues embedded in the camera motions : changes of locomotion mode, number of contacts with the ground for each feet, amplitudes of the oscillations, etc. For example, the simulated fatigue seems to be an important factor for some participants, as quoted in the subjective questionnaires: *“I watched if I could get over the hill in one smooth motion or if I had to slow down or stop”*. Future work could now focus on evaluating the influence of each visual cue on the resulting perception and estimation.

As observed in the post-hoc questionnaire and as informal feedback, it seems that the participants have well appreciated our new CM, and even suggested some interesting applications such as video games or virtual visits. Some participants even suggested to create a simulator to have a preview of how walking would “feel” when getting older or “fatter”.

#### 4.2.7 Conclusion

To sum up, our novel CM produces a multi-states and personified navigation. The users are able to perceive the properties of the virtual human in first-person mode. Moreover, the different locomotion modes are also detected correctly when using a factor on the advance speed to compensate the underestimation inherent to VR.

### 4.3 Influence of Camera Motions on Perception of Traveled Distances in Virtual Environments

As for today, camera motions still lack formal evaluations of their intrinsic properties. For instance, what is the influence of using this type of camera motion on the perception of properties of VE, such as the perception of traveled distances, the sense of orientation, or the perception of scale?

Therefore this section focus on the effect of the previous Camera Motions presented [subsection 4.1.2](#), i.e. the effect of compensated oscillating camera motions, on the perception of traveled distances in virtual environments. The goal of this experiment is to investigate if oscillating camera motions result in an increased accuracy of traveled distance perception in Virtual Environments (VE).

VE are often used in experiments that involve path integration or wayfinding. Indeed, VE enable to control more precisely the parameters of the experiment. For example, Meilinger et al. [Meilinger 08] used a photorealistic virtual environment representing a medieval city in order to study the influence of a set of different distracting tasks on the working memory task involved in memorizing a recently experienced route. Also with the help of VE, Riecke et al. [Riecke 02] found that, in absence of vestibular and proprioceptive cues, visual flow information alone was sufficient to support path integration for simple navigations, composed of one or two segments. Using VE, some studies could even demonstrate an increase in path integration accuracy for more complex paths [Wiener 06]. On the other hand, it appears that VR, lacking proprioceptive and vestibular sensations, can also result in systematic misperceptions of the general form of traveled paths [Riecke 07].

In our experiment, participants were presented with visual projections of a straight path. For half of the trials, the camera moved linearly (as in a car simulation), and for the re-

maining trials the camera oscillates around three axes in addition to the linear movement in order to simulate visual flow generated by human walking. We used the same compensated oscillating camera motions as proposed in [Lécuyer 06] and [Hillaire 08]. The participants' task was to estimate and reproduce the traveled distance.

### 4.3.1 Method

#### 4.3.1.1 Participants

Twelve participants aged between 22 and 59 (Mean  $M = 30$ , Standard Deviation  $SD = 12.6$ ) performed this experiment. There were 8 men and 4 women. One participant was left-handed, all the other participants were right-handed. All participants were naive with respect to the experimental setup and to the purpose of the experiment.

#### 4.3.1.2 Set-up

The experiment was carried out in a darkened room. Participants sat 3 meters in front of a half-cylindrical projection screen of 9.5 m by 2.4 m, but only the center of the screen was used (Figure 4.9). The resulting image was 3.25 m wide and 2.4 m high, and had a resolution of  $1400 \times 1050$  pixels. The physical field of view was  $55^\circ$  horizontally and  $45^\circ$  vertically. We used monoscopic rendering, with a frame rate of 50 Hz. The projector used was a Barco Galaxy 7+.



Figure 4.9 – Experimental setup.

The experiment was performed within an empty 3D virtual environment. All possible landmarks were removed so to avoid that the sizes of virtual objects give information about depths. The ground was made of a green color (#4db34d in hexadecimal RGB format), and the sky of a gray/blue color (RGB value: #e6e6f2). In order to provide participants with visual flow during navigation, a set of 100 000 gray points (RGB value: #4d804d) was displayed on the ground (see Figure 4.10). Each point had a radius of 5 cm, was randomly positioned in the environment, and had a random lifetime of  $5 \pm 3$  s. Using these limited lifetime dots, we avoided all problems of pattern repetitions peculiar to the use of textures.



Figure 4.10 – Visual display with random lifetime dots.

#### 4.3.1.3 Distracting task

In order to avoid time counting strategies when estimating traveled distance, participants had to complete a secondary task in parallel to the main task of estimating the traveled distance. During the passive navigation phase, they heard one to four random digits (from “1” to “9”), directly spoken into headphones every  $2 \pm 1$  s. The task was to memorize all the digits.

#### 4.3.1.4 Interaction

Directly after the completion of each passive navigation, participants had to enter the digits they heard with the keyboard and then press the “Enter” key in order to move on to the reproduction phase. During the reproduction phase, participants used the “Up” key (forward translation) and the “Down” key (backward translation) to move through the VE. As long as they pressed the key, the camera continued to move in the given direction at a constant velocity ( $V_0 = 1.2 \text{ m} \cdot \text{s}^{-1}$ ). The motion stopped when the key was released. Note that there was a short acceleration and deceleration phase when the keys were pressed or released in order to avoid any strong discontinuity in the motion’s speed. When participants estimated that they reproduced the correct distance, they validated their choice with the “Enter” key and the next trial started.

#### 4.3.1.5 Experimental plan

The participants were exposed to two sets of 28 trials: one set for each motion condition, e.g., linear camera motion vs. oscillating camera motion.

- The *linear camera motion* was a linear translation of the camera at a constant speed ( $V_0 = 1.2 \text{ m} \cdot \text{s}^{-1}$ ) as if the camera was on rails, or as if the user was driving a car.
- The *oscillating camera motion* was the same linear translation as in the linear camera motion ( $V_0 = 1.2 \text{ m} \cdot \text{s}^{-1}$ ), but additionally, the camera position was slightly moved on the vertical, lateral and forward axes depending on time. The camera motion used corresponds exactly to the model proposed by Lécuyer et al. [Lécuyer 06] and Hillaire et al. [Hillaire 08]. The main parameters of the camera motion were set

to: 80 cm step length, 6 cm oscillation amplitude on the vertical axis and 2.5 cm oscillation amplitude on the two other axes. The period on the lateral axis was twice the period on the two other axes. These values correspond approximately to the physical values observed for a person of 1.70 m height. The focus point was constantly set to the center of the screen. This point was used to compute a compensation of the camera as explained in [Lécuyer 06] and [Hillaire 08].

Participants were divided into 2 groups. One group ( $n = 6$ ) was first presented with the Linear Camera Motion trials, while the other group ( $n=6$ ) was first presented with the Oscillating Camera Motion trials.

In each condition, the participants were exposed to 7 successive blocks of 4 trials with different distances (5, 7, 10 and 13 meters). In each block, the presentation order of these trials was randomized. During a learning phase, prior to each condition (linear or oscillating camera motion), participants were provided with a set of 4 trials that did not enter in the final data set. The entire experiment lasted approximately 30 min.

### 4.3.2 Collected Data

The traveled distance and the distance reproduced by the participants (in meters) were automatically recorded at the end of each trial. The digits heard and entered for the distracting task were also recorded.

At the end of the experiment, participants were asked to fill out a subjective questionnaire in which they had to explain which strategies they used to complete the task. Using a seven-point Likert scale they were asked to evaluate both modes of camera motion according to five criteria: (1) *perception of distances*, (2) *immersion feeling*, (3) *impression of realism*, (4) *sensation of walking*, and finally (5) *simulator sickness*.

### 4.3.3 Results

Two different error measures were analyzed: the signed distance error and the absolute distance error. The signed distance error corresponds to the reproduced distance minus the required distance. The absolute distance error corresponds to the absolute value of the reproduced distance minus the required distance.

#### 4.3.3.1 Signed Distance Errors

The participants' performance in reproducing the navigated distance is characterized by an overall tendency to undershoot the distances (see Figure 4.11a and Figure 4.11b). Indeed, among the 12 participants, 8 participants undershot distances for all conditions and distances. Two participants overshot distances only for short distances and only for the linear camera motion. One participant overshot distances for all distances and only for the linear camera motion. Last, only one participant overshot all the distances for both conditions.

An ANOVA on signed distance errors (factors: navigated distance [5 m, 7 m, 10 m, 13 m] and camera motion [oscillating, linear]) revealed a significant effect of navigated distance

( $F(1) = 19.0, p < 0.001$ ). This effect reflects that the participants' tendency to undershoot the required distance increased with the length of the traveled distance.

Moreover, as illustrated on Figure 4.11a vs. Figure 4.11b, there appear to be more outliers and more overshootings with the linear camera motion than with the oscillating camera motion. This suggests that the use of oscillating camera motions can reduce variance and increase global accuracy. Indeed, for short distances (5 m and 7 m), the standard deviations of participants' signed responses were found significantly smaller in the oscillating camera motion condition (0.83) than in the linear camera motion condition (1.27) ( $t(11) = 2.71, p = 0.02$ ). For long distances (10m and 13m) the standard deviations of participants' signed responses did not differ significantly (linear motion condition: 1.60; oscillating condition: 1.38;  $t(11) = 0.98, p = 0.35$ ).

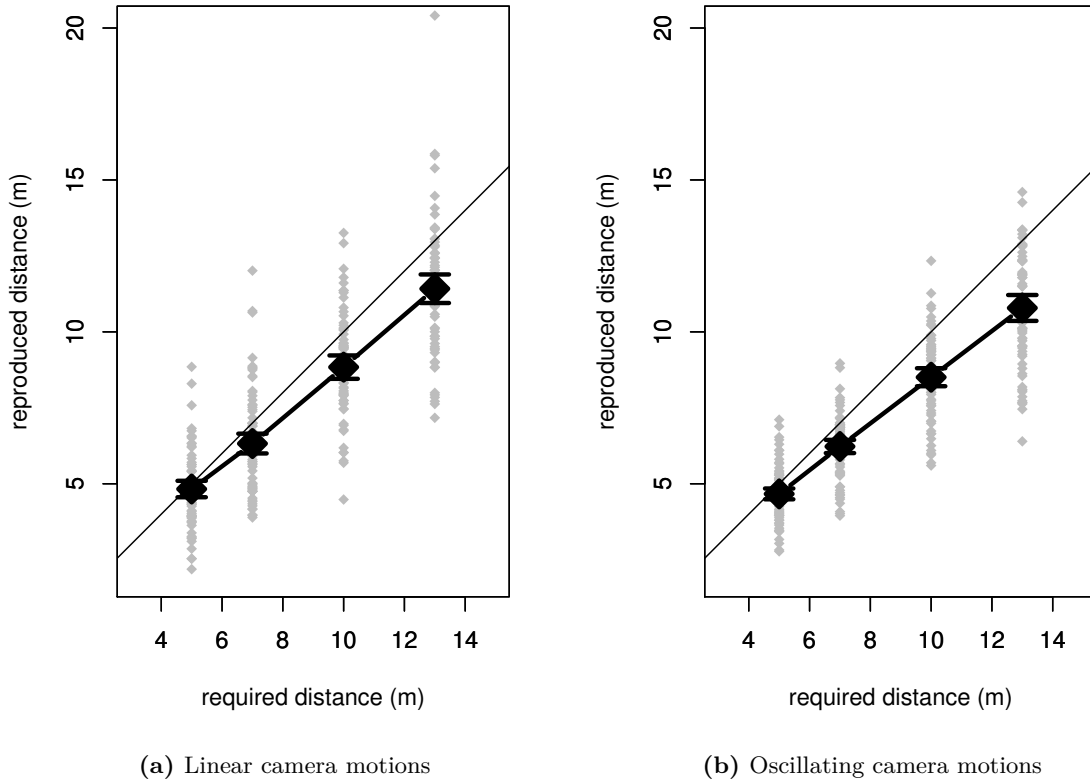


**Figure 4.11** – Distances reproduced by the participants vs. Required distances for both camera conditions.

#### 4.3.3.2 Absolute Distance Errors

An ANOVA (factors: navigated distance [5 m, 7 m, 10 m, 13 m] and camera motion [oscillating, linear]) revealed a significant effect of navigated distance ( $F(3) = 16.58, p < 0.001$ ) as well as a significant interaction between navigated distance and camera motion ( $F(3) = 3.02, p < 0.05$ ). To further characterize the nature of the interaction we pooled data over short distances (5 m and 7 m) and over long distances (10 m and 13 m) and analyzed the data again (see Figure 4.12). A T-test revealed a marginally



significant difference for short distances between the oscillating and linear camera motion ( $t(11) = 2.05$ ,  $p = 0.065$ ). Together with the significant interaction described above, and the reduction in variability, this tendency suggests that distance reproduction performance for short distances is more accurate with oscillating camera motion than with linear camera motion. For long distances, however, both kinds of camera motion rendered similar results.

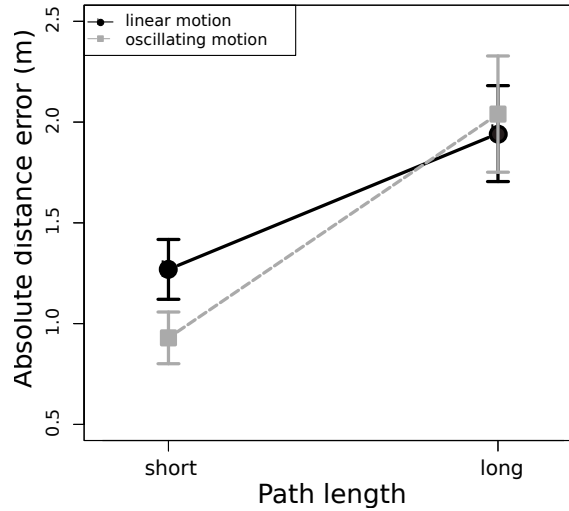


**Figure 4.12** – Absolute distance errors for short distances (5 m, 7 m) and long distances (10 m, 13 m).

#### 4.3.3.3 Questionnaire

The results of the subjective questionnaire confirmed the results of Lécuyer et al. [Lécuyer 06]. A Wilcoxon signed rank test showed significant differences for *distance perception* ( $z = -2.17$ ,  $p = 0.03$ ), *walking sensation* ( $z = -2.68$ ,  $p < 0.01$ ) and a marginally significant difference for *realism* ( $z = -1.77$ ,  $p = 0.08$ ). For these three criteria, on average participants seem to have preferred the oscillating camera motions (see Figure 4.13). However, the criteria of *immersion* and *simulator sickness* failed to be significant.

The participants were also asked to explain the strategies they used in order to complete the main task. Eight reported to have counted the number of steps during the oscillating motion, even if the secondary task made it complicated. In addition to this main strategy, five of them also tried to remember or “feel” the elapsed time for the linear motion or for both motions. Five participants reported to have tried to memorize the “rhythm” of occurrence of the digits of the secondary task, even if the digits appeared randomly. Three of the participants stated that they used a strategy involving the visual flow.

#### 4.3.4 Discussion

Results from this study suggest that the oscillating camera motion increases the accuracy of the perception of traveled distance, at least for short distances. This is supported by the significant decrease in standard deviations of participants’ responses and the marginally

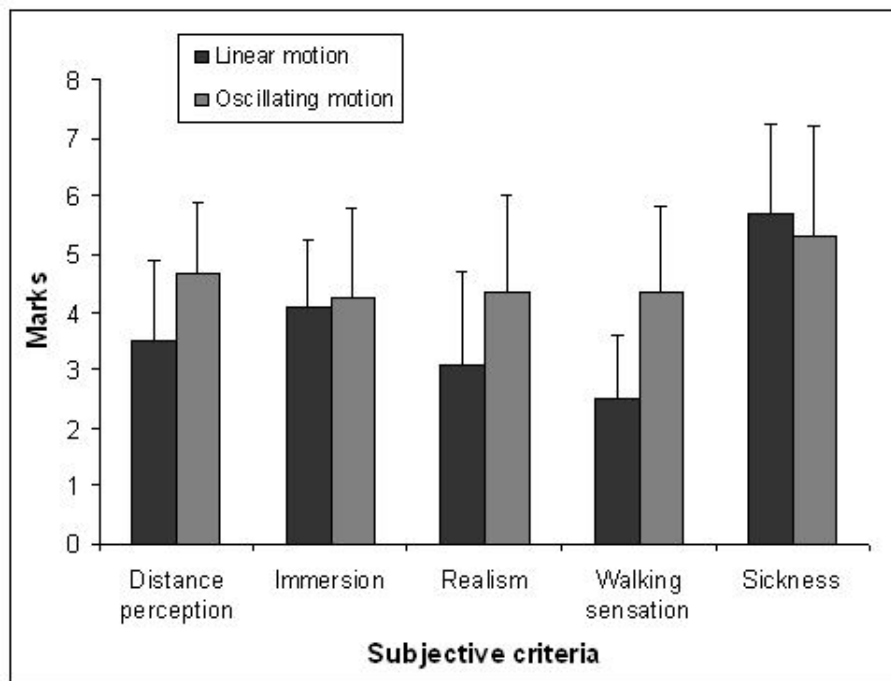


**Figure 4.13** – Subjective evaluation of oscillating camera motion vs. linear camera motion.

significant decrease of absolute distance error values, in the oscillating camera motion condition and for short distances.

Participants globally undershot traveled distances. Undershooting distances is a result that is often found and discussed in the literature [Plumert 04] [Interrante 06]. However, it is sometimes found that participants overshoot traveled distances, such as in [Riecke 05]. The main differences between our experiment and experiments found in related work (e.g., Riecke et al. [Riecke 05]) concern the generated visual flow and the field of view. For instance, the field of view used in our setup is smaller than the one used in Riecke et al. [Riecke 05].

The difference in performance concerning the estimation of traveled distance between oscillating camera motion and linear camera motion is found to be marginally significant. This marginality might be due to the secondary task used. This secondary task is a classical distracting task in experimental studies on distance perception which avoids that participants count the elapsed time. But it also prevent them counting the number of steps with the oscillating camera motion. It is possible that without the secondary task, the accuracy of the reproduced distances could have been increased with the oscillating camera motions. Indeed, if participants would have been able to count precisely the number of steps, they would have been able to reproduce the distances very accurately by reproducing the same number of steps. Moreover, we found that the effect of camera condition was marginally significant only for short distances. One explanation could be that our secondary task was more difficult for the long paths. Indeed, the number of digits that participants had to remember increased with the length of the path. Thus, the complexity increased and it presumably introduced more variance for long paths.

It could also be interesting to conduct this experiment again with an eye-tracking system in order to adapt the oscillating camera motion to the point on screen the user is actually looking at, such as in [Hillaire 08]. This implementation has been subjectively preferred

by participants in [Hillaire 08]. Thus, it might also improve the perception of traveled distance.

The results of our subjective questionnaires confirmed some of the results found in [Lécuyer 06] and [Hillaire 08]. Our questionnaires showed that participants preferred the compensated oscillating camera motion over the linear camera motion. They found that oscillating camera motions increased both the distance perception and the walking sensation. Besides, the subjective questionnaires showed no significant differences between the oscillating camera motion and the linear camera motion for the immersion criterion. It is maybe a consequence of the limited field of view, or of the visual environment that was not really realistic (random lifetime dots without other landmarks). The simulator sickness criterion also failed to be significant. One explanation could be the poor diversity of traveled paths. Indeed, traveled paths were only straight lines. Participants never had to turn or make complex trajectories. More complex paths could make them feel more dizzy. Another explanation is that the random lifetime dots seem to have disturbed the participants more than what we expected. The resulting visual flow could be tiring for the eyes and it might have had a high influence on the simulator sickness criterion, more than the camera motion condition.

#### 4.3.5 Conclusion

We investigated the use of camera motion to improve the perception of traveled distances in VE. We found that the accuracy of the reproduced distances seems to be increased by compensated oscillating camera motions, at least for short traveled distances. Taken together, our results suggest a positive influence of the camera motions on the perception of distances and on the sensation of walking in VE.

## 4.4 Conclusion

In this chapter, we proposed novel Camera Motions for multi-states and personified navigation. We proposed a generic approach to display the multiple modes of locomotion, and to take into account the properties of the avatar or the topography of the virtual environment. Our CM are adapted to walking, running and sprinting locomotions. Moreover, the physiology of the virtual human is taken into account: the locomotion is constrained by the physical capacity of the virtual human which depends on its age, gender, weight and fitness. Moreover, the locomotion also depends of the fatigue and recuperation of the virtual human. Finally, our new CM integrates the topography of the VE to render feedbacks adapted to the slope.

We conducted an experimental campaign composed of a series of experiments to evaluate the perception of our new multi-states and personified CM by naive participants when walking in VE in a first-person mode. We found notably that participants could discriminate (and perceive transitions) between the different locomotion modes, by relying exclusively on our CM. They could also perceive some properties of the avatar being used, like the virtual human fitness and age.

This chapter also investigated the influence of standard CM on the perception of traveled

distances in VE. We found that, for short traveled distances, the accuracy of the reproduced distance was increased by compensated CM. Our results suggest that CM can be used to improve the perception of short distances in the VE, as well as the sensation of walking.

# Conclusion

WE have proposed our contributions to the study of 3D interaction techniques and sensory feedback for improving navigation and walking in Virtual Reality.

We focused on two different research axes. In the first axis, we proposed a new interaction technique, the Shake-Your-Head (SYH), to improve navigation in VE using desktop and low cost VR equipment. In the second axis, we proposed two novel kinds of sensory feedback to enhance the sensation of walking and immersion in VR. The King Kong Effects (KKE) were designed to simulate and enhance the perception of the virtual steps of the virtual human. The personified and multi-states Camera Motions (CM) were designed to improve the range of information perceived visually during the navigation, in particular the properties of the virtual human and VE.

For each of the proposed techniques, we adopted a user-centered approach and conducted several evaluations. In particular, we conducted quantitative and qualitative evaluations of the proposed techniques to evaluate their performances as well as users preferences.

**The Shake-Your-Head.** First, we proposed the Shake-Your-Head technique for navigation in VE. This technique relies on the motions of the user's head to control the navigation. When the user walks-in-place in front of the screen, the oscillations of his head are measured to control the advance speed in the VE. Our technique is based on a low-cost webcam and can therefore be used in desktop VR context. This technique simulates walking in the VE, as well as jumping and crawling.

We conducted an experiment to compare the SYH technique to standard keyboard/joystick navigations. In this experiment, participants had to walk along slalom trajectories. We performed the evaluation in both desktop and immersive setups. We did not find any significant decrease in accuracy to complete the task with the SYH for simple slalom trajectories. Moreover, we found that the SYH requires only a small learning time. Finally, the SYH was more appreciated by the participants compared to joystick and keyboard-based navigations, and perceived as increasing the presence.

Then, we conducted an in-depth analysis of the trajectories produced with the SYH in the immersive setup. We notably found that the strategies of navigation between the different techniques were rather different. The participants exhibited a more precise control of their advance speed with the SYH, but more anticipation of the turns with the joystick. In particular, the trajectories with the joystick were smoother and more predictable. Taken together, our results suggest that the SYH technique provided a better control of advance speed while the joystick was more precise for controlling direction. These results could be used to further improve the SYH technique.

**The King Kong Effects.** We have introduced the King Kong Effects (KKE) technique to improve the sensation of walking in the VE using visual and vibrotactile feedback to simulate the steps of the virtual human. This technique is inspired from Hollywood movies

where the displacements of gigantic creatures are suggested through visual vibrations of the camera. We proposed to use vibrations in vertical and lateral directions to simulate the contacts of heels and toes with the ground. In addition, we have introduced vibrotactile feedback under user's feet to simulate both contacts. For the vibrotactile modality, we have proposed two different models: one model based on rigid contact of the feet with the ground and one model based on the ground reaction forces at each step.

We have conducted a series of experiments to determine the parameters of the KKE providing the best sensation of walking in the VE. We found that vertical visual vibrations were preferred over lateral oscillations. Moreover, we found that vibrations simulating only the contact of the heel were preferred over simulations of contact on heels and toes. Concerning the vibrotactile modality, we found that the model based on solid contact of the feet with the ground provides the best sensation of walking. Moreover, the simulation of the contact of the heel only was also preferred. Finally, a multimodal evaluation of the different components of the KKE showed that the different modalities used together can increase the sensation of walking in the VE.

**Personified and Multi-States Camera Motions.** We have introduced a novel approach to the Camera Motion (CM) technique. The standard CM are limited to the simulation of the walk only. Moreover, the properties of the virtual human and VE are not taken into account. We proposed a new model for personified and multi-states CM. Our CM can simulate walking, running and sprinting in the VE. Moreover, the locomotion is constrained by the physical capacity of the virtual human which depends on its age, gender, weight and fitness. Finally, the produced feedback is adapted to the slope of the VE.

We conducted a series of experiment to evaluate the perception of the different modes of locomotion (walking, running and sprinting) by the participants. We found that the participants could discriminate between two different locomotion modes by relying exclusively on our CM. Moreover, they could also perceive some properties of the avatar being used, such as its fitness and age. We also conducted a second evaluation on the influence of this type of visual feedback on the perception of traveled distances in the VE. We found that the CM can be used to improve the perception of short traveled distances in VE.

## Perspectives and Future Work

The work presented in this manuscript suggests some potential improvements, which could be addressed in short-term or long-term future work.

Hereafter, we present future research possibilities corresponding to the continuation of the different techniques introduced in this manuscript.

**The Shake-Your-Head.** First, the **control laws** used to control the turns of the Shake-Your-Head technique could be improved. Indeed, the analysis of the trajectories strongly suggested that this component of the SYH technique is not yet as efficient as joystick to control the direction. Moreover, the control laws used for jumping or crawling could also be improved. Indeed, the less accurate results on the complex trajectories could be explained by difficulties to control the jumps or crawling.

Second, more **modes of locomotion** could be integrated into the simulation. Indeed, the running and sprinting modes proposed in [chapter 4](#) could be integrated into the SYH to increase the range of possible navigation interactions with the SYH.

Third, a more precise or **biomechanically-inspired model** could be used to control the locomotion. Indeed, instead of a set of heuristic, the SYH would gain to be based on more formal knowledge of the human locomotion. Therefore, the control laws could be extended to simulate new locomotion modes for example.

Last, new **evaluations** of the SYH could be done. For example, the SYH could be evaluated by participants who are not used to the keyboard and joystick navigations. Indeed, all the experimental participants were very familiar to those techniques but naive to the SYH. The SYH could also be evaluated in more complex situations, such as navigations in complex environments or navigations in parallel to other more complex tasks.

**The King Kong Effects.** First, new **modalities** could be integrated into the KKE to increase the perception of the virtual steps. For example, the auditory modality could be used by introducing existing footstep sounds synthesis techniques into the KKE. Moreover, the footstep sounds could provide additional information about the ground properties, such as its material (snow, gravel or concrete for example). Vestibular information could also be introduced using the Galvanic Vestibular System [[Nagaya 05](#)] for example.

Second, concerning tactile/vibratory feedback, we identified the model providing the best sensation of walking between the two proposed. However, **new models** could yield to even better results. In particular, the KKE are not aiming at a physically realistic simulation of the sensory feedbacks produced at each step but could be considered as a metaphor to increase the sensation of contact with the ground at each step. Therefore, new models could be designed and should be tested and compared to the models presented in this manuscript.

Last, the influence of multimodal simulation on the sensation of walking could be more extensively studied. In particular, new **evaluations** of the KKE could be done.

**Personified and Multi-States Camera Motions.** First, the current model of CM is only adapted to the slope of the VE. Other **properties of the VE** could also be taken into account and simulated, such as the material of the ground (water, snow, or mud for example). The CM could also adapted to take into account some specific navigations and specificities of the VE, such as stairs for example.

Second, the CM could be **used together with other feedback techniques** like the vibrotactile component of the KKE. Indeed, some parameters computed, such as the advance speed or the fatigue of the virtual human, could be useful to improve the range and pertinence of other sensory feedback techniques.

Last, other **evaluations** of the properties of the CM could be made. Indeed, we evaluated the influence of CM on the perception of traveled distances in the VE, but the influence on other factors such as scale could be tested. Moreover, we could evaluate the influence of CM on more complex paths than slaloms, as well as their influence on the sens of orientation of the participants.



In addition to the future work mentioned above, this Ph.D. thesis could also pave the way to new research directions and long-term views.

### **Towards Low-Cost Multimodal Navigation in VE**

During the walk, and more generally any natural human locomotion, different senses are used to perceive and control the locomotion [Harris 99]. Natural human locomotion is fundamentally a multimodal experience, including but not limited to visual, auditory, vestibular and kinesthetic information. The number and complexity of the simulated modalities when navigating in current VR applications are still limited by the current technology. Each modality is often rendered separately to the user, and integrating different techniques together can be a complex or costly problem.

Recently, new kinds of interaction or sensory feedback devices have been developed. For example, the Microsoft Kinect [Microsoft 12] is a low-cost tracking interface designed to let the users interact with immersive systems using their bodies. Therefore, this system can be used to provide vestibular or proprioceptive cues. Similarly, new devices for auditory or haptic/vibrotactile modalities are getting more accessible. Thus, in the longer term, we can imagine that low-cost VR applications could propose full-body interaction and feedback for navigation in VR. These applications could be used everyday by millions of users in virtual visits in historical or architectural/urban applications for example. However, for this to become a reality, the question of unified multimodal models must probably be solved first.

### **Towards Biomechanically Driven Navigation in VE**

In the different chapters of this manuscript, we regularly needed to use previous knowledge or models that simulate the human locomotion with different levels of precision. For example, in chapter 2 we defined a simple finite state automaton to describe the different modes of locomotion allowed by our interaction technique. In chapter 3, we used some biomechanically inspired data to control the steps of the virtual human in a realistic way. Finally, in chapter 4 we used both approaches to define a more complete locomotion simulator used to simulate different properties of virtual human and VE.

Taken together, our different techniques suggest that one key-component of the simulation of walking in VE could be a **locomotion model** that would simulate the different modes and properties of natural human locomotion. This model would take into account the morphology and physiology of the virtual human and various properties of the VE. It could be used to control the navigation and the interaction protocol (i.e. constrain the possible and available motions at a given time). It could be also useful to design and tune the different sensory feedbacks (i.e. compute the events such as steps or changes in the mode of locomotion).

Therefore, the standard interaction loop used in VR application could be revisited by introducing and integrating this locomotion model as a central component of the simulation (Figure 4.14). This new architecture opens new possibilities to improve the interaction and immersion during navigation in VE. Indeed, developing new interaction techniques or sensory feedbacks could become faster and easier. The time and resources spent could be more focused on designing the techniques themselves. Moreover, multimodal integration

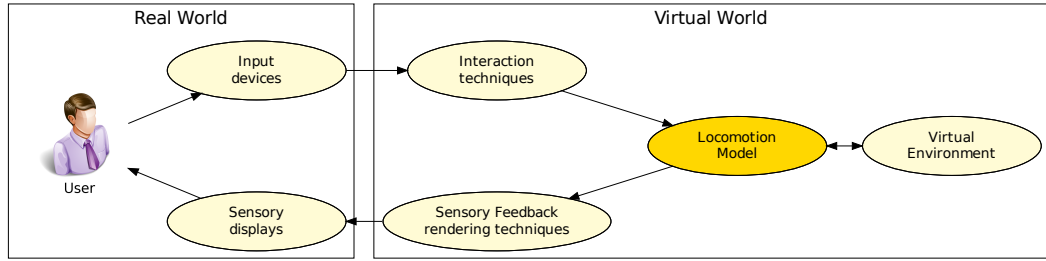


**Figure 4.14** – Novel architecture of interaction loop proposed for navigation in VR. Introducing a biomechanically-inspired model for driving both sensory feedbacks and interaction techniques.

could also be simplified. Indeed, in addition to providing an extended range of information about the locomotion, the locomotion model could also serve as a synchronization mechanism between the different sensory feedback techniques. Finally, any improvement made on the locomotion model could automatically apply to all the existing techniques, reducing the difficulty to maintain the coherency between the different techniques used.

Naturally, a lot of work is still required in order to achieve seamless multimodal navigation in VE. As navigation and walking in VR should benefit from incoming improvements in navigation devices and techniques, the next decade will probably witness tremendous advances in the field and, at the same time, will open the way to new and exciting research challenges.



# Appendix: Résumé Long en Français

# A

BEAUCOUP d'applications de Réalité Virtuelle (RV) dépendent des tâches de navigation et doivent permettre aux utilisateurs de marcher et naviguer librement dans l'Environnement Virtuel (EV). La navigation est souvent essentielle pour les applications d'entraînement. Par exemple, la SNCF (compagnie de chemin de fer française) a développée une simulation d'entraînement pour les conducteurs de train qui doivent marcher le long des voies ferrées afin d'effectuer différentes opérations de maintenance [David 01]. De plus, la visualisation architecturale de bâtiments [Fuchs 01] ou les visites virtuelles de musées [Miller 92] ont également besoin de fournir à l'utilisateur la possibilité de naviguer facilement et efficacement dans l'EV.

Naviguer dans un grand EV peut être une expérience passionnante. Entre autres, les jeux vidéos à la première personne proposent souvent des environnements larges et riches à explorer. Par exemple, dans le jeu vidéo "The Elder Scrolls V: Skyrim" une île de plus de 35 km<sup>2</sup> peut être explorée librement par le joueur. En conséquence, les joueurs peuvent passer de nombreuses heures à explorer et découvrir différents paysages pendant qu'ils complètent les différentes missions du jeu.

La navigation dans les EV peut être décrite comme une boucle d'interaction [Bowman 05] (Figure A.1). Les utilisateurs manipulent des périphériques d'interaction (1) qui génèrent des entrées pour le système de RV. Ensuite, les techniques d'interaction (2) convertissent les entrées de l'utilisateur en instructions et commandes qui modifient le contenu de l'EV (3). En retour, les techniques de retour sensoriel (4) calculent les différents rendus sensoriels de l'EV et de ses modifications. Finalement, les retours sensoriels sont présentés à l'utilisateur avec différents types de périphériques (interfaces visuelles comme les CAVE ou visiocasques, interfaces haptiques, etc.) (5), permettant à l'utilisateur de finalement percevoir les changements se produisant dans l'EV et, en particulier sa navigation.

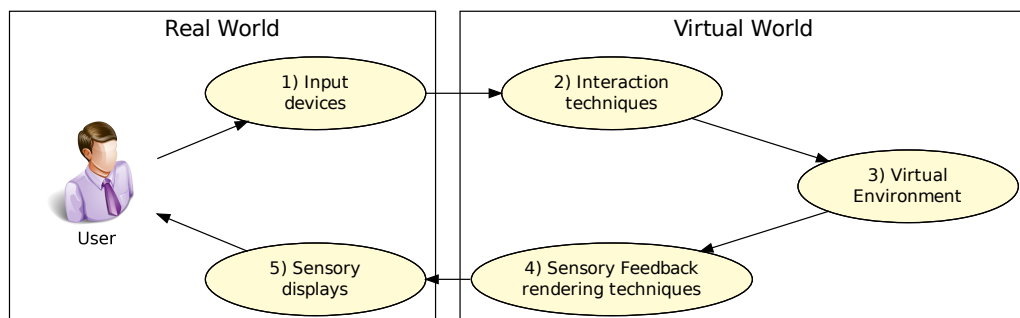


**Figure A.1** – Boucle d'interaction pour la navigation en Réalité Virtuelle.

De nombreux périphériques d'interaction (1) ont été proposés pour la navigation en RV

[Bowman 05]. Jusqu'à présent, les périphériques de locomotion existant vont des simples clavier/joystick [Stanney 02] à des périphériques mécaniques complexes. Une solution classique consiste à suivre les mouvements 3D de l'utilisateur et de les utiliser comme entrées pour la simulation. Par exemple, la technique "Walking-In-Place" (WIP, c.-à-d. marcher sur place) [Slater 95] est basée sur cette approche. Cette technique suit les mouvements de l'utilisateur lorsqu'il marche sur place afin de contrôler la navigation dans l'EV. D'autres périphériques mécaniques complexes, comme les tapis roulant [Iwata 99a] ou des plateformes sous les pieds de l'utilisateur [Iwata 01] peuvent également être utilisés. Ces périphériques sont conçus afin de suivre et de contrôler les mouvements de l'utilisateur. De fait, ils fournissent donc aussi fréquemment des retours sensoriels (5) à l'utilisateur.

Les techniques d'interaction (2) traduisent les entrées de l'utilisateur en commandes pour interagir avec l'EV. En particulier, les techniques d'interaction peuvent être utilisées pour compenser certaines des limitations des périphériques d'interaction. Entre autre, l'utilisateur peut être confronté à des situations où l'EV est plus large que l'espace de travail physique. Par conséquent, les techniques de navigation doivent trouver un moyen de maintenir la position de l'utilisateur dans l'espace de travail disponible. Par exemple, la technique du "Redirected Walking" [Steinicke 08a] (c.-à-d. marche redirigée) utilise les retours visuels afin de tromper les utilisateurs et de les faire marcher sur des trajectoires curvilignes dans le monde réel tout en leur donnant l'impression de marcher en ligne droite dans l'EV. Si l'espace de travail est suffisamment large, les utilisateurs marcheront en cercle et par conséquent ne remarqueront jamais les limites de l'espace de travail.

Cependant, les techniques et périphériques d'interaction existant souffrent toujours de quelques limitations. Les techniques et périphériques d'interaction doivent atteindre différents objectifs concurrents. En effet, ils doivent souvent être efficaces, écologiques<sup>1</sup>, résoudre le problème de l'espace de travail limité et ne pas avoir un coût prohibitif. Par exemple, la technique du "Redirected Walking" [Steinicke 08a] semble efficace et écologique, mais nécessite un large espace de travail. Par conséquent, une technique d'interaction qui atteindrait tout ces objectifs en même temps demeure toujours un problème de recherche ouvert.

Concernant les retours sensoriels (4 et 5), les utilisateurs doivent percevoir l'EV à travers différentes modalités et de multiples retours sensoriels. En effet, durant la marche, les humains peuvent percevoir leurs mouvements à travers les sens visuel, auditif et proprioceptif [Harris 99]. Par exemple, les matériaux composant le sol virtuel peuvent être rendus grâce à différentes modalités. La neige, le gravier, le sable ou le béton peuvent être rendus par la modalités auditive [Nordahl 10] par des méthodes de synthèse de sons. Ces matériaux peuvent aussi être rendus par la modalité vibrotactile [Visell 08] en utilisant des petits actuateurs placés sur les chaussures de l'utilisateur ou sous le sol. Les Mouvements de Caméra (MC) [Lécuyer 06] peuvent aussi être utilisés pour rendre la modalité visuelle. Les MC ont été introduits pour simuler le flux visuel correspondant aux mouvements de la tête durant la marche. La caméra virtuelle oscille le long des trois axes de l'espace et reproduit les mouvements de la tête. Il est intéressant de noter qu'il a été montré que cette technique augmente la sensation de marcher, ainsi que l'immersion dans l'EV [Lécuyer 06].

Les périphériques/techniques de rendu sensoriel existant souffrent aussi de certaines limi-

---

<sup>1</sup>Les interactions écologiques sont définies par la théorie de Gibson sur l'écologie de la perception visuelle [Gibson 86] : l'affordance, c.-à-d. la corrélation entre perception et action, élimine le besoin de faire la différence entre mondes réels et virtuels. En effet, une perception valide est une perception qui rend possible le succès des actions dans l'environnement [Gibson 86].

tations. De nombreuses techniques sont souvent basées sur une seule modalité. L'étendue des retours sensoriels fournis est limitée, et la sensation d'immersion dans l'EV est souvent détériorée. D'un autre côté, chaque technique simule seulement un type précis de retours. Par conséquent, de nombreuses techniques sont requises afin de fournir une simulation sensorielle globale. Ainsi, de nouveaux retours sensoriels sont nécessaires pour améliorer l'immersion et les sensations des utilisateurs durant la navigation en EV.

Par conséquent, de nouvelles techniques de navigation semblent nécessaires afin d'obtenir des navigations efficaces et écologiques pour les applications de RV, tout en restant abordables financièrement. De plus, de nouvelles techniques de retour sensoriel sont nécessaires pour améliorer l'immersion, basées sur de nouvelles modalités ou sur des approches multimodales.

## A.1 Approche

Ce manuscrit de thèse se concentre sur l'étude et la mise au point de nouvelles techniques d'interaction et de retour sensoriels pour améliorer la navigation en RV. En particulier, nous proposons d'étudier la marche humaine comme méthode d'interaction afin de concevoir des techniques de navigation aussi écologiques que possible. En effet, un de nos objectifs est de faire disparaître la frontière entre le monde réel et le monde virtuel autant que possible durant la navigation. Idéalement, l'utilisateur doit interagir et naviguer dans l'EV de la même manière qu'il interagit avec le monde réel (Figure A.2). De plus, les navigations basées sur la marche humaine auraient également l'avantage de libérer les mains de l'utilisateur pour d'autres tâches.



**Figure A.2** – Nos objectifs sont d'améliorer la navigation en RV en augmentant les performances de navigation, l'écologie des interactions, l'immersion et la sensation de marcher dans l'EV. Par exemple, la navigation devrait être aussi proche que possible des navigations dans le monde réel.

Tout d'abord, notre étude et conception de nouvelles techniques d'interaction se concentre sur quatre objectifs principaux :

- **Conformité et extension de l'espace de travail** : Les techniques de navigation doivent adresser le problème posé par les limites de l'espace de travail afin de

permettre des navigations dans de grand EV potentiellement infinis.

- **Navigations efficaces** : Les techniques de navigation doivent par exemple permettre de naviguer rapidement et précisément dans l'EV.
- **Navigations écologiques** : Les techniques de navigation doivent être aussi écologique que possible afin de permettre d'interagir sans obstacle avec l'EV.
- **Coût modéré** : Le coût des techniques doit éviter d'être prohibitif afin de permettre un large panel d'applications possibles.

Ensuite, notre étude se concentre sur les moyens d'augmenter l'étendu des retours sensoriels afin d'améliorer l'immersion et la sensation de marcher durant la navigation dans l'EV [Lécuyer 06]. Trois différents objectifs sont considérés :

- Propose **De nouveaux effets** qui reproduisent les indices sensoriels existant disponibles dans le monde réel.
- Propose **De nouvelles métaphores** de retour sensoriel afin d'étendre l'étendue des informations rendues aux utilisateurs, avec parfois des effets non réalistes mais très évocateurs.
- Créer **des retours multimodal** de la marche afin d'améliorer l'immersion dans l'EV avec de multiples modalités sensorielles.

Pour chacune de nos nouvelles techniques, nous avons adoptées une approche centrée sur l'utilisateur. En particulier, dans chaque cas, nous avons conduit des expérimentations qualitatives et quantitatives pour évaluer leurs performances ainsi que les préférences des utilisateurs.

## A.2 Contributions

### A.2.1 Le Shake-Your-Head

Dans le [chapter 2](#), nous proposons une nouvelle technique pour contrôler la navigation en RV, appelée “Shake-Your-Head” (SYH) ([Figure A.3](#)). Notre technique, basée sur la technique du “Walking-In-Place” (c.-à-d. marche sur place), nécessite que l'utilisateur bouge réellement et mesure spécifiquement les mouvements produits par la tête lors de la marche sur place afin de contrôler la navigation. L'utilisateur peut être debout ou assis (comme dans les jeux vidéo traditionnels ou les configurations de RV de bureau). Les mouvements de la tête sont capturés par un système de suivi à bas coût composé d'une webcam standard. La simulation de la locomotion calcule des mouvements de marche virtuels, ainsi que la possibilité de tourner, sauter et ramper.

Nous avons conduit une expérience afin de comparer la technique du SYH avec des navigations standard au clavier/joystick. Dans cette expérience, les participants devaient marcher le long de trajectoires formant un slalom. Nous avons effectué l'évaluation dans les deux configurations possibles : immersive et assis à un bureau. Nous n'avons pas trouvé de diminution significative dans la précision pour compléter la tâche avec le SYH pour les slaloms simples. De plus, nous avons trouvé que le SYH requière seulement un très court



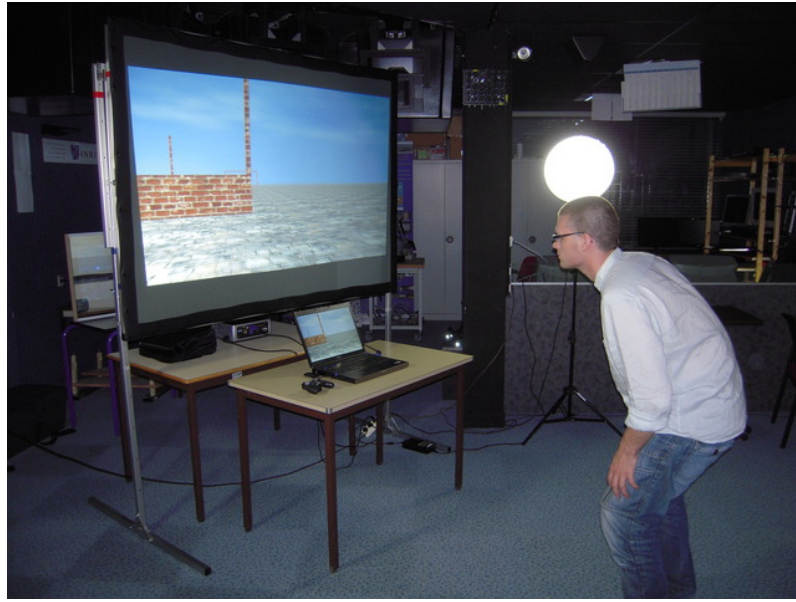


**Figure A.3** – Implémentation du SYH.

temps d'apprentissage. Finalement, le SYH a été plus apprécié par les participants comparé aux navigations basé joystick et clavier, et perçut comme augmentant la présence dans l'EV.

Ensuite, nous avons conduit une analyse détaillée des trajectoires produites par le SYH en configuration immersive. Nous avons notamment trouvé que les stratégies de navigation utilisées entre les différentes techniques étaient assez différentes. Les participants ont montré un contrôle plus précis de leur vitesse d'avance avec le SYH, mais plus d'anticipation dans les virages avec le joystick. En particulier, les trajectoires avec le joystick étaient plus lisses et plus prédictibles. Pris ensemble, nos résultats suggèrent que la technique du SYH fournit un meilleur contrôle de la vitesse d'avance, alors que le joystick était plus précis pour contrôler la direction. Ces résultats pourraient être utilisés pour améliorer d'avantage la technique du SYH.

### **A.2.2 Les King Kong Effects**

Dans le [chapter 3](#), nous introduisons une nouvelle technique de retour sensoriel pour la navigation en RV appelée “King Kong Effects” (KKE) ([Figure A.4](#)). Les KKE simulent les contacts des pieds avec le sol à chaque pas virtuel. Des modèles de vibrations visuelle et tactile sont utilisés pour augmenter les sensations de marche dans l'EV. Les KKE sont inspirés de films Hollywoodiens connus comme “King Kong” ou “Jurassic Park ” où la marche de créatures gigantesques est accentuée afin de faire “ressentir” aux spectateurs les pas de la créature approchant. Notre technique reproduit, d'une certaine manière, les effets spéciaux vus dans ces films pour les technologies de RV de bureau de manière interactive. Nous avons proposé d'utiliser des vibrations de la caméra dans les directions horizontales et verticales pour simuler le contact des talons et des orteils avec le sol. De plus, nous avons introduit un retour vibrotactile sous les pieds de l'utilisateur afin de simuler ces deux types de contact. Pour la modalité vibrotactile, nous avons proposé deux différent modèles : un modèle basé sur le contact rigide des pieds avec le sol et un modèle

basé sur les forces de réaction au sol à chaque pas.

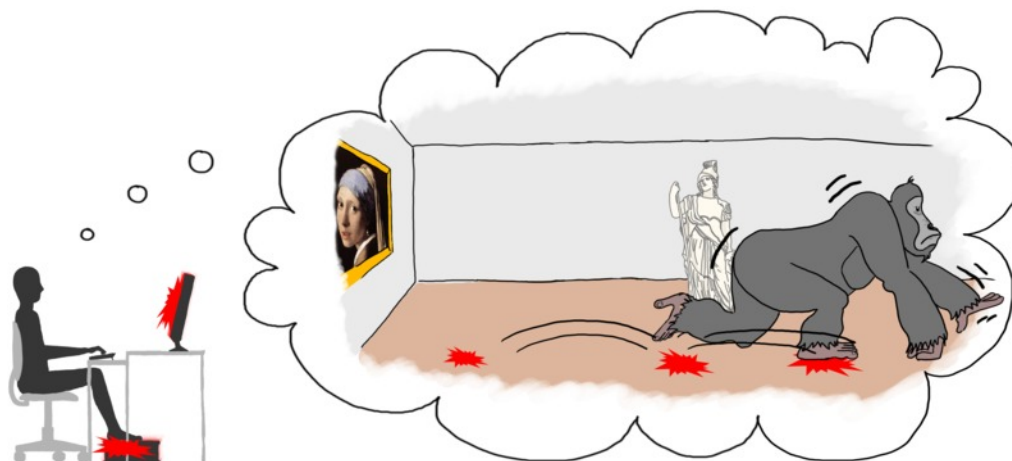


**Figure A.4** – Concept des KKE

Nous avons conduit une série d'expériences afin de déterminer les paramètres des KKE fournissant la meilleure sensation de marche dans l'EV. Nous avons trouvé que les vibrations visuelles verticales étaient préférées par rapport aux oscillations latérales. De plus, nous avons trouvé que les vibrations ne simulant que le contact du talon étaient préférées par rapport aux simulations des contacts du talon et des orteils. Concernant la modalité vibrotactile, nous avons trouvé que le modèle basé sur les contacts rigides du pied avec le sol fournit une meilleure sensation de marcher. De plus, la simulation du contact du talon seul a également été préférée. Finalement, une évaluation multimodale des différents composants des KKE a montré que les différentes modalités utilisées ensemble peuvent augmenter la sensation de marche dans l'EV.

### **A.2.3 Mouvements de Caméra Personnifiés et Multi-États**

Dans le [chapter 4](#) nous proposons une nouvelle approche pour concevoir les Mouvements de Caméra (MC) pour les navigations en vue à la première personne en RV. Les modèles précédents de MC étaient limités aux simulations de la marche. Nos MC sont multi-états : ils sont adaptés aux différents modes de locomotion de l'être humain et peuvent ainsi rendre la marche, la course et le sprint. De plus, les MC existants ne prennent pas en compte la morphologie de l'humain virtuel. Nous proposons des MC personnalisés adaptés à l'humain virtuel basés sur son sexe, son âge, son poids et sa condition physique. Les retours visuels des MC sont différents si l'humain virtuel est plus lourd ou en meilleure condition physique par exemple. De plus, contrairement aux MC existants, nos MC sont adaptés à la pente dans l'EV.

Nous avons conduit une série d'expériences pour évaluer la perception des différents modes de locomotion (marche, course, sprint) par les participants. Nous avons trouvé que les participants peuvent faire la différence entre deux modes de locomotion en se basant exclusivement sur nos MC. De plus, ils peuvent également percevoir certaines des propriétés de l'humain virtuel utilisé, comme son âge ou sa condition physique. Nous avons également conduit une seconde évaluation sur l'influence de ce type de retour visuel sur la perception des distances parcourues dans l'EV. Nous avons trouvé que les MC peuvent être utilisés pour améliorer la perception des courtes distances parcourues dans l'EV.

## A.3 Perspectives et Prochain Travaux

Le travail présenté dans ce manuscrit suggère quelques améliorations potentielles, qui pourraient être adressées dans des prochains travaux à court et long terme.

### A.3.1 Prochain Travaux

Cette section présente des futures possibilités de recherche correspondant à la continuation des différentes techniques introduites dans ce manuscrit.

#### A.3.1.1 Le Shake-Your-Head

Premièrement, les **lois de contrôle** utilisées pour gérer les virages de la technique Shake-Your-Head peuvent être améliorées. En effet, l'analyse des trajectoires suggère fortement que ce composant de la technique SYH n'est pas encore aussi efficace que le joystick pour contrôler la direction. De plus, les lois de contrôle utilisés pour sauter et ramper peuvent également être améliorées. En effet, les résultats moins précis sur les trajectoires complexes peuvent être expliqués par une difficulté à contrôler les saut ou ramper.

Deuxièmement, plus de **modes de locomotion** pourraient être intégrés dans la simulation. En effet, les modes de course et de sprint proposés dans le [chapter 4](#) pourraient être intégrés dans le SYH pour augmenter l'ensemble des interactions de navigation possibles avec le SYH.

Troisièmement, un **modèle** plus précis ou **biomécaniquement inspiré** pourrait être utilisé pour contrôler la locomotion. En effet, au lieu d'un ensemble d'heuristiques, le SYH gagnerait à être basé sur des connaissances plus formelles de la locomotion humaine. Ainsi, les lois de contrôle pourraient être étendues pour simuler de nouveaux modes de locomotion par exemple.

Finalement, des nouvelles **évaluations** du SYH pourraient être faites. Par exemple, le SYH pourrait être évalué par des participants n'étant pas familier avec les navigations au clavier et joystick. En effet, tous les participants de l'expérience étaient très familier avec ces techniques mais étaient naïfs concernant le SYH. Le SYH pourrait aussi être évalué dans des situations plus complexes, comme des navigations dans des environnements complexes ou des navigations en parallèle à d'autres tâches plus complexes.

#### A.3.1.2 Les King Kong Effects

Premièrement, de nouvelles **modalités** pourraient être intégrées dans les KKE pour augmenter la perception des pas virtuels. Par exemple, la modalité auditive pourrait être utilisée en introduisant des techniques existantes de synthèse de son dans les KKE. De plus, les sons de pas pourraient fournir des informations additionnelles sur les propriétés du sol, comme les matériaux le composant (neige, gravier ou béton par exemple). Des informations vestibulaires pourraient aussi être introduites avec le Système Galvanique Vestibulaire [Nagaya 05] par exemple.

Deuxièmement, concernant les retours tactiles/vibratoires, nous avons identifié le modèle fournissant la meilleure sensation de marcher parmi les deux modèles proposés. Cependant, de **nouveaux modèles** pourrait conduire à de meilleurs résultats. En particulier, les KKE ne visent pas à simuler de manière physiquement réaliste les retours sensoriels produits à chaque pas, mais peuvent être considérés comme étant une métaphore pour augmenter la sensation de contact avec le sol à chaque pas. Par conséquent, de nouveaux modèles pourraient être conçus et comparés aux modèles présentés dans ce manuscrit.

Finalement, l'influence d'une simulation multimodale sur la sensation de marcher pourrait être étudiée plus en détail. En particulier, de nouvelles **évaluations** des KKE pourraient être faites.

#### A.3.1.3 Mouvements de Caméra Personnifiés et Multi-États

Premièrement, le modèle de MC présenté est adapté uniquement à la pente de l'EV. D'autres **propriétés de l'EV** pourraient aussi être prise en compte et simulées, comme par exemple les matériaux constituant le sol (eau, neige ou boue par exemple). Les MC pourraient aussi être adaptés pour prendre en considération certain types de navigation spécifiques et certaines spécificités de l'EV, comme par exemple les escaliers.

Deuxièmement, les MC pourraient être **utilisés avec d'autres techniques de retour** comme la composant vibrotactile des KKE. En effet, certains paramètres calculés, comme la vitesse d'avance ou la fatigue de l'humain virtuel, pourraient être utiles pour améliorer la diversité et la pertinence des autres techniques de retour sensoriel.

Finalement, d'autres **évaluations** des propriétés des MC pourraient être faites. En effet, nous avons évalués l'influence des MC sur la perception des distances parcourues dans l'EV, mais l'influence d'autres facteurs comme l'échelle pourraient être testés. De plus, nous pourrions évaluer l'influence de MC sur des trajectoires plus compliquées que celles réalisées, ainsi que leur influence sur le sens de l'orientation des participants.

### A.3.2 Perspectives

En plus des futur travaux mentionnés ci-dessus, cette thèse de doctorat peut également ouvrir la voie à de nouvelles directions de recherche et des vues sur le long terme.

#### A.3.2.1 Vers des Navigations Multimodales à Bas Coût en EV

Durant la marche, et plus généralement toute locomotion humaine, différents sens sont utilisés pour percevoir et contrôler la locomotion [Harris 99]. La locomotion humaine est fondamentalement une expérience multimodale, incluant mais n'étant pas limitée aux informations visuelles, auditives, vestibulaires et kinesthésiques. Le nombre et la complexité des modalités simulées durant les navigations dans les applications de RV actuelles sont toujours limités par la technologie actuelle. Chaque modalité est souvent rendue séparément à l'utilisateur, et intégrer différentes techniques ensemble peut être un problème complexe et coûteux.

Récemment, de nouveaux types de périphériques d'interaction ou de retour sensoriel ont été développés. Par exemple, la Kinect de Microsoft [Microsoft 12] est une interface de

suivit de mouvement à bas coût conçue pour laisser les utilisateurs interagir avec les systèmes immersifs en utilisant leur mouvements. Par conséquent, ce système peut être utilisé pour fournir des informations vestibulaires ou proprioceptives. De manière similaire, de nouveaux périphériques pour le rendu des modalités auditive ou haptique/vibrotactile deviennent de plus en plus accessibles. Ainsi, sur le long terme, nous pouvons imaginer que les applications de RV à bas coût pourraient proposer des interactions et retours utilisant tout les corps des utilisateurs pour naviguer en RV. Ces applications pourraient être utilisées par des millions d'utilisateurs lors de visites virtuelles de monuments historiques ou de projets urbains/architecturaux par exemple. Cependant, pour que ceci devienne une réalité, la question des modèles de retour multimodaux unifiés doit probablement être résolue en premier lieu.

### A.3.2.2 Vers des Navigations Biomécaniquement Réalistes en EV

Dans les différents chapitres de ce manuscrit, nous avons régulièrement eu besoin d'utiliser des connaissances existantes ou modèles qui simulent la locomotion humaine avec différents niveaux de précision. Par exemple, dans le [chapter 2](#) nous avons défini un automate à états finis pour décrire les différents modes de locomotion permis par notre technique d'interaction. Dans le [chapter 3](#), nous avons utilisé des données inspirées de la biomécanique pour contrôler les pas de l'humain virtuel de manière réaliste. Finalement, dans le [chapter 4](#) nous avons utilisé les deux approches pour définir un simulateur de locomotion plus complexe, utilisé pour simuler différentes propriétés de l'humain virtuel et de l'EV.

Prise ensemble, nos différentes techniques suggèrent que un élément clé de la simulation de la marche en EV pourrait être un **modèle de locomotion** qui simulerait les différents modes et propriétés de la marche humaine réelle. Ce modèle prendrait en considération la morphologie et la physiologie de l'humain virtuel et divers propriétés de l'EV. Il pourrait être utilisé pour contrôler la navigation et le protocole d'interaction (c.-à-d. pour contraindre les mouvements possibles et disponibles à un moment donné). Il pourrait également être aussi utile pour concevoir et paramétrer les différents retours sensoriels (c.-à-d. calculer les événements tels que les pas ou les changements de mode de locomotion).

Par conséquent, la boucle d'interaction standard utilisée dans les applications de RV pourrait être revisitée en introduisant et intégrant ce modèle de locomotion comme un élément central de la simulation ([Figure A.5](#)).

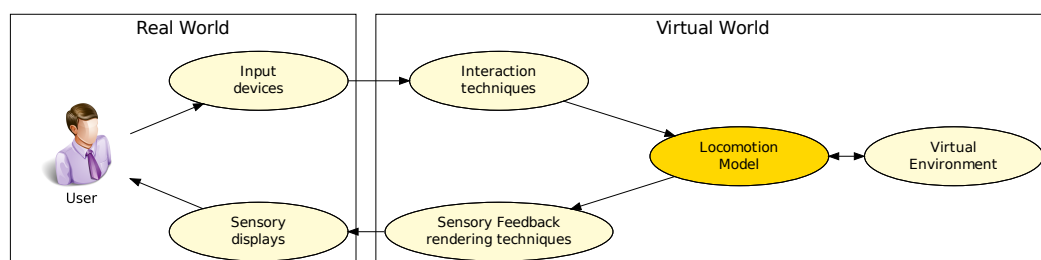


**Figure A.5** – Nouvelle architecture de boucle d'interaction proposée pour la navigation en RV. Introduction d'un modèle d'inspiration biomécanique pour contrôler à la fois les retours sensoriels et les techniques d'interaction.

Cette nouvelle architecture ouvre de nouvelles possibilités pour améliorer les interactions

et l’immersion durant la navigation en EV. En effet, développer de nouvelles techniques d’interaction ou des retours sensoriels deviendrait plus simple et plus rapide. Le temps et les ressources dépensés pourraient être ainsi d’avantage concentrés sur la conception des techniques elles mêmes. De plus, l’intégration multimodale des différentes techniques serait également simplifiée. En effet, en plus de fournir un ensemble étendu d’informations disponibles sur la locomotion, le modèle de locomotion pourrait également servir de mécanisme de synchronisation entre les différentes techniques de retour sensoriel. Finalement, toute amélioration faite sur le modèle de locomotion serait automatiquement répercutée sur toutes les techniques existantes, réduisant ainsi la difficulté à maintenir la cohérence entre les différentes techniques utilisées.

Naturellement, beaucoup de travail est toujours requis afin de pouvoir atteindre une navigation multimodale transparente dans l’EV. Étant donné que la navigation, et plus particulièrement la marche, en RV devrait bénéficier des améliorations à venir des périphériques et techniques de navigation, la prochaine décennie devrait probablement être témoin de formidables avancements dans ce domaine, et en même temps, devrait ouvrir la voie à de nouveaux et excitants défis de recherche.

# Author's Publications

## Submitted

- [S1] **Léo Terziman**, Maud Marchal, Franck Multon, Bruno Arnaldi, and Anatole Lécuyer. *Personified and Multi-States Camera Motions for First-Person Navigation in Virtual Reality*. Conditionally accepted to IEEE Transactions on Visualization and Computer Graphics (special issue of IEEE Conference on Virtual Reality), 2013.

## Published

### ■ International Conferences

- [P1] **Léo Terziman**, Maud Marchal, Franck Multon, Bruno Arnaldi, and Anatole Lécuyer. *The King-Kong Effects: Improving Sensation of Walking in VR with Visual and Tactile Vibrations at each Step*. Proceedings of the IEEE Symposium on 3D User Interfaces, pages 19-26, 2012.
- [P2] **Léo Terziman**, Maud Marchal, Franck Multon, Bruno Arnaldi, and Anatole Lécuyer. *Short Paper: Comparing Virtual Trajectories Made in Slalom Using Walking-In-Place and Joystick Techniques*. Proceedings of the EuroVR / EGVE Joint Virtual Reality Conference, pages 55-58, 2011.
- [P3] **Léo Terziman**, Maud Marchal, Mathieu Emily, Franck Multon, Bruno Arnaldi, and Anatole Lécuyer. *Shake-your-head: Revisiting walking-in-place for desktop virtual reality*. Proceedings of the ACM Symposium on Virtual Reality Software and Technology, pages 27-34, 2010.
- [P4] **Léo Terziman**, Anatole Lécuyer, Sébastien Hillaire, and Jan M. Wiener. *Can camera motions improve the perception of traveled distance in virtual environments?* Proceedings of the IEEE Conference on Virtual Reality, pages 131-134, 2009.

### ■ Books

- [P5] **Léo Terziman**, Gabriel Cirio, Maud Marchal, and Anatole Lécuyer. *Walking with the Senses: Non-visual perceptual techniques for walking in simulated environments*, chapter *Novel Interactive Techniques for Walking in Virtual Reality*. Yon Visell and Frederico Fontana (Eds.), Logos Verlag, 2012. ISBN : 978-3-8325-2967-3.

### ■ Other Invited Papers and Presentations

- [P6] **Léo Terziman**, Maud Marchal, Mathieu Emily, Franck Multon, Bruno Arnaldi, and Anatole Lécuyer. *Shake-your-head: Walking in virtual worlds*. Poster of the INSA de Rennes 2nd Young Researchers Scientific Day, 2011.



- [P7] **Léo Terziman**, Maud Marchal, Mathieu Emily, Franck Multon, Bruno Arnaldi, and Anatole Lécuyer. *Shake-your-head: Revisiting walking-in-place for desktop virtual reality*. 4th Japan-France Cooperative Workshop on "Improving the VR Experience", 2010.
- [P8] **Léo Terziman**, Maud Marchal, Mathieu Emily, Franck Multon, Bruno Arnaldi, and Anatole Lécuyer. *A novel walking-in-place technique for navigating in virtual worlds using head motions*. 5èmes Journées de l'AFRV, 2010.
- [P9] Gerd Bruder, Jan Souman, and **Léo Terziman**. *Walking experiences in virtual worlds*. Tutorial of the EuroVR / EGVE / VEC Joint Virtual Reality Conference, 2010.

# Bibliography

- [Alexander 76] Alexander, R. M. *Mechanics of bipedal locomotion*. Perspectives in experimental biology, vol. 1, pages 493–504, 1976. [23](#)
- [Alexander 03] Alexander, R. M. Principles of animal locomotion. Princeton University Press, 2003. [20](#), [72](#)
- [Berthoz 97] Berthoz, A. Le sens du mouvement. Odile Jacob, 1997. [16](#), [17](#), [18](#), [23](#), [24](#)
- [Blondel 01] Blondel, N., Berthoin, S., Billat, V. & Lensel, G. *Relationship Between Run Times to Exhaustion at 90, 100, 120, and 140% of  $v\text{VO}_2\text{max}$  and Velocity Expressed Relatively to Critical Velocity and Maximal Velocity*. International journal of sports medicine, vol. 22, no. 1, pages 27–33, 2001. [22](#), [92](#)
- [Bordeux 99] Bordeaux, C., Boulic, R. & Thalmann, D. *An efficient and flexible perception pipeline for autonomous agents*. Computer graphics forum, vol. 18, no. 3, pages 23–30, 1999. [26](#)
- [Boulic 90] Boulic, R., Magnenat-Thalmann, N. & Thalmann, D. *A global human walking model with real-time kinematic personification*. The visual computer, vol. 6, no. 6, pages 344–358, 1990. [18](#)
- [Bowman 05] Bowman, D. A., Kruijff, E., LaViola, Jr., J. J. & Poupyrev, I. 3d user interfaces: Theory and practice. Addison-Wesley, 2005. [9](#), [31](#), [69](#), [123](#), [124](#)
- [Bowman 08] Bowman, D. A., Coquillart, S., Fröhlich, B., Hirose, M., Kitamura, Y., Kiyokawa, K. & Stuerzlinger, W. *3D User Interfaces: New Directions and Perspectives*. IEEE Computer Graphics and Applications, vol. 28, no. 6, pages 20–36, 2008. [26](#)
- [Bradski 98] Bradski, G. R. *Computer Vision Face Tracking For Use in a Perceptual User Interface*. Intel Technology Journal, vol. 2, no. 2, pages 12–21, 1998. [52](#)
- [Breedlove 07] Breedlove, S., Rosenzweig, M. & Watson, N. Biological psychology: an introduction to behavioral, cognitive, and clinical neuroscience. Sinauer Associates, 2007. [17](#)
- [Bruder 12] Bruder, G., Interrante, V., Phillips, L. & Steinicke, F. *Redirecting Walking and Driving for Natural Navigation in Immersive Virtual Environments*. IEEE Transactions on Visualization and Computer Graphics, vol. 18, no. 4, pages 538–545, 2012. [37](#)

- [Cirio 09] Cirio, G., Marchal, M., Regia-Corte, T. & Lécuyer, A. *The Magic Barrier Tape: a Novel Metaphor for Infinite Navigation in Virtual Worlds with a Restricted Walking Workspace*. In Proceedings of the 16th Symposium on Virtual Reality Software and Technology, pages 155–162, 2009. [35](#), [36](#)
- [Cirio 12a] Cirio, G., Marchal, M., Lécuyer, A. & Cooperstock, J. R. *Vibrotactile Rendering of Splashing Fluids*. IEEE Transactions on Haptics, vol. PP, no. 99, page 1, 2012. [40](#), [46](#), [47](#)
- [Cirio 12b] Cirio, G., Vangorp, P., Chapoulie, E., Marchal, M., Lécuyer, A. & Drettakis, G. *Walking in a Cube: Novel Metaphors for Safely Navigating Large Virtual Environments in Restricted Real Workspaces*. IEEE Transactions on Visualization and Computer Graphics, vol. 18, no. 4, pages 546–554, 2012. [35](#)
- [Cochran 82] Cochran, G. A primer of orthopaedic biomechanics. Churchill Livingstone New York, 1982. [19](#)
- [Courtine 03] Courtine, G. & Schieppati, M. *Human walking along a curved path. I. Body trajectory, segment orientation and the effect of vision*. European Journal of Neuroscience, vol. 18, no. 1, pages 177–190, 2003. [55](#)
- [Courty 02] Courty, N. *Animation référencée vision: de la tâche au comportement*. PhD thesis, INSA de Rennes, 2002. [25](#)
- [David 01] David, P. & Lourdeaux, D. *A simulator using virtual reality techniques for training driver to manual interventions on the tracks*. In World Conference on Railway Research. Poster presentation, 2001. [9](#), [123](#)
- [de Barros 09a] de Barros, P. G., Lindeman, R. W. & Loughlin, T. J. *Characterizing Head Movement in First-Person Games*. In Proceedings of the ACM SIGGRAPH Symposium on Interactive 3D Graphics and Games, 2009. [42](#)
- [de Barros 09b] de Barros, P. G., Lindeman, R. W. & Loughlin, T. J. *Head-movement evaluation for first-person games*. In Proceedings of the international conference on Human Factors in Computing Systems, pages 4399–4404, 2009. [42](#)
- [Dean 07] Dean, J., Alexander, N. & Kuo, A. D. *The Effect of Lateral Stabilization on Walking in Young and Old Adults*. IEEE Transactions on Biomedical Engineering, vol. 54, no. 11, pages 1919–1926, 2007. [22](#)
- [Doke 05] Doke, J., Donelan, J. M. & Kuo, A. D. *Mechanics and energetics of swinging the human leg*. Journal of Experimental Biology, vol. 208, no. 3, page 439, 2005. [22](#)
- [Doke 07] Doke, J. & Kuo, A. D. *Energetic cost of producing cyclic muscle force, rather than work, to swing the human leg*. Journal of Experimental Biology, vol. 210, no. 13, page 2390, 2007. [22](#)
- [Donelan 01] Donelan, J. M., Kram, R. & Kuo, A. D. *Mechanical and metabolic determinants of the preferred step width in human walking*. Proceedings of the Royal Society of London. Series B: Biological Sciences, vol. 268, no. 1480, pages 1985–1992, 2001. [22](#)

- [Endo 98] Endo, T., Katayama, A., Tamura, H., Hirose, M., Tanikawa, T. & Saito, M. *Image-based walk-through system for large-scale scenes*. In Proceedings of the IEEE conference on Virtual Systems and Multimedia, pages 269–274, 1998. [32](#)
- [Engel 08] Engel, D., Curio, C., Tcheang, L., Mohler, B. & Bülthoff, H. H. *A psychophysically calibrated controller for navigating through large environments in a limited free-walking space*. In Proceedings of the ACM Symposium on Virtual Reality Software and Technology, pages 157–164, 2008. [37](#), [38](#)
- [FCAT 98] FCAT. Terminologia anatomica: international anatomical terminology. Thieme Medical Publishers, 1998. [18](#)
- [Feasel 08] Feasel, J., Whitton, M. C. & Wendt, J. D. *LLCM-WIP: Low-Latency, Continuous-Motion Walking-in-Place*. In IEEE Symposium on 3D User Interfaces, pages 97–104, 2008. [33](#), [34](#), [35](#), [49](#)
- [Fernandes 03] Fernandes, K. J., Raja, V. & Eyre, J. *Cybersphere: the fully immersive spherical projection system*. Communications of the ACM, vol. 46, no. 9, pages 141–146, 2003. [30](#), [31](#)
- [Firstbeat 05] Firstbeat. *Indirect EPOC Prediction Method Based on Heart Rate Measurement*. Rapport technique, Firstbeat Technologies Ltd., 2005. [22](#)
- [Fontana 03] Fontana, F. & Bresin, R. *Physics-based sound synthesis and control: crushing, walking and running by crumpling sounds*. In Proceedings of the Colloquium on Musical Informatics, pages 109–114, 2003. [44](#)
- [Fraysse 09] Fraysse, F., Dumas, R., Cheze, L. & Wang, X. *Comparison of global and joint-to-joint methods for estimating the hip joint load and the muscle forces during walking*. Journal of Biomechanics, vol. 42, no. 14, pages 2357–2362, 2009. [22](#)
- [Fuchs 01] Fuchs, P., Moreau, G., Papin, J.-P. & Berthoz, A. Le traité de la réalité virtuelle. Les Presses de l’Ecole des Mines, 2001. [9](#), [27](#), [28](#), [29](#), [32](#), [123](#)
- [Gard 04] Gard, S., Miff, S. & Kuo, A. D. *Comparison of kinematic and kinetic methods for computing the vertical motion of the body center of mass during walking*. Human movement science, vol. 22, no. 6, pages 597–610, 2004. [22](#)
- [Gauthier 90] Gauthier, G. M. & Vercher, J. L. *Visual vestibular interaction: vestibulo-ocular reflex suppression with head-fixed target fixation*. Experimental Brain Research, vol. 81, pages 150–160, 1990. [18](#)
- [Gibson 86] Gibson, J. The ecological approach to visual perception. Lawrence Erlbaum, 1986. [10](#), [124](#)
- [Gordon 09] Gordon, K., Ferris, D. & Kuo, A. D. *Metabolic and Mechanical Energy Costs of Reducing Vertical Center of Mass Movement During Gait*. Archives of Physical Medicine and Rehabilitation, vol. 90, no. 1, pages 136–144, 2009. [22](#)
- [Gore 90] Gore, C. J. & Withers, R. T. *The effect of exercise intensity and duration on the oxygen deficit and excess post-exercise oxygen consumption*.

- European Journal of Applied Physiology and Occupational Physiology, vol. 60, pages 169–174, 1990. [22](#)
- [Grieve 68] Grieve, D. *Gait Patterns and the Speed of Walking*. Biomedical Engineering, vol. 3, pages 119–122, 1968. [20](#)
- [Harris 99] Harris, L. R., Jenkin, M. R. & Zikovitz, D. C. *Vestibular Cues and Virtual Environments: Choosing the Magnitude of the Vestibular Cue*. In Proceedings of the IEEE conference on Virtual Reality, pages 229–236, 1999. [10](#), [46](#), [120](#), [124](#), [130](#)
- [Harris 02] Harris, L. R., Jenkin, M. R., Zikovitz, D. C., Redlick, F., Jaekl, P. M., Jasiobedzka, U., Jenkin, H. L. & Allison, R. S. *Simulating Self-Motion I: Cues for the Perception of Motion*. Virtual Reality, vol. 6, no. 2, pages 75–85, 2002. [41](#)
- [Heyward 06] Heyward, V. H. Advanced fitness assessment and exercise prescription. Human Kinetics, 5 edition, 2006. [92](#)
- [Hillaire 07] Hillaire, S., Lécuyer, A., Cozot, R. & Casiez, G. *Depth-of-field blur effects for first-person navigation in virtual environments*. In Proceedings of the ACM symposium on Virtual reality software and technology, page 206, 2007. [42](#)
- [Hillaire 08] Hillaire, S., Lécuyer, A., Cozot, R. & Casiez, G. *Using an Eye-Tracking System to Improve Camera Motions and Depth-of-Field Blur Effects in Virtual Environments*. In Proceedings of the IEEE conference on Virtual Reality, pages 47–50, 2008. [41](#), [109](#), [110](#), [111](#), [114](#), [115](#)
- [Hillaire 09a] Hillaire, S., Lécuyer, A., Breton, G. & Corte, T. *Gaze behavior and visual attention model when turning in virtual environments*. In Proceedings of the ACM Symposium on Virtual Reality Software and Technology, pages 43–50, 2009. [26](#), [42](#)
- [Hillaire 09b] Hillaire, S., Lécuyer, A., Regia-Corte, T., Cozot, R. & Breton, G. *A Real-Time Visual Attention Model for Predicting Gaze Point During First-Person Exploration of Virtual Environments*. In Proceedings of the 16th Symposium on Virtual Reality Software and Technology, 2009. [41](#)
- [Hirasaki 99] Hirasaki, E., Moore, S., Raphan, T. & Cohen, B. *Effects of walking velocity on vertical head and body movements during locomotion*. Experimental Brain Research, vol. 127, no. 2, pages 117–130, 1999. [42](#)
- [Interrante 06] Interrante, V., Ries, B. & Anderson, L. *Distance Perception in Immersive Virtual Environments, Revisited*. In Proceedings of the IEEE conference on Virtual Reality, pages 3–10, 2006. [114](#)
- [Itti 98] Itti, L., Koch, C. & Niebur, E. *A model of saliency-based visual attention for rapid scene analysis*. IEEE Transactions on pattern analysis and machine intelligence, vol. 20, no. 11, pages 1254–1259, 1998. [24](#), [25](#)
- [Iwata 99a] Iwata, H. *The Torus Treadmill: Realizing Locomotion in VEs*. IEEE Computer Graphics and Applications, vol. 19, no. 6, pages 30–35, 1999. [10](#), [29](#), [124](#)

- [Iwata 99b] Iwata, H. *Walking About Virtual Environments on an Infinite Floor*. In Proceedings of the IEEE conference on Virtual Reality, pages 286–293, 1999. [27](#), [29](#)
- [Iwata 99c] Iwata, H. & Yoshida, Y. *Path Reproduction Tests Using a Torus Treadmill*. Presence: Teleoperators and Virtual Environments, vol. 8, no. 6, pages 587–597, 1999. [29](#)
- [Iwata 01] Iwata, H., Yano, H. & Nakaizumi, F. *Gait Master: A Versatile Locomotion Interface for Uneven Virtual Terrain*. In Proceedings of the IEEE conference on Virtual Reality, pages 131–137, 2001. [10](#), [28](#), [124](#)
- [Iwata 05] Iwata, H., Yano, H., Fukushima, H. & Noma, H. *CirculaFloor: A Locomotion Interface Using Circulation of Movable Tiles*. In Proceedings of the IEEE Conference on Virtual Reality, volume 0, pages 223–230, 2005. [30](#)
- [Iwata 07] Iwata, H., Yano, H. & Tomiyoshi, M. *String Walker*. In ACM SIGGRAPH Emerging Technologies, page 20, 2007. [27](#)
- [Kim 12] Kim, J.-S., Gracanin, D. & Quek, F. *Sensor-fusion walking-in-place interaction technique using mobile devices*. In Proceedings of the IEEE workshop on Virtual Reality, pages 39–42, 2012. [33](#), [35](#)
- [Kuffner 99] Kuffner, J. & Latombe, J. *Fast Synthetic Vision, Memory, and Learning Models for Virtual Humans*. In Proceedings of the Computer Animation, pages 118–127, 1999. [26](#)
- [Kume 98] Kume, Y., Shirai, A., Kusahara, M. & Sato, M. *Foot Interface: Fantastic Phantom Slipper*. In International Conference on Computer Graphics and Interactive Techniques, 1998. [39](#)
- [Kuo 01] Kuo, A. D. *A Simple Model of Bipedal Walking Predicts the Preferred Speed-Step Length Relationship*. Journal of biomechanical engineering, vol. 123, no. 3, page 264, 2001. [22](#), [23](#), [72](#)
- [Kuo 05] Kuo, A. D. *An optimal state estimation model of sensory integration*. Journal of neural engineering, vol. 2, pages S235–S249, 2005. [23](#)
- [Kuo 07] Kuo, A. D. *The six determinants of gait and the inverted pendulum analogy: a dynamic walking perspective*. Human Movement Science, vol. 26, no. 4, pages 617–656, 2007. [23](#)
- [Latypov 06] Latypov, N. N. *The virtosphere*, 2006. [30](#), [31](#)
- [LaViola 00] LaViola, Jr., J. J. *A Discussion of Cybersickness in Virtual Environments*. ACM SIGCHI Bulletin, vol. 32, no. 1, pages 47–56, 2000. [45](#)
- [LaViola 01] LaViola, Jr., J. J., Feliz, D., Keefe, D. & Zeleznik, R. *Hands-free multi-scale navigation in virtual environments*. In Proceedings of the ACM symposium on Interactive 3D graphics, pages 9–15, 2001. [32](#)
- [Lécuyer 06] Lécuyer, A., Burkhardt, J.-M., Henaff, J.-M. & Donikian, S. *Camera Motions Improve the Sensation of Walking in Virtual Environments*. In Proceedings of the IEEE conference on Virtual Reality, pages 11–18,

2006. [10](#), [11](#), [41](#), [42](#), [50](#), [52](#), [55](#), [59](#), [69](#), [70](#), [79](#), [88](#), [89](#), [109](#), [110](#), [111](#), [113](#), [115](#), [124](#), [126](#)
- [Maeda 05] Maeda, T., Ando, H., Amemiya, T., Nagaya, N., Sugimoto, M. & Inami, M. *Shaking the world: galvanic vestibular stimulation as a novel sensation interface*. In ACM SIGGRAPH Emerging Technologies, page 17, 2005. [43](#)
- [Marchal 10] Marchal, M., Lécuyer, A., Cirio, G., Bonnet, L. & Emily, M. *Walking Up and Down in Immersive Virtual Worlds: Novel Interactive Techniques Based on Visual Feedback*. In Proceedings of the IEEE Symposium on 3D User Interfaces, pages 19–26, 2010. [42](#), [43](#), [96](#)
- [McGeer 90] McGeer, T. *Passive dynamic walking*. The International Journal of Robotics Research, vol. 9, no. 2, page 62, 1990. [23](#)
- [Meilinger 08] Meilinger, T., Knauff, M. & Bühlhoff, H. H. *Working Memory in Wayfinding—A Dual Task Experiment in a Virtual City*. Cognitive Science, vol. 32, no. 4, pages 755–770, 2008. [24](#), [108](#)
- [Microsoft 12] Microsoft. 2012. <http://www.microsoft.com/en-us/kinectforwindows/>. [120](#), [130](#)
- [Miller 92] Miller, G., Hoffert, E., Chen, S. E., Patterson, E., Blackketter, D., Rubin, S., Applin, S. A., Yim, D. & Hanan, J. *The virtual museum: Interactive 3d navigation of a multimedia database*. The Journal of Visualization and Computer Animation, vol. 3, no. 3, pages 183–197, 1992. [9](#), [123](#)
- [Motmans 05] Motmans, R. *DINBelg Antropometric Tables*, 2005. <http://www.dinbelg.be/anthropometrie.htm>. [91](#)
- [Multon 98] Multon, F. *Contrôle du Mouvement des Humanoïdes de Synthèse*. PhD thesis, Université de Rennes 1, 1998. [18](#)
- [Nagaya 05] Nagaya, N., Sugimoto, M., Nii, H., Kitazaki, M. & Inami, M. *Visual perception modulated by galvanic vestibular stimulation*. In Proceedings of the ACM International Conference on Augmented Tele-Existence, pages 78–84, 2005. [43](#), [119](#), [129](#)
- [Neth 11] Neth, C. T., Souman, J. L., Engel, D., Kloos, U., Bühlhoff, H. H. & Mohler, B. J. *Velocity-dependent dynamic curvature gain for redirected walking*. In Proceedings of the IEEE Conference on Virtual Reality, pages 151–158, 2011. [37](#)
- [Nitzsche 04] Nitzsche, N., Hanebeck, U. & Schmidt, G. *Motion Compression for Telepresent Walking in Large Target Environments*. Presence: Teleoperators & Virtual Environments, vol. 13, no. 1, pages 44–60, 2004. [37](#)
- [Nordahl 06] Nordahl, R., Serafin, S., Bottcher, N. & Gelineck, S. *Physically based sonic interaction synthesis for computer games*. In Proceedings of the Conference Audio Mostly, 2006. [44](#)
- [Nordahl 10] Nordahl, R., Serafin, S. & Turchet, L. *Sound synthesis and evaluation of interactive footsteps for virtual reality applications*. In Proceedings of the IEEE Conference on Virtual Reality, pages 147–153, 2010. [10](#), [44](#), [45](#), [85](#), [124](#)



- [Novacheck 98] Novacheck, T. F. *The biomechanics of running*. Gait & Posture, vol. 7, no. 1, pages 77–95, 1998. [20](#), [21](#), [72](#), [75](#), [94](#)
- [Okamura 98] Okamura, A. M., Dennerlein, J. T. & Howe, R. D. *Vibration feedback models for virtual environments*. In Proceedings of the IEEE Conference on Robotics and Automation, volume 1, pages 674–679, 1998. [73](#), [75](#)
- [Olivier 08] Olivier, A.-H. *Analyse dans le plan courbure-vitesse d'un changement de direction lors de la marche*. PhD thesis, Université Européenne de Bretagne, 2008. [17](#), [26](#)
- [OpenCV 10] OpenCV. 2010. <http://sourceforge.net/projects/opencvlibrary/>. [53](#)
- [Papetti 10] Papetti, S., Fontana, F., Civolani, M., Berrezag, A. & Hayward, V. *Audio-tactile display of ground properties using interactive shoes*. In Proceedings of the international conference on Haptic and Audio Interaction Design, pages 117–128, 2010. [39](#), [46](#)
- [Park 04] Park, S., Horak, F. & Kuo, A. D. *Postural feedback responses scale with biomechanical constraints in human standing*. Experimental Brain Research, vol. 154, no. 4, pages 417–427, 2004. [22](#)
- [Pausch 95] Pausch, R., Burnette, T., Brockway, D. & Weiblen, M. E. *Navigation and Locomotion in Virtual Worlds via Flight into Hand-Held Miniatures*. In Proceedings of the ACM conference on Computer Graphics and Interactive Techniques, pages 399–400, 1995. [32](#)
- [Péruch 95] Péruch, P., Vercher, J. L. & Gauthier, G. M. *Acquisition of spatial knowledge through visual exploration of simulated environments*. Ecological Psychology, vol. 7, pages 1–20, 1995. [24](#)
- [Pham 07] Pham, Q., Hicheur, H., Arechavaleta, G., Laumond, J. & Berthoz, A. *The formation of trajectories during goal-oriented locomotion in humans. II. A maximum smoothness model*. European Journal of Neuroscience, vol. 26, no. 8, pages 2391–2403, 2007. [67](#)
- [Plumert 04] Plumert, J. M., Kearney, J. K. & Cremer, J. F. *Distance perception in real and virtual environments*. In Proceedings of the ACM Symposium on Applied Perception in Graphics and Visualization, pages 27–34, 2004. [114](#)
- [Polaine 05] Polaine, A. *The Flow Principle in Interactivity*. In Proceedings of the Australasian conference on Interactive Entertainment, page 158, 2005. [62](#)
- [Razzaque 01] Razzaque, S., Kohn, Z. & Whitton, M. C. *Redirected walking*. In Proceedings of EUROGRAPHICS, pages 289–294, 2001. [36](#), [37](#)
- [Razzaque 02] Razzaque, S., Swapp, D., Slater, M., Whitton, M. C. & Steed, A. *Redirected walking in place*. In Proceedings of the EUROGRAPHICS workshop on Virtual Environments, pages 123–130, 2002. [33](#), [34](#), [35](#), [37](#), [53](#)
- [Reed-Jones 07] Reed-Jones, R. J., Reed-Jones, J. G., Trick, L. M. & Vallis, L. A. *Can Galvanic Vestibular Stimulation Reduce Simulator Adaptation Syndrome?* In Proceedings of the International Driving Symposium on Human Factors in Driver Assessment, Training, and Vehicle Design, 2007. [44](#)

- [Riecke 02] Riecke, B., Veen, H. & Bühlhoff, H. H. *Visual homing is possible without landmarks: A path integration study in virtual reality*. Presence: Teleoperators & Virtual Environments, vol. 11, no. 5, pages 443–473, 2002. [23](#), [108](#)
- [Riecke 05] Riecke, B., Schulte-Pelkum, J. & Bühlhoff, H. H. *Perceiving Simulated Ego-Motions in Virtual Reality - Comparing Large Screen Displays with HMDs*. In Proceedings of the SPIE, volume 5666, pages 344–355, 2005. [41](#), [114](#)
- [Riecke 07] Riecke, B. & Wiener, J. *Can People Not Tell Left from Right in VR? Point-to-origin Studies Revealed Qualitative Errors in Visual Path Integration*. In Proceedings of the IEEE Conference on Virtual Reality, pages 3–10, 2007. [23](#), [108](#)
- [Riecke 09] Riecke, B., Våljamäe, A. & Schulte-Pelkum, J. *Moving Sounds Enhance the Visually-Induced Self-Motion Illusion (Circular Vection) in Virtual Reality*. ACM Transactions on Applied Perception, vol. 6, no. 2, page 7, 2009. [23](#), [44](#)
- [Rovers 05] Rovers, A. F. & van Essen, H. A. *FootIO - Design and Evaluation of a Device to Enable Foot Interaction over a Computer Network*. Proceedings of the IEEE World Haptics Conference, vol. 0, pages 521–522, 2005. [39](#)
- [Schwaiger 07] Schwaiger, M., Thümmel, T. & Ulbrich, H. *Cyberwalk: Implementation of a Ball Bearing Platform for Humans*. In Human-Computer Interaction. Interaction Platforms and Techniques, pages 926–935. 2007. [29](#), [30](#)
- [Serafin 07] Serafin, S., Kjaer, H.-P., Taylor, C. & Avanzini, F. *Audio-Haptic Physically Based Simulation and Perception of Contact Textures*. In Proceedings International Conference on Auditory Display, 2007. [46](#)
- [Serafin 09] Serafin, S., Turchet, L. & Nordahl, R. *Extraction of ground reaction forces for real-time synthesis of walking sounds*. In Proceedings of the Audio Mostly Conference, pages 99–105, 2009. [44](#), [45](#)
- [Slater 95] Slater, M., Usoh, M. & Steed, A. *Taking Steps: The Influence of a Walking Technique on Presence in Virtual Reality*. ACM Transaction on Computer-Human Interaction, vol. 2, no. 3, pages 201–219, 1995. [9](#), [33](#), [35](#), [49](#), [52](#), [124](#)
- [Stanney 02] Stanney, K. M. *et al.* Handbook of virtual environments: Design, implementation, and applications. Lawrence Erlbaum Associates, 2002. [9](#), [27](#), [28](#), [29](#), [32](#), [124](#)
- [Steinicke 08a] Steinicke, F., Bruder, G., Jerald, J., Frenz, H. & Lappe, M. *Analyses of human sensitivity to redirected walking*. In Proceedings of the ACM symposium on Virtual Reality Software and Technology, pages 149–156, 2008. [10](#), [37](#), [124](#)
- [Steinicke 08b] Steinicke, F., Bruder, G., Ropinski, T. & Hinrichs, K. H. *Moving Towards Generally Applicable Redirected Walking*. In Proceedings of the Virtual Reality International Conference, pages 15–24, 2008. [37](#)

- [Su 07] Su, J. *Motion compression for telepresence locomotion*. Presence: Teleoperators and Virtual Environments, vol. 16, no. 4, pages 385–398, 2007. [37](#)
- [Sugihara 98] Sugihara, T. & Miyasato, T. *The Terrain Surface Simulator ALF*. In Proceedings of the International Conference on Artificial Reality and Telexistence, volume 8, pages 170–174, 1998. [40](#)
- [Suma 12] Suma, E. A., Lipps, Z., Finkelstein, S., Krum, D. M. & Bolas, M. *Impossible Spaces: Maximizing Natural Walking in Virtual Environments with Self-Overlapping Architecture*. IEEE Transactions on Visualization and Computer Graphics, vol. 18, pages 555–564, 2012. [38](#)
- [Sun 03] Sun, Y. & Fisher, R. *Object-based visual attention for computer vision*. Artificial Intelligence, vol. 146, no. 1, pages 77–123, 2003. [25](#)
- [Templeman 99] Templeman, J. N., Denbrook, P. S. & Sibert, L. E. *Virtual Locomotion: Walking in Place through Virtual Environments*. Presence: Teleoperators and Virtual Environments, vol. 8, no. 6, pages 598–617, 1999. [33](#), [35](#)
- [Tongen 10] Tongen, A. & Wunderlich, R. E. *Biomechanics of Running and Walking*. Mathematics and Sports, vol. 43, pages 315–328, 2010. [21](#)
- [Treisman 80] Treisman, A. M. & Gelade, G. *A feature-integration theory of attention*. Cognitive psychology, vol. 12, no. 1, pages 97–136, 1980. [24](#)
- [Usuh 99] Usuh, M., Arthur, K., Whitton, M. C., Bastos, R., Steed, A., Slater, M. & Brooks, Jr., F. P. *Walking > walking-in-place > flying, in virtual environments*. In Proceedings of the ACM SIGGRAPH conference on Computer Graphics and Interactive Techniques, pages 359–364, 1999. [34](#), [35](#), [63](#)
- [Vaughan 92] Vaughan, C., Davis, B. & Jeremy, C. Dynamics of human gait. Human Kinetics, 1992. [18](#), [19](#), [72](#)
- [Visell 08] Visell, Y., Cooperstock, J. R., Giordano, B. L., Franinovic, K., Law, A., McAdams, S., Jathal, K. & Fontana, F. *A Vibrotactile Device for Display of Virtual Ground Materials in Walking*. Lecture Notes in Computer Science, vol. 5024, page 420, 2008. [10](#), [40](#), [44](#), [74](#), [124](#)
- [Visell 10a] Visell, Y. & Cooperstock, J. R. *Design of a vibrotactile display via a rigid surface*. In Proceedings of the IEEE Haptics Symposium, pages 133–140, 2010. [40](#)
- [Visell 10b] Visell, Y., Law, A., Ip, J., an Severin Smith, R. R. & Cooperstock, J. R. *Interaction capture in immersive virtual environments via an intelligent floor surface*. In Proceedings of the IEEE Conference on Virtual Reality, pages 313–314, 2010. [46](#), [69](#)
- [Wendt 10] Wendt, J. D., Whitton, M. C. & Brooks, Jr., F. P. *GUD WIP: Gait-Understanding-Driven Walking-In-Place*. In Proceedings of the IEEE Conference on Virtual Reality, pages 51–58, 2010. [33](#), [34](#), [35](#), [49](#)
- [Whitton 05] Whitton, M. C., Cohn, J., Feasel, J., Zimmons, P., Razzaque, S., Poulton, S., McLeod, B. & Brooks, Jr., F. P. *Comparing VE Locomotion*

- Interfaces*. In Proceedings of IEEE Conference on Virtual Reality, pages 123–130, 2005. [34](#)
- [Wiener 06] Wiener, J. & Mallot, H. *Path complexity does not impair visual path integration*. Spatial Cognition and Computation, vol. 6, no. 4, pages 333–346, 2006. [24](#), [108](#)
- [Williams 07] Williams, B., Narasimham, G., Rump, B., McNamara, T. P., Carr, T. H., Rieser, J. & Bodenheimer, B. *Exploring Large Virtual Environments with an HMD when Physical Space is Limited*. In Proceedings of the ACM symposium on Applied Perception in Graphics and Visualization, pages 41–48, 2007. [35](#)
- [Wilmore 94] Wilmore, J. H. & Costill, D. L. Physiology of sport and exercise. Human Kinetics, 1994. [22](#)
- [Yan 04] Yan, L., Allison, R. S. & Rushton, S. K. *New simple virtual walking method - walking on the spot*. In Proceedings of the Symposium on Immersive Projection Technology, 2004. [34](#), [35](#)
- [Yano 00] Yano, H., Noma, H., Iwata, H. & Miyasato, T. *Shared walk environment using locomotion interfaces*. In Proceedings of the ACM conference on Computer Supported Cooperative Work, pages 163–170, 2000. [28](#), [29](#)
- [Zanbaka 05] Zanbaka, C., Lok, B., Babu, S., Ulinski, A. & Hodges, L. *Comparison of Path Visualizations and Cognitive Measures Relative to Travel Technique in a Virtual Environment*. IEEE Transaction on Visualization and Computer Graphics, vol. 11, pages 694–705, 2005. [34](#)



## Résumé

La navigation à la première personne en Environnement Virtuel (EV) est essentielle à beaucoup d'applications de Réalité Virtuelle (RV), comme les simulations d'entraînement ou les visites virtuelles de musées ou de projets architecturaux. Les techniques de navigation doivent fournir un moyen efficace et écologique d'explorer les EV. De plus, comme dans toute autre application de RV, l'immersion des utilisateurs est aussi primordiale pour obtenir une bonne simulation.

Dans cette thèse, nous avons proposé des nouvelles techniques d'interaction 3D et de retour sensoriel pour améliorer la navigation. Ainsi, nos contributions peuvent être découpées en deux parties : (1) une nouvelle technique d'interaction pour une navigation efficace et écologique en RV et (2) de nouvelles techniques de retour sensoriel conçues pour améliorer l'immersion et la sensation de marche des utilisateurs durant la navigation. Pour chacune des techniques proposées, nous avons conduit des évaluations poussées afin de valider que nos techniques atteignent leurs objectifs.

Dans la première partie, nous avons proposé une nouvelle technique de navigation pour la RV, le Shake-Your-Head (SYH). Cette technique suit les mouvements de la tête de l'utilisateur lorsqu'il marche sûr place devant son écran afin de produire une navigation simulant la marche, ainsi que les sauts ou ramper. Nous avons trouvé que notre technique peut être utilisée efficacement sur des trajectoires complexes et est simple d'apprentissage. De plus, cette technique a été très appréciée par les utilisateurs.

Dans la seconde partie, nous avons proposé une technique, les King Kong Effects (KKE), pour simuler les informations visuelles et vibrotactiles produites à chaque pas. Nous avons également proposé de nouveaux Mouvements de Caméra (MC) améliorés pour simuler les mouvements de la tête lors de la marche, de la course et du sprint. De plus, nos MC sont adaptés à l'âge, au genre, au poids et à la condition physique de l'humain virtuel, ainsi qu'à la pente dans l'EV. Les KKE améliorent la sensation de marcher dans l'EV et ont également été très appréciés des utilisateurs. De plus, nous avons montrés que les différents paramètres des MC sont correctement perçus par les utilisateurs.

## Abstract

First-person navigation in Virtual Environments (VE) is essential to many Virtual Reality (VR) application such as training simulation or virtual visits of museum or architectural projects. Navigation techniques must provide an efficient and ecological way to explore the VE. Moreover, as in any VR application, the immersion of the users is also a primordial component of a successful simulation.

In this Ph.D. thesis, we proposed new 3D interaction and sensory feedback techniques to improve the navigation in VR. Therefore, our contribution can be decomposed into two main parts: (1) a new interaction technique for efficient and ecological navigation in VR and (2) new sensory feedback techniques designed to improve the immersion and sensation of walking of the users during the navigation. For each of the proposed techniques, we conducted extensive evaluations to validate that their objectives were completely fulfilled.

In the first part, we proposed the Shake-Your-Head (SYH) technique as a new navigation technique for VR. This technique tracks the movements of the user head when walking-in-place in front of the screen to produce a navigation simulating the walk, as well as jumping or crawling. We found that our technique can be used efficiently on complex trajectories and is easy to learn. Moreover, this technique was highly appreciated by the users.

In the second part, we proposed the King Kong Effects (KKE) technique to simulate visual and vibrotactile information produced at each step. We also proposed improved Camera Motions (CM) to simulate the head motions when walking, running and sprinting. Moreover, our CM are adapted to the virtual human age, gender, weight and fitness, as well as the slope of the VE. The KKE increase the sensation of walking in VE and was also highly appreciated by the users. Moreover, the different parameters of the CM were correctly perceived by the participants.